ABSTRACT

LODGE, MARECA. Investigating the Role of Fructose Metabolism on Macrophage Function and Phenotype. (Under the direction of Dr. Arion Kennedy).

Over-consumption of fructose in adults and children has been linked to increased risk of Non-Alcoholic Fatty Liver Disease (NAFLD). Recent studies have highlighted the effect of fructose on liver inflammation, fibrosis, and immune cell activation. Researchers have linked fructose consumption to *de novo* lipogenesis, inflammatory signaling and fibrosis within hepatocytes, the bulk cell type of the liver. Many works have summarized the effects of fructose on hepatocyte cell signaling, function and phenotype as well as the metabolic fate of fructose within these cells. Over consumption of fructose leads to disease, aiding in immune cell recruitment and activation. Chronic immune cell activation can lead to inflammation, fibrosis and potentially liver cancer. Macrophages are just one type of immune cell that contributes to liver inflammation and fibrosis. However, little work summarizes the direct impact of fructose on macrophage infiltration, function, and phenotype within the liver. By understanding the effect of fructose on macrophage activation and function, we can gain insight into the progression and regulation of liver disease. In this work we used both *in vitro* and *in vivo* methods to analyze fructose metabolism within residential macrophages of the liver, Kupffer cells. We discovered fructose decreased viability of immortalized Kupffer cells (IMKC). By use of real-time polymerase chain reaction fructose induced gene expression of pro-inflammatory cytokines tumor necrosis factor alpha (*Tnfα*) and interleukin 6 (*Il6*) in M1 polarized IMKC. In addition, fructose increased expression of genes associated with the anti-inflammatory response, fibrosis, cell proliferation, and differentiation in unpolarized IMKC. To gain insight into fructose regulated gene expression, we used C13 fructose to metabolically trace fructose carbons using mass spectrometry. Fructose

carbons were present in glycolysis and the pentose phosphate pathway (PPP). Inhibition of the PPP increased genes associated with the anti-inflammatory response, fibrosis, cell proliferation, and differentiation. *In vivo*, we demonstrated via genetic mapping and flow cytometry chronic fructose diet decreased Kupffer cell populations while increasing transitioning monocytes in mice. Single cell RNA sequencing (scRNAseq) revealed fructose elevated expression of genes associated with the anti-inflammatory response, fibrosis, cell proliferation, and differentiation in liver and hepatic macrophages. In addition, fructose elevated genes involved in fructose metabolism and the pentose phosphate pathway in hepatic macrophages. Lastly, we analyzed the ability of hepatocytes and the non-parenchymal (NPC) fraction of the liver containing macrophages to uptake and utilize fructose during acute and chronic exposure. By using C13 fructose portal vein perfusion coupled with cell fraction isolation techniques, hepatocytes and NPCs uptake free circulating fructose at time of acute and chronic exposure. These results significantly impact the field by increasing our understanding of fructose metabolism within highly active immune cells. The implications of this work will benefit carbohydrate metabolism research, the understanding of macrophage function and phenotype in disease and aid in potential therapeutic mechanisms for NAFLD through PPP metabolism within macrophages.

Investigating the Role of Fructose Metabolism on Macrophage Function and Phenotype

by

Mareca Lodge

A dissertation submitted to the Graduate Faculty of

North Carolina State University

in partial fulfillment of the

requirements for the degree of

Doctor of Philosophy

Biochemistry

Raleigh, North Carolina

2023

APPROVED BY:

Dr. Arion Kennedy	Dr. Melanin Simpson
Dr. Matt Koci	Dr. Scott Laster
Dr. Xiaojing Liu	

DEDICATION

I dedicate this work first and foremost to my family. I especially dedicate this work to my parents, April and Russell Lodge, my brother Holden Lodge and my husband Christopher Dubois. Without any of you this work would not be possible. Thank you for the incredible support in every way. I could not have asked for a better support system during my time in this program. I want to thank my mom for her prayers and constant encouragement during the hardest of days. Thank you, dad, for challenging me to work hard daily and to enjoy my time in Raleigh. Thank you, Holden, for being someone I can look up to and can go for guidance when I am troubled. Thank you, Chris, for your love and devotion to our family. You have been a steady point of comfort that has made my time in Raleigh and this program more enjoyable.

BIOGRAPHY

Mareca Lodge grew up in Montoursville, Pennsylvania where she actively participated in band, choir, softball, cheerleading and any chance to lead others. As early as elementary school Mareca knew she wanted to teach and pursued every opportunity in high school and beyond to gain experience in teaching, being a leader and communicating with individuals. She had two influential science teachers that pushed her to pursue a teaching career in science, specifically biology, which led her to accept an offer from Mansfield University to join their biology undergraduate program. At Mansfield, Mareca expanded her knowledge of science by taking biochemistry and tissue culture where she fell in love with cell culture and molecular mechanisms. It was at this point that she applied to and got accepted into the molecular and structural biochemistry department of North Carolina State University to pursue her Ph.D. in biochemistry. With the help of the Kennedy lab at NCSU Mareca shared her love for teaching science by mentoring undergraduate students, participating in the preparing the professoriate program, leading discussions in class and being a recitation leader. After finishing her project on understanding the mechanism of fructose metabolism within macrophages she accepted a position at North Carolina School of Science and Mathematics where she is a biology instructor. Mareca hopes to continue encouraging students to ask questions about the world around them and to follow their passions wherever they may take them.

ACKNOWLEDGMENTS

Here I acknowledge an absolutely essential person in all of my work and the last 5 years of living in Raleigh, Dr. Alex Breuer. Alex, you have not only encouraged and developed my mind as a scientist, but you have shown me what a true friend is. My expectations of joining a lab with a post doc was merely to have someone to train me in the skills I would need to complete my project and degree. Instead, I learned both these and how to be confident in myself as a researcher, and educator, a person and a woman of God. Your friendship and mentorship has been invaluable and I strongly believe if it weren't for you I would not have loved my time in Raleigh, NC as much as I have. I cannot thank you enough for all you have done for me. Truly my gratitude is endless.

I acknowledge my PI Dr. Arion Kennedy for her superior knowledge in the field and her persistence to ask important questions to further our understanding of metabolic diseases. Without her guidance I would not have had the courage to tackle a project of this scale. Thank you for being optimistic and positive about my results from the very beginning. You have always presented an environment in which I feel safe and comfortable to ask questions. Having limited research experience, I was nervous to start any assay, but you encouraged me to try and to stand strong in my skills as a researcher. I appreciate your support in my desires to pursue teaching training. Although not a role of high importance in our department, you continuously fought for me to have these teaching experiences and for that I am thankful. Because of these, I strengthened my skills in science communication and further confirmed my goals for educating others in science and the changing world around us. Thank you for creating a space in which I felt heard and seen in my challenges and triumphs. Thank you for being a strong woman of science that I am able to look up to. You have always believed in my abilities even when I didn't. You have made my experience unforgettable and have prepared me for my future in science education.

To Dr. Xiaojing Liu for all of your encouraging words and mass spectrometry knowledge. Every day in which you are in lab brought me such joy. Your endless positivity motivated me to push myself to come prepared and excited every day to tackle the hardest parts of my project. Thank you for challenging me to think critically about the assays I was using and how to best analyze and use my MS data.

I acknowledge my committee for their counsel in my 5 years at NCSU. Thank you for your collective insight into my project and offering suggestions where you saw challenges in my work. Thank you for challenging me to push myself to answer challenging questions and to not give up when experiments get tough. You have all been a valuable asset to my career and I am thankful for each of you.

To the students of the biochemistry department, I want to thank you for the best 5 years of my life. I am forever grateful for the friendships I have made in this department. We have made such a tight knit group of friends that I hope we continue to support and challenge each other in years to come. Thank you for participating in all of my parties, outings and endless taco lunches. These friendships pushed me to continue working on days that felt like I was never going to finish. Your peer reviews made me a better presenter and kept me working hard on my project.

TABLE OF CONTENTS

LIST OF TABLES VIII

LIST OF FIGURES IX

CHAPTER 1: Introduction

1.1 Sources of Fructose 1

1.2 Fructose Uptake and Utilization 1
- 1.2.1 Current Dogma Fructose Metabolism 1
- 1.2.2 Importance of GLUT in Fructose Metabolism 2
- 1.2.3 Importance of KHK in Fructose Metabolism 3

1.3 Fructose in Intestinal Disease 4

1.4 Fructose in the Microbiota 4

1.5 Fructose and NAFLD 5

1.6 Fructose and Obesity 6
- 1.6.1 Fructose Regulated Adipocyte Inflammation 6

1.7 Macrophage Phenotype and Metabolism 7

1.8 Liver Macrophages 9

1.9 Regulation of Fructose Intake and Metabolism to Prevent Metabolic Disease 10

1.10 Figures and Legends 12

CHAPTER 2: Fructose Metabolism Regulates Inflammatory Gene Expression Through the Pentose Phosphate Pathway Within Macrophages 14

2.1 Abstract 14

2.2 Introduction 14

2.3 Materials and Methods 17

2.4 Results 22
- 2.4.1 Fructose Consumption Induces Proliferation of IMKC While Reducing Metabolic Activity and Cell Viability 22
- 2.4.2 Fructose Metabolism Induces Macrophage Inflammatory Gene Expression 23
- 2.4.3 C13 Fructose Labeling Reveals Fructose Carbon Shuttling Patterns 23
- 2.4.4 Pentose Phosphate Pathway Regulates Fructose Mediated Inflammatory Gene Expression 25

2.5 Discussion 26

2.6 Figures and Legends 30

CHAPTER 3: Characterize the Effects of Acute and Chronic Fructose Exposure in vivo in Mouse Liver and Macrophage Subsets 44
3.1 Abstract 44
3.2 Introduction 44
3.3 Materials and Methods 46
3.4 Results 49
3.4.1 Chronic Fructose Diet induces Liver and Body Weight Gain 49
3.4.2 Chronic Fructose Diet Reveals Gene Signature of Hepatic Macrophages 50
3.4.3 Fructose Increases Anti-inflammatory Gene Expression in Acute and Chronic Studies 51
3.5 Discussion 51
3.6 Figures and Figure Legends 55
CHAPTER 4: Analyze the Effect of Fructose Metabolism and Localization Within Primary Liver Macrophages After Chronic and Short-Term Fructose Exposure 61
4.1 Abstract 61
4.2 Introduction 61
4.3 Materials and Methods 63
4.4 Results 67
4.4.1 Closed-Loop Perfusion Results in Decreased Cell Viability 67
4.4.2 New C13 Fructose Perfusion Increased Cell Yield and Viability 68
4.5 Discussion 69
4.6 Figures and Figure Legends 72
CHAPTER 5: Conclusions 77
5.1 Fructose Metabolism and Macrophages 77
5.2 Pentose Phosphate Pathway and Inflammation 77
5.3 Gene Associated with NASH phenotype 78
5.4 Impact of Fructose Concentration and Delivery on NAFLD Development 78
5.5 Limitations of Study 79
5.6 Final Summary of Work 82

REFERENCES 83

LIST OF TABLES

Table 1: Representative Cell Yield and Viability from Closed Loop Circulation……72

Table 2: Representative Cell Yield and Viability from PLOS……73

Table 3: Representative Cell Yield and Viability from C13 Study……..75

LIST OF FIGURES

Figure 1.1: Fructose Metabolism in Low and High Concentrations. 12
Figure 2.1: Fructose Induces Inflammation in Metabolically Active Tissues. 13
Figure 1: Fructose uptake in Macrophages. 30
Figure 2: Fructose Uptake Mediated by HK. 31
Figure 3: Fructose Decreases Cell Viability in IMKC and J774.1. 32
Figure 4: Fructose Induces IMKC Proliferation and Decreases J774.1 Proliferation. 33
Figure 5: Fructose Reduces AP-1 Factor c-Jun Phosphorylation in M1 J774.1. 34
Figure 6: 25mM Fructose Increases Anti-inflammatory and Fibrosis Gene Expression in M0 IMKC. 35
Figure 7: Fructose Regulates Genes Involved in Inflammation, and Fibrosis in J774.1 and RAW 36
Figure 8: 5mM Fructose Metabolic Partitioning in IMKC. 37
Figure 9: 25mM Fructose Metabolic Partitioning in IMKC. 38
Figure 10: 5mM Fructose Metabolic Partitioning in J774.1 and RAW. 39
Figure 11: Pharmacological Inhibition of the PPP Increases Fructose Induced Expression of Anti-Inflammatory and Fibrosis Genes in M0 IMKC. 40
Figure 12: Pharmacological Inhibition of the PPP Increases IL6 Gene Expression in Fructose Treated J774.1. 41
Figure 13: Establishing G6PDH Knockdown. 42
Figure 14: SiRNA Inhibition of the PPP Increases Fructose Induced Expression of Anti-Inflammatory and Fibrosis Genes in M0 IMKC. 43
Figure 15: Chronic Fructose Diet Induces Liver and Adipose Tissue Weight Gain. 55
Figure 16: Fructose Increases Long Chain Carnitines and DGs and Liver Damage. 56
Figure 17: Chronic Fructose Diet Decreases Kupffer Cells and Increases Transitioning Monocytes. 57
Figure 18: Impact of Chronic Fructose Diet on Molecular Pathways and Genes Associated with Metabolism, Inflammation, and Fibrosis. 58
Figure 19: Chronic Fructose Diet Increases Anti-Inflammatory and Profibrotic Associated Gene Expression in Liver and $CD11b^{+}F4/80^{+}$ Cells. 59

Figure 20: Fructose Increases Anti-inflammatory and Fibrosis Gene Expression in Primary M1 Polarized KC. 60
Figure 21: Closed Loop Perfusion leads to NPC and Hepatocyte Separation. 72
Figure 22: Fructose Carbon Partitioning in NPC and Hepatocyte Fractions. 73
Figure 23: Mice on Fructose Diet do not Gain Weight. 74
Figure 24: Fructose Metabolites After Acute and Chronic Fructose Exposure. 75
Figure 25: Fructose Metabolite Shuttling After Acute and Chronic Fructose Exposure. .. 76

CHAPTER 1: Introduction

1.1 Sources of Fructose

Understanding how fructose affects our health has been a controversial subject for over a decade. Multiple studies have linked fructose consumption to increased obesity, lipid accumulation within nonalcoholic fatty liver disease (NAFLD), and other metabolic diseases [1] [2]. Although fructose is a naturally occurring fruit sugar that is found in many fruits and vegetables, it is important to note that fructose within the diet is often in the form of sucrose or high fructose corn syrup (HFCS). The increased ingestion of foods sweetened with these products raised fructose consumption from 20g/day to nearly 100g/day [3]. Sucrose, commonly known as table sugar, is a non-reducing disaccharide of glucose bound to fructose through an α-1,β-2-glycosidic linkage. HFCS has been developed to enhance sweetness of drinks and baked goods as it's cheaper to make than sucrose. Because fructose is sweeter and more soluble than glucose it has been suggested as an alternative sweetener for sugary products [4]. Glucose converting enzyme glucose isomerase is added to corn syrup to convert glucose molecules into fructose, thus adding additional sweetness with less product [5]. Within the standard glucose glycemic index, sucrose consumption spikes blood glucose levels less than glucose, whereas HFCS is much higher in the index. High levels of added fructose can be found in yogurts, fast food, and highly consumed sugar sweetened beverages. Although fructose is most often consumed in the form of sucrose, both sucrose and HFCS have been identified to elevate levels of triglycerides, free fatty acids and insulin release after consumption [6]. Due to the negative effects of high sucrose or HFCS consumption on health, it is imperative to fully distinguish the molecular mechanisms of fructose on the development of metabolic disease.

1.2 Fructose Uptake and Utilization

1.2.1 Current Dogma Fructose Metabolism

The current dogma for fructose metabolism and metabolic disease suggests enterocytes and hepatocytes metabolize fructose leading to dysregulation of lipid metabolism, inflammation and intestinal microbiome producing toxic metabolites. Until recently, the metabolic fate of fructose was thought to occur primarily in the liver, as expression of phosphorylating enzyme ketohexokinase-C (KHK) is highly expressed in the liver compared to the intestines [7]. Cholsoon

et. al. revealed at low doses of fructose, fructose in the form of sucrose or free fructose in HFCS has the same metabolic fate [8]. Fructose carbons are rapidly converted to glucose, glycerate and TCA metabolites within the small intestine. These byproducts are shuttled through the portal vein to the liver for further processing. However, dose dependent studies of fructose diet in mice indicate an intestinal saturation point where fructose is no longer metabolized. The remaining fructose is absorbed through the intestinal lining and travels to the liver through the portal vein where it begins metabolism **(Figure 1.1)**. In addition, unmetabolized fructose is utilized by intestinal gut microbiome producing TCA metabolites and short chain fatty acid butyrate [9] [10]. This study changed the way the field looks at fructose metabolism and disease, highlighting the importance of understanding the direct impacts of high fructose consumption on cell function and phenotype.

1.2.2 Importance of GLUT in Fructose Metabolism

Polysaccharides such as sucrose cannot be absorbed within the intestine and must first be broken down into monomeric forms of glucose, fructose and galactose. At this point, fructose is first absorbed within the intestinal lumen epithelial cells (enterocytes) where glucose transporters (GLUT) 2 and 5 are highly expressed [11]. The process of fructose transport is passive and insulin independent unlike glucose. Although GLUT2 can participate in fructose absorption, GLUT5 is the primary transporter as it has a much higher affinity for fructose and is found in most mammals within the small intestine [12]. Knock out mouse models of intestinal GLUT5 led to 75% reduction of fructose absorption, low peripheral blood levels of fructose and an overall reduction in weight gain when fed high fructose diets [13]. GLUT5 is developmentally regulated, with GLUT5 gene expression significantly lower in fetal intestine compared to adults [14]. Consumption of fructose in toddlers leads to cases of malabsorption and early onset weight gain within children [15] [16]. In healthy adults, normal resting levels of fructose within peripheral blood are 0.04mM but following fructose consumption can increase to 0.4mM. A recent C13 tracing study within mice found the intestine to fully metabolize low concentrations of fructose (5% of daily caloric intake) via phosphorylation and fructolysis, a process that intercedes with glycolysis [8]. These metabolites can be converted to glucose via gluconeogenesis, used within the cell, or be sent to the liver via the portal vein. However, intestinal cells can become saturated with higher concentrations (10% or higher caloric intake) leading to transportation via GLUT2/8 to the portal vein for further

processing by the liver. This is shown by minimal C13 fructose carbon labeled glucose within the portal vein as well as higher C13 fructose carbon labeled fructose 1 phosphate (F1P) within the liver.

1.2.3 Importance of KHK in Fructose Metabolism

Within the liver, GLUT2 and 8 are responsible for fructose uptake where phosphofructokinase mediated metabolism is not restricted as it is with glucose. Following entry into a liver cell, fructose is metabolized by KHK and aldolase B. Phosphorylation of fructose can lead to ATP depletion and uric acid production as this process is not feedback regulated [17] [18]. Fructose can also be phosphorylated with hexokinases I and II although HK affinity is higher for glucose[19]. The KHK gene encodes for two isotopes KHKC and KHKA. KHKC is primarily expressed in humans and mice in liver, kidney, and the jejunum with low expression levels in pancreas and white adipose tissue in mice [19] . KHKA is ubiquitously expressed and has a slower enzymatic rate compared to KHKC. KHKC is more active in metabolic tissues as the Km is 0.8mmol/l compared to KHKA at 7 mmol/l with fructose. Although both isoforms can phosphorylate fructose, the majority of fructose uptake and metabolism is mediated by KHKC in the intestine and liver [20]. Pharmacological inhibition and global knockdown of both isoforms of KHK, reduces fructose caloric intake leading to reductions in body weight, adipose tissue expansion and hepatic lipid accumulation, liver injury and fibrosis [21] [22]. Knockdown of KHK in epithelial cells of the small and large intestines in mice leads to reductions in fructose caloric intake but does not impact chronic fructose induced lipid accumulation in adipose tissue or liver [20]. In contrast, hepatocytes were found to be the primary cells responsible for driving fructose induced metabolic syndrome. Interestingly, during the development of hepatocellular carcinoma and breast cancer, there is a switch from KHKC to KHKA activity which leads to phosphorylation of phosphoribosyl pyrophosphate synthetase 1 driving nucleotide synthesis [23] [24].

KHK phosphorylates fructose to fructose-1-phosphate (F1P) which begins metabolism via aldolase B. Fructose is then broken into 2, triose phosphates dihydroxyacetone phosphate (DHAP) and glyceraldehyde 3 Phosphate (G3P). These intermediates are then converted into lactate, glucose, glycogen or fatty acids. Because of this, fructose largely impacts the available triose pools within the liver leading to increased cycling of glycolysis, gluconeogenesis, lipogenesis, and oxidative phosphorylation. Although fructose is mainly shuttled from the intestine to the liver via

the portal vein, it is projected that 20-30% of ingested fructose may enter systemic circulation where it can be deposited in other metabolic tissues including the proximal tubes within the kidney and adipose tissue. The concentration and frequency of consumed fructose determines the metabolic fate of these carbons [25].

1.3 Fructose and Intestinal Disease

If consumption and metabolism of fructose is not regulated correctly it can lead to intestinal and liver diseases. Fructose metabolism within the intestine begins with phosphorylation to F1P by KHK in enterocytes. Elevated intracellular levels of F1P can be toxic, leading to endoplasmic reticulum stress and inflammation which has been reported to induce barrier deterioration and shorten colon length [26]. Samuel et. al. discovered fructose promotes hypoxic cell survival via extended villi length, partly through F1P inhibition of hypoxic adaptation protein pyruvate kinase isozyme M2 (PKM2). The villi length extension led to increased weight gain, nutritional absorption and fat accumulation [27]. High levels of fructose led to misshapen colon and cecum as well as infiltration of inflammatory macrophages, neutrophils, dendritic cells and natural killer T cells within the lamina propria. These cells increase expression of inflammatory cytokines interleukin 1 beta (IL1β), interleukin 2 (IL2), and interleukin 6 (IL6) within the small intestine of mice (**Figure 2.1**) [28], [29].

1.4 Fructose and Microbiota

Recently fructose has surfaced as a contributor to irritable bowel syndrome (IBS). High fructose diet led to abundance changes of intestinal microbiota families, primarily through increasing *Bacteroides* and *Lactobacilli* [28]. Interestingly, these bacteria have a high ability to synthesize enzymes for carbohydrate metabolism. Bacterial fermentation of excess fructose leads to increased short chain fatty acids as well as hydrogen and carbon release, mimicking IBS symptoms [30]. When in excess, fructose malabsorption can occur when dietary concentrations exceed absorption capacity within enterocytes [31]. In addition to increased bacterial growth, Kawabata et.al found fructose diet to induce leaky gut symptoms by decreasing protein expression of tight junction protein, occludin [32]. This led to epithelial cell permeability and inflammatory cell infiltration. These findings suggest an indirect mechanism by which fructose regulates inflammation in the intestine by promoting microbiome dependent on carbohydrate metabolism, increasing leaky gut leading to hypoxia and increased immune cell infiltration. Although fructose metabolism begins

within the intestine, it can often bypass initial metabolism and be shuttled to the liver for further processing which can lead to liver complications due to high fructose consumption.

1.5 Fructose and NAFLD

NAFLD affects 25% of the adult world population with advances in this percentage on the rise [33]. NAFLD is associated with metabolic syndrome (MetS) as symptoms of weight gain, insulin resistance and inflammation are shared between both diseases. NAFLD is a progressive disease hallmarked by lipid accumulation and inflammation within hepatocytes, which make up 70% of liver structure. Over the last decade, studies have linked the monosaccharide fructose to the progression of NAFLD as fructose consumption has increased from the recommended 5% of daily energy intake to 17% within sugar sweetened beverages alone, correlating to the rise in obesity related diseases [34]. Metabolism of fructose produces triose phosphates that form acetyl-coA, the essential building block for fatty acid synthesis. With consistent production of fatty acids, these fatty acids can be stored as triglycerides, a process known as *de novo* lipogenesis (DNL). Fructose metabolism stimulates DNL through triose phosphate activated fatty acid synthesis and through transcriptional regulation of enzymes involved in DNL. Studies have shown that high concentrations of fructose in drinking water increases genes involved in fatty acid synthesis such as FAS, acetyl-CoA carboxylase (ACC) and carbohydrate responsive element binding protein (ChREBP) in mice [35] [36]. Fructose consumption has also been tied to decreased fatty acid oxidation. A recent study showed fructose diet for 10 weeks with and without high fat diet had elevated malonyl CoA levels which elevated saturated acyl carnitines in fructose groups, aiding in the decrease of fatty acid oxidation. Softic et al. demonstrate that consumption of fructose-sweetened water in the presence of high-fat diet leads to increased fatty acid synthesis and hepatic insulin resistance compared with glucose-sweetened water. Interestingly, knockdown of KHK in this model attenuates fructose-mediated insulin resistance and NAFLD [37]. In addition to increasing lipid accumulation (steatosis), human diet studies have found prolonged fructose consumption can lead to increased prevalence of liver fibrosis [38]. The effects of fructose on hepatocytes have been well reviewed [39] [40]. Although intestines and liver are the major organs contributing to fructose metabolism, fructose metabolism impacts other metabolic tissue such as adipose tissue.

1.6 Fructose and Obesity

Obesity is a serious health risk that can decrease quality of life through increased risk for type 2 diabetes, hypertension, cardiovascular disease and premature mortality. Obesity and NAFLD are often linked, and it is predicted that nearly 20% of the world population will become obese by 2025 [41]. A recent mouse study has uncovered a link between fructose consumption and developing obesity through increased weight gain, hyperinsulinemia, and increased serum triglycerides [42]. After carbohydrate consumption, circulating fructose can be deposited within adipose tissue, affecting local cell metabolism and phenotype. It is important to note that adipose tissue is dynamic in cell populations and cross talk fluidity. Because of this, multiple cell types may be exposed to dietary carbohydrates. Fructose exposure increases adipogenesis within adipose tissue, aiding in the increase of lipid accumulation [43]. Fructose metabolism differs between cell types due to available protein transporters, making the prediction of how fructose affects phenotype and function of cells a challenge. Adipocytes lack KHK, leaving HK responsible for phosphorylating fructose to fructose 6 phosphate (F6P) where it diverges into glycolysis metabolism [44]. Fructose at high concentrations induces fatty acid and palmitate release and in the presence of glucose increases NADP and C02 for lipid storage [45].

1.6.1 Fructose Regulates Adipocyte Inflammation

Adipocytes maintain homeostasis by secreting cytokines to signal immune cell recruitment to clear pathogens. Fructose increases secretion of pro-inflammatory cytokines interleukin 18 (IL18), Il1b and TNFα (Fig. 2). Interestingly, anti-inflammatory proteins interleukin 10 (IL10) and nuclear receptor factor 2 (Nrf2) were also elevated, potentially for a mechanism to compensate for pro-inflammatory flux [46]. Additionally, insulin sensing molecule PPARy was also shown to be upregulated with fructose treatment. 8 weeks of fructose administration studies show activation of IL6 with a reduction in PPARy [47]. Another study indicated 30% fructose for 8 weeks decreased IL10 secretion without affecting TNFα levels [48]. In addition to adipokines, extracellular vesicle secretion is known to signal to surrounding cells. Small extracellular vesicles (EV) may contain mircoRNAs (miRNA) which facilitate changes in adipocyte differentiation, adipogenesis, inflammation and lipid accumulation. Discovering that secreted vesicles can have endocrine effects on multiple cell types and tissues has opened the field up to new questions involving diet induced signaling. In cultured adipocytes and rat adipose tissue, fructose increased specific

miRNA 143-5p which plays a role in lipid metabolism, adipogenesis and insulin resistance (Figure 2.2) [49]. In contrast, miRNA 223-3p was reduced. Previous studies have linked the decrease in 223-3p to a reduction in pro-inflammatory activation of macrophages [50]. As the study of fructose metabolism remains a race, it is clear fructose can have indirect effects on endocrine signaling and inflammation, although the complete story is yet to be revealed.

1.7 Macrophage Phenotype and Metabolism

Within metabolic tissues such as intestine, liver and adipose, residential or recruited immune cells may be exposed to high concentrations of fructose. Immune cells communicate with surrounding microenvironmental cells in metabolic tissues to maintain homeostasis. Myeloid cells and lymphocytes are known to contribute to inflammation and fibrosis in metabolic tissues. However, there remains a gap in knowledge on how fructose regulates immune cell function and phenotype, specifically in macrophages, in the context of metabolic disease. A wide range of studies have demonstrated that fructose in concert with high fat diet leads to increased infiltration of macrophages within hepatic tissue [51-53]. The scope of tracing infiltrating macrophage lineage is widening as emerging evidence suggests recruitment from myeloid progenitor cells of the bone marrow as well as mature macrophages from surrounding tissue such as peritoneal and intestinal macrophages [54].

Residential or recruited macrophages may express a fluid phenotype, displaying both proinflammatory and anti-inflammatory properties. Traditionally, external stimuli such as lipopolysaccharide (LPS) or cytokines secreted from other immune cells such as interferon gamma (IFNγ) activate toll-like receptor (TLR) responses of macrophages. These signaling cascades are thought of as pro-inflammatory (M1) because they lead to upregulation and secretion of cytokines such as IL6 and tumor necrosis factor alpha (TNFα) [55]. These cytokines aid in wound repair by activating T cells and other immune cells to clear pathogens. This metabolically energetic process is maintained through increased flux of glycolysis through upregulated glycolytic proteins from increased succinate and HIF1α levels [56]. In addition to glycolysis, the oxidizing phase of the pentose phosphate pathway (PPP) is also highly upregulated in M1 polarized macrophages to maintain cellular levels of ROS for macrophage phagosome stabilization [57]. In situations where there is pro-longed inflammation, macrophages can take on an anti-inflammatory phenotype where they release extracellular matrix rebuilding proteins to signal wound healing [55]. Alternatively

activated macrophages (M2) are activated in response to immune cell signaling of IL4 and IL13 [58] [59]. Unlike M1, oxidative phosphorylation (OXPHOS) and the tricarboxylic acid cycle (TCA) are highly important for M2 metabolism [60] [61]. The challenge of identifying macrophage phenotype lies within the varying types of macrophage subsets along with overlapping of cell membrane protein markers. As technology such as single-cell RNA (scRNAseq) sequencing is becoming more widely available, distinguishing between residential and recruited macrophage subsets as well as pro-inflammatory or anti-inflammatory macrophages is becoming better understood [62].

Glucose is the primary fuel source of proinflammatory macrophages, with glycolysis providing energy for the production and secretion of cytokines. However, a recent study with peripheral blood monocytes discovered fructose to shuttle carbons through oxidative phosphorylation (OXPHOS) rather than glycolysis (Fig. 1) [63]. In turn, TCA metabolites such as succinate, malate and fumarate were elevated to a higher extent than glucose, most likely to produce energy and reducing agents to maintain increased OXPHOS. Interestingly, when inhibiting the OXPHOS pathway, cells provided only fructose were not able to recover and use glycolysis for additional energy, leaving these cells metabolically inflexible, where glucose conditions were able to switch back and forth. Inflammatory cytokines IL6, IL1β, IL18 and TNFα were secreted at higher concentrations in fructose treated monocytes compared to glucose [63]. This response was in part mediated by upregulated mTORC1 signaling. Of note, glutamine carbons mainly contributed to TCA cycle intermediates and cytokine secretion within fructose treatments. Thus, fructose can directly affect immune cell regulation by inducing inflammation within monocytes.

In addition to inflammatory cytokines, macrophages and T cells secrete macrophage migration inhibitory factor (MIF) which has been shown to be important in the protection of liver disease through regulation of inflammation and immunity [64]. MIF deficient mice on 20% fructose diet for 9 weeks showed increased hepatic fatty acid accumulation through upregulated CD36 signaling. Whether wild type (WT) or MIF deficient mice, fructose supplementation induced levels of lipogenesis proteins sterol regulatory element binding protein 1 (SREBP-1) and carbohydrate regulatory element binding protein (chREBP) as well as their downstream targets acetyl-CoA carboxylase (ACC) and fatty acid synthase (FAS). Unsurprisingly, the changes in protein levels were accompanied by lipid accumulation and increased gene expression of IL6 within liver

hepatocytes. Although the mechanism is not fully understood, AMP activated protein kinase (AMPK) was decreased in MIF deficient fructose fed mice potentially aiding in the upregulation of lipogenesis proteins. In addition to lipid accumulation, mice on a WT or MIF deficient background given fructose supplementation had enlarged and increased numbers of residential macrophages, Kupffer cells, within the liver. Although Kupffer cells (KCs) have liver regenerative properties, they can also play a role in liver destruction and promote inflammation.

1.8 Liver Macrophages

Current literature categorizes three unique macrophage populations that reside in the liver. The first and most abundant in normal liver conditions are KCs, followed by transitioning monocytes and non-Kupffer cell derived macrophages [65]. The main role of liver macrophages is to clear pathogens by phagocytosis or anti-microbial protein secretion. Clearance of pathogens from blood circulation happens within the portal vein and blood capillaries of the liver. KCs reside within the liver sinusoid along with other pathogen clearing cells such as dendritic cells and hepatic stellate cells, making them the first line of immune defense [66]. KCs originate from yolk sac derived bone marrow monocytes at early ages of fetal development [67]. Until recently, residential macrophage maintenance in normal liver conditions was thought to mainly derive from circulating monocytes. However, liver regenerative studies have shown that emerging macrophage populations come from self-renewal and IL-6 induced proliferation of KCs [68] [69]. KC renewal can be marked by increased cells expressing CLEC2, CD207, VSIG4, and TIMD4 as these cell surface proteins are exclusively expressed on KCs [70]. Conversely, in pro-longed disease states like steatosis, KCs lose the ability to self-renew and populations are regenerated by monocyte derived macrophages that differentiate into a KC phenotype [70]. As described above, KCs may become active by cellular signaling which induces a pro- or anti-inflammatory phenotype. Studies have shown that induction of an M2 phenotype in NAFLD may be a leading therapeutic target as M2 leads to increased apoptosis of inflammatory cells which reduced inflammation, cell damage and increased liver repair [71]. In addition to cytokine signaling activation, KCs can be stimulated by fructose mediated fatty acid exposure. Fructose may play an indirect role in activating KCs as fructose mediated fatty acid synthesis has been shown to increase TLR4 inflammatory signaling in macrophages [72]. Fructose also increases intestinal permeability which leads to increased LPS and endotoxin levels within the liver. The increase in LPS led to an increase in liver KCs as well

as prevalence of liver fibrosis [73]. Although works have summarized the indirect effects of fructose on liver damage and KC function, the role of direct fructose metabolism on KC function and phenotype remains to be elucidated and is the focus of this proposed work.

1.9 Regulation of Fructose Intake and Metabolism to Prevent Metabolic Disease

Reducing fructose intake and metabolism of fructose can be an effective therapy for treating obesity and NAFLD. Patients are advised to limit the consumption of sugary drinks, such as soda, juice, and sports drinks. In addition, it is recommended to select low fructose-containing fruits and vegetables and avoid foods that contain high concentrations of fructose and high-fructose corn syrup. While effective, this can be challenging for patients to adhere. Targeting fructose metabolism with KHK inhibitors has been shown to have several potential therapeutic benefits, including treating obesity, type 2 diabetes, and fatty liver disease. KHK inhibitors have been shown to reduce weight gain in animal models. In one study, patients with type 2 diabetes experienced significant reductions in blood sugar levels. KHK inhibitors have also been shown to improve insulin sensitivity and reduce the risk of heart disease in patients with type 2 diabetes. There have been multiple clinical trials of KHK inhibitors, but the results are mixed. One of the most promising clinical trials was a Phase 2 trial of PF-06835919, a KHK inhibitor developed by Pfizer [74]. In this trial, PF-06835919 was shown to be effective in reducing liver fat and inflammation in patients with non-alcoholic fatty liver disease (NAFLD) [75]. Another Phase 2 trial of TAK-875, a KHK inhibitor developed by Takeda. In this trial, TAK-875 was shown to be effective in reducing blood sugar levels in patients with type 2 diabetes. However, not all clinical trials of KHK inhibitors have been successful. For example, a Phase 2 trial of a KHK inhibitor developed by Eli Lilly, was terminated early due to safety concerns. Thus, the inconsistencies and termination of clinical trials suggests a need for further research to identify molecular mechanisms of fructose metabolism. In addition, improvements on safety and efficacy of KHK inhibitors will lead to better treatments for metabolic disorders.

In the following Chapters, we determine fructose can directly influence hepatic macrophage phenotype and function. We find chronic fructose consumption decreases Kupffer cell populations while increasing transitioning monocytes. In addition, fructose exposure increases gene expression of fibrotic proteins *Col1a1* and *Timp1*. scRNAseq revealed fructose increased expression of genes *Gpnmb, Mmp12, Ilrn1,* and *Rsad2* in liver tissue as well as hepatic macrophages. Fructose also

elevated expression of genes involved in fructose metabolism and the PPP, although these changes were not specific to KCs. These results were also seen *in vitro* where fructose decreased cell viability of IMKC and J774.1. Interestingly, fructose increased proliferation of IMKC but decreased proliferation of J774.1. Fructose increased gene expression of *Gpnmb, Mmp12, Ilrn1,* and *Rsad2* in M0 IMKC and pro-inflammatory gene expression of *Il6* and *Tnfα* in M1 IMKC. C13 fructose metabolic tracing revealed carbon shuttling into glycolysis and the PPP with little carbons entering the tricarboxylic acid cycle (TCA). Inhibition of the PPP using G6PDH siRNA led to increased gene expression of *Gpnmb, Mmp12* and *Ilrn,* specifically in M0 IMKC. Taken together, our results indicate the potential for fructose to decrease KC viability and increase expression of genes that regulate inflammation, fibrosis, proliferation, and polarization in KC. It is possible the decrease in KC is to allow for the influx of transitioning monocytes to replace KC. In addition, the PPP metabolism may play a suppressive role as inhibition increases fructose induced anti-inflammatory gene expression.

1.10 Figures and Figure Legends

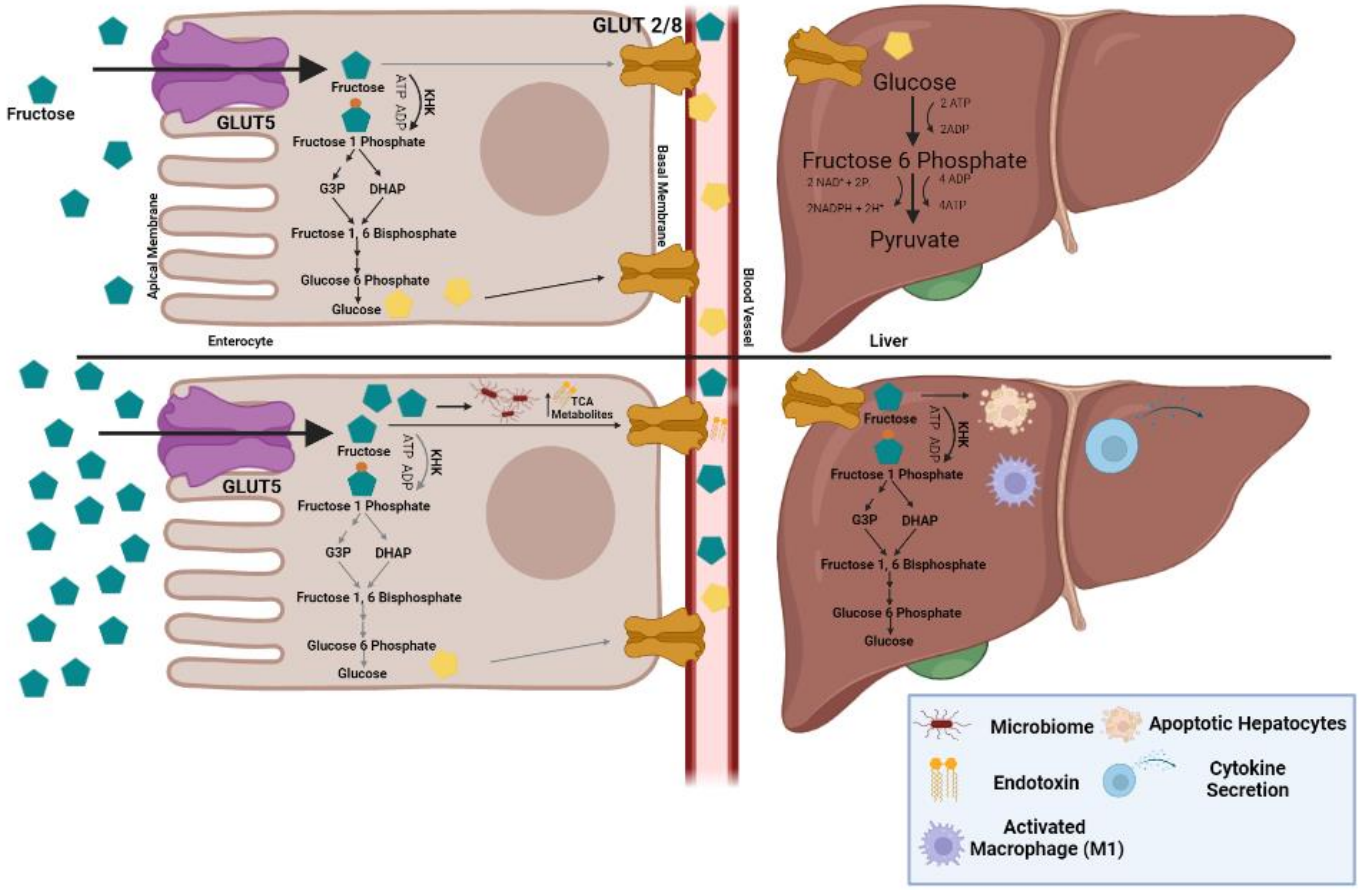

Figure 1.1: Fructose Metabolism in Low and High Concentrations. Fructose is taken up through GLUT5 transporters in enterocytes. Fructose is phosphorylated by KHK through phosphate transfer from ATP to make fructose -1- phosphate (F1P). At low concentrations of fructose, F1P continues through fructolysis converging with glycolysis through upper-level glycolytic metabolites glyceraldehyde 3 phosphate (G3P) and dihydroxyacetone phosphate (DHAP). These metabolites may combine in the process of gluconeogenesis and glucose is released through GLUT 2 or 8 into the blood stream. Glucose is then deposited into the liver via the portal vein and undergoes glycolysis for metabolic processes in the liver. In high concentrations of fructose, KHK becomes saturated and can no longer phosphorylate fructose. This leads to intestinal saturation and fructose is transported into the bloodstream through GLUT 2 or 8. Some fructose may undergo metabolism, although this is at a much lower rate than in low concentrations of fructose. Additionally, fructose induces leaky gut where endotoxins are released into the blood stream. Fructose is then deposited into the liver through the portal vein where it leads to increased immune cell activation and cell death.

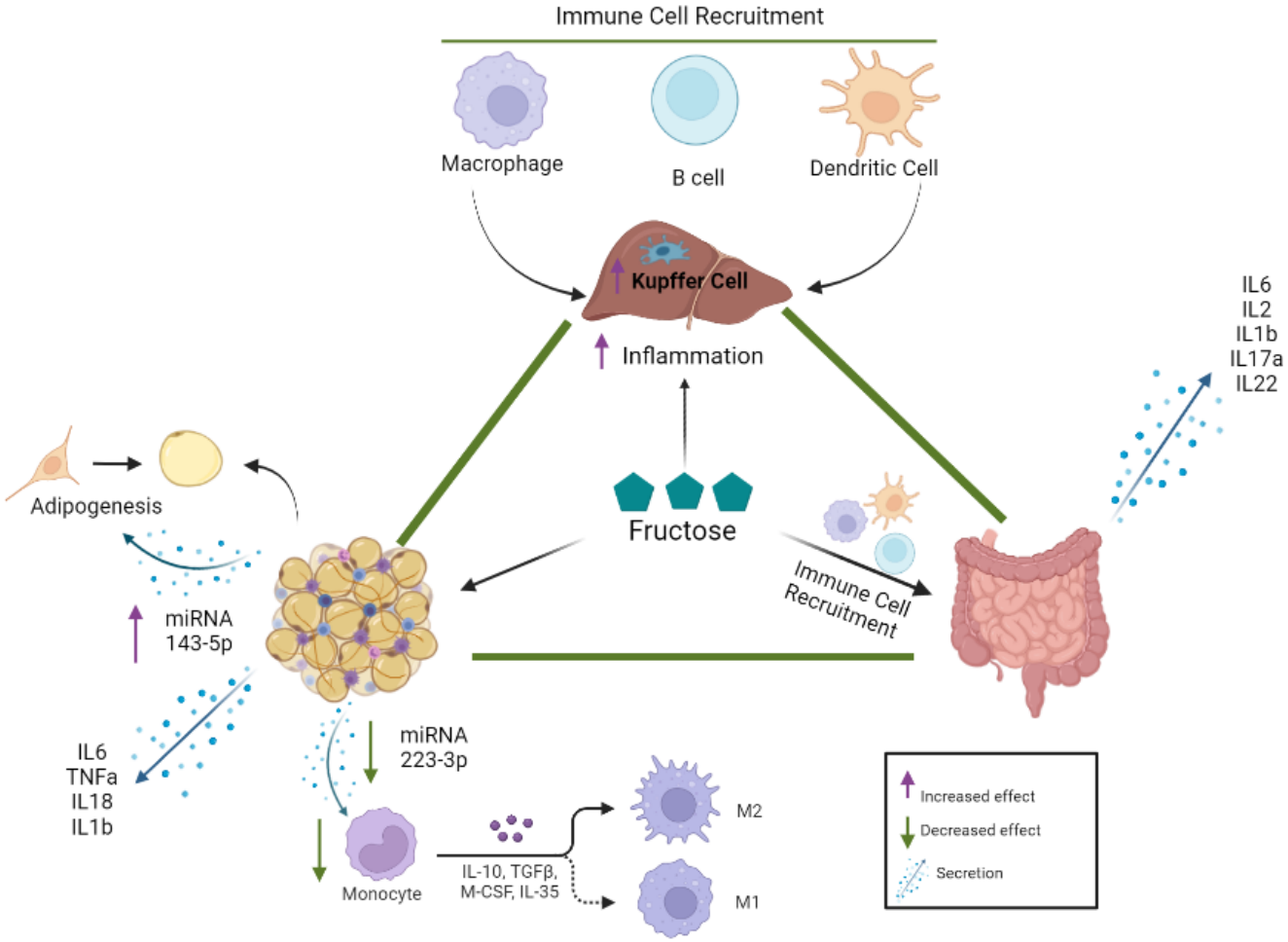

Figure 2.1: Fructose Induces Inflammation in Metabolically Active Tissues. Fructose increases immune cell recruitment and activation in the liver and the intestine. Within the intestine, fructose increases pro-inflammatory cytokine secretion. Fructose increases adipogenesis within adipose tissue as well as increases secretion of inflammatory cytokines. Fructose leads to increased macrophage differentiation due to increased miRNA cell signaling.

CHAPTER 2: Fructose Metabolism Regulates Inflammation through the Pentose Phosphate Pathway in Macrophages

2.1 Abstract

Fructose diet studies show over-consumption aids in development of Non-Alcoholic Fatty Liver Disease (NAFLD). Chronic inflammation progresses NAFLD to Non-Alcoholic Steatohepatitis as the liver becomes fibrotic and inflamed. High fructose consumption is correlated with an increase of residential macrophages, Kupffer Cells (KCs), within the liver. The increase in macrophages potentially increases inflammation as activated macrophages (M1) drive inflammation through cytokine secretion of interleukin 6 (IL6) and tumor necrosis factor α (Tnfα). Little work summarizes the direct impact of fructose on macrophage phenotype and function. We demonstrate high fructose concentrations reduce metabolic activity and viability while increasing proliferation within Immortalized KCs (IMKC). Fructose induced gene expression of inflammatory proteins *Tnfα* and *Il6* in M1 IMKC. Interestingly, fructose increased expression of fibrosis and anti-inflammatory genes *Gpnmb*, *Mmp12* and *Il1rn* in M0 macrophages. By Mass spectrometry, C13 fructose tracing detected fructose metabolites in the pentose phosphate pathway (PPP). Inhibition of the PPP using 6 Aminonicotinamide (6AN) reduced fructose induced *Tnfα* and *Gpnmb* expression within M1 of IMKC. However, 6AN further increased *Il6* expression in fructose treated M1. In addition, 6AN augmented fructose induced expression of *Il6*, *Mmp12,* and *Rsad2* in M0. Targeting the PPP enzyme glucose 6 phosphate dehydrogenase (G6PDH) using silencing RNA (siRNA) in fructose cells, increased *Gpnmb*, *Il6, Mmp12, Il1rn* and *Rsad2* in M0, confirming the involvement of the PPP. Taken together, the PPP may be protective in regulating fructose mediated inflammation in macrophages *in vitro*.

2.2 Introduction

Non-Alcoholic Fatty Liver Disease (NAFLD) is quickly becoming a global health issue [76]. Prevalence of Steatosis has reached 25% of the worldwide population with the more aggressive form of Non-Alcoholic Steatohepatitis (NASH) reaching nearly 14% [77]. As NAFLD is linked to obesity related insulin resistance, type 2 diabetes mellitus and high blood pressure with atherogenic dyslipidemia, it becomes a greater risk for cardiac stroke and potentially death [77]. Carbohydrate consumption has been linked to driving NAFLD progression. In recent years, the monosaccharide fructose has been given the title of "lipogenesis regulator" as the consumption and metabolism of

fructose increases *de novo* lipogenesis (DNL) [39]. As fructose becomes more prevalent in sweetened juices, carbonated sodas and processed foods, the average consumer may easily consume 3x the recommended daily dose of fructose. A recent study demonstrated that 80 g/day of fructose or sucrose (40g glucose/40g fructose) over 7 weeks was enough to induce fatty acid synthesis and hepatic *de novo* lipogenesis within male participants [78] . Along with induced lipogenesis, fructose has been shown to increase hepatic inflammation [38].

Because of the rising availability of fructose rich products, many researchers are investigating direct and indirect effects of fructose on parenchymal and non-parenchymal cells of the liver [79]. One target of investigation lies within the immune cell populations of the liver. Residential and recruited immune cells are needed to maintain healthy, functional livers by clearing pathogens and toxins as well as upholding the structure and function of the liver [80] [81]. Monocytes and macrophages play a large role in maintaining tissue function and phenotype as they scavenge for toxins and secrete messenger proteins (cytokines) which allow for crosstalk amongst cells in tissue [82]. Within a disease state, many macrophage populations are present, each working together or against one another, fueling the progression of NAFLD through secretion of proteins that can cause extracellular matrix (ECM) dysregulation, inflammation and immune cell recruitment and activation [83] [84]. Residential macrophages, Kupffer cells (KC) and recruited macrophages have been shown to play a massive role in the progression of NAFLD as they often display a pro-inflammatory phenotype (M1) secreting cytokines interleukin 6 (IL6), tumor necrosis factor α (Tnfα) and interleukin 1β (IL-1β) [85-87]. *In vitro* studies by Tang et. al demonstrates free fatty acid activation of KCs increases their pro-inflammatory phenotype [88]. As fructose has been shown to induced fatty acid synthesis, it is likely that fructose treatment can indirectly aid in macrophage inflammatory regulation through fatty acid activation [89] [90]. Although fructose may have indirect effects on KC activation, fructose may directly impact KC inflammation through metabolic processing.

The induction of M1 phenotype is often due to increased metabolic flux within glycolysis and the pentose phosphate pathway (PPP), which produces NADPH pools needed for cytokine production [91] [92]. Pro-inflammatory secretion studies of KC depletion within rats and mice demonstrate a protective effect on the liver as the depletion prevented steatosis, hepatic insulin resistance and hepatic inflammation/apoptosis [93] [94]. The protective effect of KC depletion may be due to

decreased inflammation through monocyte and macrophage infiltration. Although being protected from inflammation may slow down chronic inflammation, one mouse study of 20% fructose water on high fat diet for 12 weeks showed fructose treatment increased lymphocyte infiltration and triglyceride accumulation within the liver even when KCs were not activated [95]. These findings highlight the need for understanding the effects of fructose on NAFLD progression, as fructose stimulation has been shown to indirectly offer a protective/non-protective phenotype of KCs within the context of NAFLD.

In this study, we show fructose uptake within IMKC, J774.1 and RAW cells which increases their inflammatory phenotype. Fructose at a concentration of 5mM had no effect on cell metabolic activity within IMKC, but reduced activity and viability of non-activated (M0) and lipopolysaccharide activated (M1) macrophages at 25mM concentrations. The reduction in viability was not due to increased cytotoxicity or apoptosis. 5mM fructose concentrations decreased J774.1 metabolic activity and viability in both M0 and M1 conditions. Fructose increased proliferation of M0 IMKC at 5mM, but induced proliferation of M0 and M1 IMKC at 25mM. However, 5mM fructose decreased proliferation of M0 and M1 J774.1. Inflammatory marker *Il6* was significantly upregulated in fructose conditions within IMKC and had no effect in RAW cells while decreasing *Il6* in J774.1. Fructose reduced *ll-1b* and increased *Tnfα* within all macrophages at 5mM and 25mM concentrations. Similar across all macrophages, fructose induced transmembrane glycoprotein NMB (*Gpnmb*) which has been linked to an anti-inflammatory phenotype. Additionally, *Mmp12*, *Il1rn*, and *Rsad2*, which are involved in fibrosis, polarization and proliferation, were also upregulated in M0 and M1 IMKC. Surprisingly, fructose carbon partitioning through the pentose phosphate pathway (PPP) was observed in all macrophage lines. Inhibition of the PPP through 6 Aminonicotinamide (6AN) and glucose 6 phosphate dehydrogenase (G6PDH) knockdown led to elevated *Gpnmb*, *Il6* and *Rsad2* expression within M0 IMKC. Taken together, these results indicate a suppressive role of the PPP in fructose mediated inflammation.

2.3 Materials and Methods

Cell Culture

Immortalized Kupffer Cells (IMKC), J774A.1 and RAW macrophages were used. IMKC and RAW cells were cultured in RPMI (VWR 1640) with 10% fetal bovine serum (FBS), 5% L-Glutamine, 1% Penicillin/Streptomycin. All cells were cultured for 24 hours at 37°C with 5% CO2 in the atmosphere before treatment and seeding at 4 x 10^5 cells/ml. For all J774.1 experiments, cells were cultured in Dulbecco's modified Eagle's medium (Corning 97060-876) supplemented with 10% fetal bovine serum (FBS), 5% L-Glutamine, 1% Penicillin/Streptomycin and 25mM glucose (Culturing DMEM). J774.1 cells were treated with 200 nM/mL PMA (VWR 102515-692) for macrophage differentiation. IMKCs were treated with 5mM glucose or fructose in the absence or presence of 0.1ug/ml LPS (Fisher Scientific 50-112-2025). J774.1 and RAW cells were treated with 5mM glucose or fructose in the absence or presence of 1ng/ml LPS. Cells were harvested 24 hours after treatment for protein, RNA or media collection. Protein was harvested by washing once with 1X PBS and adding RIPA buffer (150mM Sodium Chloride, 1% Triton X, 0.5% Sodium Deoxycholate, 0.1% SDS, 50mM Tris, and 1mM EDTA) with protease inhibitor cocktail 1:100 (HALT). Plates were harvested for RNA by Tri-reagent (Fisher Scientific). Media was collected and stored at -80°C.

BrdU Assay

IMKC and J774.1 were plated in 96 well plates with a seeding density of 2.5 x 10^4 in culturing media. J774.1 cells were treated with 200nM PMA for 24 hours. Cells were treated with glucose or fructose (5mM J774.1 and 25mM IMKC/J774.1) treatment 24 hours. BrdU reagent was added at time of treatment using the BrdU Assay Kit (#6813 Cell signaling technology) and absorbance measured at 450 nm on plate reader.

MTT Assay

IMKC and J774.1 were plated in 96 well plates with a seeding density of 2.5 x 10^4 in culturing media and adhered overnight. Culturing media was removed and replaced with fresh, no phenol red media (RPMI 1640) with MTT labeling reagent at 1.2mM. Cells were incubated at 37°C for 2

hours before removing media and adding 50µl DMSO to dissolve MTT. Cells were then incubated at 37°C for 10 minutes and absorbance measured at 450 nm on plate reader.

Western Blotting

Protein samples were thawed and spun at 15,000 RPM at 4°C to pellet. Supernatant was used for BCA protein assay kit (Thermo Scientific) to quantify concentration of protein. Samples were prepared using 2X Laemmli Sample Buffer (Bio-rad) in a 1:1 ratio of protein to loading buffer solution. Samples were run on 4-15% 12 well SDS page gel following Bio-Rad protocol. The gel was transferred for 1 hour and blocked using one-block blocking buffer (Genesee Scientific) for 1 hour. Phospho c-Jun, c-Jun, CHOP, G6PDH, Ketohexokinase and Hexokinase 1/2 and βactin antibodies were purchased from cell signaling. Ki67 was purchased from Abcam. All antibodies were used at 1:1000 dilutions except βactin at 1:3000 dilution. Primary antibodies were incubated for 1 hour at room temperature or overnight at 8°C shaking. The membrane was washed 3X with PBS-1% tween-20 for 5 minutes, then incubated with secondary antibody. Goat anti-mouse and Goat anti- rabbit were bought from Fisher Scientific and used at a 1:20,000 dilution. The secondary was removed, and the membrane was washed 3X with PBS-1% tween-20 for 5 minutes. Membrane bands were analyzed by Li-COR Odyssey and quantified by Image Lite Version 5.2 software.

Gene Expression

Samples were isolated for RNA according to manufacturer's protocol using Direct-zol™ RNA MicroPrep kit (Genesee Scientific). RNA concentration was obtained by nanodrop, and cDNA was made using qscript cDNA supermix following instructions of manufacturer (Quantabio). cDNA was synthesized at 1000 ng using BioRAD iQ5 thermocycler. Cycles were: Priming for 5 minutes at 25°C, RT: 30 minutes at 42°C and RT inactivation for 5 minutes at 85°C. cDNA was used to analyze gene expression by real time polymerase chain reaction (RT q-PCR) using PerfeCta qPCR FastMixII (QUantbio). TaqMan assays used were Timp 1, Col1a1, Mmp9, Il6, Tnfα, Il1b, Gpnmb, Mmp12, Il1rn, Rsad2, Il18-bp and 18S eukaryotic endogenous control (Thermo Fisher Scientific). Samples were normalized to 18SE.

G6PDH Inhibition Studies

IMKC and J774.1 cells were plated in culturing media at 4 x 10^5/ml in 24 well plates and adhered overnight. Cells were treated as described above with or without the Glucose 6 Phosphate Dehydrogenase (G6PDH) inhibitor 6 Aminonicotinamide (Milipore Sigma CAS: 329-89-5) at 100µM for 24 hours (IMKC) or Dehydroepiandrosterone (J774.1) (DHEA- EMD Millipore 252805) at various concentrations for 24 hours. G6PDH knock down was established using Invitrogen™ Lipofectamine™ RNAiMAX Transfection Reagent (Fisher Scientific-13-778-030) and Silencer® Select Pre-Designed & Validated siRN AID s66340 (Thermo Scientific-4390771). SiRNA studies were optimized to 25pmol of SiRNA for 48 hours. SiRNA studies were performed similarly with cells plated at 2 x 10^5/ml in 24 well plates with culturing media. The next day media was changed to fresh culture media, or fresh culture media with 25 pmol siRNA supplied. 24 hours later media was changed again to fresh culturing media as a control, 25mM glucose or fructose (IMKC), 5mM Glucose or fructose (J774.1), M0/M1 treatment with/without additional 25pmol of G6PDH siRNA. After 24 hours of treatment samples were collected for RNA and protein.

ELISA

Kit was purchased from Invitrogen (Thermo Fisher BMS6032) and protocol was followed per kit recommendations. Media was spun at 500xg for 10 min to pellet cell debris before being added to wells.

Apoptosis Assay

IMKC and J77.1 cells were plated at 2 x 10^4 in a 96 black walled plate. Treatment was supplied 24 hours later as previously discussed. Cells were tested for viability, cytotoxicity and apoptotic activity following manufacturers protocol. ApoTox-Glo Triplex Assay (G6320 Promega).

Sample preparation for LC-MS analysis

IMKC, RAW and J774.1 cells were seeded at 5 x 10^6 /mL in 6 well plates in culturing media. Cells adhered and 24 hours later media was changed to C13 labeled 5mM glucose or C13 labeled 5 mM fructose. After 24 hours, cells were washed with ice cold saline (0.9% NaCl, 1ml, twice) and immediately placed on dry ice. Extraction solution composed of methanol/water (4:1, v/v) was

added to each well and cells were scraped, vortexed vigorously and spun down at 20,000 xg for 10 mins at 4°C. Supernatant containing polar metabolites were dried in vacuum concentrator. Dry pellets and cell media were kept frozen at -80°C until ready for LC-MS analysis.

LC-MS analysis

Metabolite analysis was performed using Ultimate 3000 UHPLC (Dionex) coupled with Q Exactive Plus mass spectrometer (Thermo Fisher Scientific) and Vanquish UHPLC (Thermo Fisher Scientific) coupled with and Orbitrap Exploris 480 mass spectrometer (Thermo Fisher Scientific), as described previously [24]. A hydrophilic interaction chromatography method (HILIC) with an Xbridge amide column (100 x 2.1 mm i.d., 3.5 µm; Waters) was used for metabolite separation at 25 °C. Mobile phase A: water with 5 mM ammonium acetate (pH 6.8), and mobile phase B: 100% acetonitrile. Linear gradient is: 0 min, 85% B; 1.5 min, 85% B; 5.5 min, 35% B; 6.9 min, 35% B; 10.5 min, 35% B; 10.6 min, 10% B; 12.5 min, 10% B; 13.5 min, 85% B; 17.9 min, 85% B; 18 min, 85% B; 20 min, 85% B. Due to the instrumentation difference between Ultimate 3000 UHPLC and Vanquish UHPLC, different flow rates were used. For Ultimate 3000 UHPLC, the flow rate is: 0-5.5 min, 0.15 ml/min; 6.9-10.5 min, 0.17 ml/min; 10.6-17.9 min, 0.3 ml/min; 18-20 min, 0.15 ml/min. For Vanquish UHPLC, the flow rate is: 0-5.5 min, 0.11 ml/min; 6.9-10.5 min, 0.13 ml/min; 10.6-17.9 min, 0.25 ml/min; 18-20 min, 0.11 ml/min. Both mass spectrometers were equipped with a HESI probe and operated in the positive/negative switching mode. When Q Exactive Plus mass spectrometer was used, the relevant parameters are as listed: heater temperature, 120 °C; sheath gas, 30; auxiliary gas, 10; sweep gas, 3; spray voltage, 3.6 kV for positive mode and 2.5 kV for negative mode; capillary temperature, 320°C; S-lens, 55. The resolution was set at 70,000 (at *m/z* 200). Maximum injection time (max IT) was set at 200 ms and automatic gain control (AGC) was set at 3×10^6. When Exploris 480 mass spectrometer was used, the relevant parameters are as listed: vaporizer temperature, 350 °C; ion transfer tube temperature, 300 °C; sheath gas, 35; auxiliary gas, 7; sweep gas, 1; spray voltage, 3.5 kV for positive mode and 2.5 kV for negative mode; RF-lens (%), 30. The resolution was set at 60,000 (at *m/z* 200). Automatic maximum injection time (max IT) and automatic gain control (AGC) were used.

Samples were reconstituted into sample solvent (40 µl water:ACN:MeOH (2:1:1, v/v/v)and 3 µl was injected to LC-MS for polar metabolite analysis. Metabolite identification was based on exact mass to charge ratio (less than 5 ppm) and retention time, which was determined using in house library. Unresolved metabolites were combined into one feature to reflect the possibility of co-eluted isomers. Integrated peak area of each metabolite was used to calculate the relative changes of metabolites in different samples. Integrated peak area of each metabolite or each isotopologue was used to calculate the ^{13}C enrichment without natural abundance correction.

Nuclear Magnetic Resonance Spectroscopy Analysis

Media was thawed and spun in 3 kDa AMICON filters at 13,000 rpm for 1 hour at 4°C. ^{1}H NMR spectra was acquired using Bruker 700 MHz NEO Spectrometer with TCI cryoprobe instrumentation with pulse program noesypr1d. Sodium trimethylsilylpropanesulfonate (D6-DSS) standard in D_2O was added at a 1:10 dilution to media and D_2O, giving a final solution with 29% D_2O and a DSS concentration of 448 µM. Samples were run at 25°C with 128 scans of 65572 datapoints, a mixing time of 100 ms, a relaxation delay of 1 s, and a spectral width of 11.7 ppm. Data were processed and analyzed in Chenomx according to standard protocols. Briefly, the residual water was removed, phase correction and baseline correction were applied (Chenomx Spline), the chemical shift indicator (CSI) was calibrated, a shim adjustment was performed, and the CSI was calibrated. Data was analyzed using Graph Pad.

Statistical Analysis

GraphPad Prism 9.3.1 software was used for all statistical analyses. Two-tailed unpaired Student's t-tests were performed for two group comparisons. Two-way ANOVA was performed for genotype versus diet studies followed by multiple T test comparisons. All data is presented as the mean ± SEM. Data was considered statistically significant for $P<0.05$ (*), $P<0.01$ (**), $P<0.001$(***), and $P<0.0001$(****).

Fructose Assay

J774.1 media was collected from experiments with M0/M1 cells treated with 5mM fructose. Media was spun down to remove cellular debris. Samples were diluted 1:40 with assay buffer. Followed protocol instructions of fructose colorimetric assay (K619-100 BioVision).

2.4 Results

2.4.1 Fructose Consumption Induces Proliferation of IMKC While Reducing Metabolic Activity and Cell Viability

To determine the effect of fructose metabolism on macrophage function, intracellular fructose was analyzed via nuclear magnetic resonance (NMR) and liquid chromatography mass spectrometry (MS). M0 and M1 macrophages were treated with 5mM and 25mM C13 labelled fructose for 24-hours before media was collected and analyzed for presence of fructose compared to unspent media. In J774.1 cells, fructose concentration within media was significantly reduced at 16 and 24 hours (Fig 1A). This response was further suggested when analyzing fructose concentration in media using a fructose assay. Samples showed a decrease in fructose in the media after 24-hours of cell exposure compared to control which was stock media (Fig 1B). To validate the reduction of fructose in the media was due to cellular uptake, intracellular fructose levels were measured by LC-MS in IMKC and J774.1. As expected, C13 labeled fructose peaks were observed after 24-hours of treatment in both 5 and 25mM concentrations in IMKC (Fig 1C-D). Fructose uptake was observed in J774.1 and RAW cells as well (Fig 1E-F respectively). To identify enzymes responsible for fructose metabolism, we measured protein expression of hexokinase 1 and 2 (HK1/HK2) which phosphorylates fructose. HK1 expression did not differ between glucose and fructose treatment, however there was a significant decrease in HK1 expression in M1 polarized IMKC (Fig 2A). HK2 expression was not observed in IMKC samples. In J774.1 cells, expression of HK1 was unchanged between all treatment groups, however, fructose significantly upregulated HK2 expression in M1 compared to glucose (Fig 2B-C respectively). Within the liver, fructose is phosphorylated by ketohexokinase (KHK), however we did not detect protein expression of KHK in IMKC or J774.1 cells.

To examine the effect of fructose uptake on macrophage metabolic activity, we performed an NADPH dependent MTT assay. 5mM fructose had no effect on IMKC metabolic activity, however, 25mM concentration decreased activity in both M0 and M1 IMKC (Fig 3A-B respectively). Fructose reduced metabolic activity in M0 and M1 J774.1 cells at 5mM, but 25mM fructose had no effect on activity (Fig 3C-D respectively). To determine if the reductions in metabolic activity were associated with cell death, we measured cell viability, cytotoxicity, and apoptosis in macrophages. Cell viability was decreased in 25mM fructose treated IMKC with no effect on

cytotoxicity and apoptosis in both M0 and M1 (Fig 3E,G and Fig 4A). Similar to IMKC, fructose decreased viability in M0 and M1 J774.1 cells (Fig 3F). Unique to J774.1, fructose increased cytotoxicity and apoptosis (Fig 3H and Fig 4B). To gain insight into fructose induced apoptosis in J774.1 cells, we analyzed apoptosis protein marker C/EBP Homologous Protein (CHOP) as it is often upregulated in cells undergoing endoplasmic reticulum stress [96]. Fructose reduced CHOP protein expression compared to glucose treated J774.1 cells (Fig 4C). Taken together, these data indicate 5mM fructose reduces proliferation and cell metabolic activity most likely due to increased cytotoxic and apoptotic mechanisms within J774.1 cells. However, 25mM fructose reduced viability and metabolic activity within IMKC without inducing cytotoxicity or apoptosis.

As glucose is known to facilitate macrophage proliferation, we sought to determine the impact of fructose on macrophage proliferation [97]. 5mM fructose increased proliferation in M0 cells but had no effect on proliferation of M1 IMKCs (Fig 4D). Interestingly, 5mM fructose decreased J774.1 proliferation in M0 and M1 (Fig 4F). 25mM fructose significantly upregulated proliferation of both M0 and M1 in IMKC (Fig 4E) while decreasing proliferation in M0 J774.1 cells (Fig 4G). To determine if the reduction in proliferation of J774.1 cells was due to decreased cell cycle progression, we measured protein expression of Ki67 as it is upregulated during active phases of the cell cycle [98]. Fructose had no effect on Ki67 expression compared to glucose in J774.1 suggesting a mechanism apart from cell cycle arrest in regulating proliferation (Fig 5A). Proliferation of macrophages can be regulated at the transcriptional level. Transcription factor c-Jun-N-Terminal Kinase (JNK) phosphorylates the transcription factor, c-Jun, often associated with proliferation regulator Activator Protein 1 (AP-1) [99] [100]. Fructose significantly decreased protein expression of total c-Jun protein as well as phosphorylated c-Jun in M0 phenotype within J774.1 cells (Fig 5B-C), suggesting c-Jun may be a potential mechanism for fructose mediated reduction of proliferation. Taken together, fructose reduces cell viability in both IMKC and J774.1. However, fructose increased proliferation in IMKC in contrast to decreased proliferation in J774.1.

2.4.2 Fructose Metabolism Induces Macrophage Inflammatory Gene Expression.

We sought to investigate how fructose affects the ability of macrophages to regulate pro- and anti-inflammatory cytokine gene expression. Fructose and LPS exposure significantly increased gene expression of pro-inflammatory cytokines *Il6* within IMKC at both 5mM and 25mM concentration (Fig 6A,E). When measuring secretion of IL6 via ELISA, 25mM fructose with LPS followed the

same pattern (Fig 6F). Interestingly, 5 mM M1 fructose significantly decreased *Il6* in J774.1 compared to glucose, however, there was no difference in *Il6* expression in RAW cells (Fig 7A, H respectively). Similar to gene expression, IL6 protein secretion was decreased in fructose treated M1 J774.1 (Fig 7B). Inflammatory cytokine *Tnfα* was elevated with 25mM fructose in M0 and M1 IMKC (Fig 6G). Of interest, 5mM fructose induced expression of *Tnfα* in both J774.1 and RAW cells although this was only detected during LPS stimulation (Fig 7C,I). Inflammatory cytokine *Il-1b* was decreased in all cell lines with fructose and LPS stimulant.

In addition to analyzing inflammatory cytokines, we also determined if fructose effects regulation of genes associated with inflammation, proliferation, and fibrosis. Fructose significantly upregulated gene expression of *Gpnmb* when compared to glucose in M0 and M1, 5 and 25mM treated IMKC and 5mM treated J774.1 cells (Fig 6D,I and Fig 7E respectfully). *Gpnmb* was upregulated in RAW cells, although only with LPS supplementation (Fig 7K). Gpnmb has recently become a protein of interest within inflammatory diseases as expression has been shown to regulate inflammation, lipid, and fibrosis accumulation [101]. 25mM Fructose caused IMKC to significantly upregulate gene expression of *Mmp12* and *Il1rn* compared to glucose in both M0 and M1 conditions (Fig 6J-K). *Rsad2* gene expression was also upregulated in IMKC when exposed to fructose, although this response was only detected in M1 (Fig 6L).

As macrophages are known to secrete proteins involved in fibrosis regulation, we analyzed *Mmp9* and *Timp1* gene expression in J774.1 and RAW cells. Fructose reduced expression of *Mmp9* in M0 J774.1 but there was no effect in RAW cells (Fig 7F,L). Interestingly, LPS treatment decreased *Mmp9* expression regardless of treatment in J774.1, however the opposite effect was seen in RAW cells (Fig 7F,L). The regulation of *Mmp9* may be more sensitive to LPS signaling than carbohydrate exposure. During extracellular matrix repair (ECM) Timp1 binds to Mmp9 and inhibits degradation of collagen matrix. Fructose significantly upregulated *Timp1* expression in both M0 and M1 J774.1 cells (Fig 7G). Taken together, these results indicate fructose stimulates macrophage inflammatory and fibrosis associated genes at both low (5mM) and high (25mM) concentrations in macrophage cell lines.

2.4.3 C13 Fructose Labeling Reveals Fructose Carbon Shuttling Patterns.

To determine the mechanism for fructose metabolism, IMKC, J774.1 and RAW cells were treated with C13 labeled fructose for 24 hours. Jones et al. recently showed 11.1 mM fructose treated monocytes had increased carbon shuttling through glycolysis and the TCA cycle. In comparison, we found glycolysis intermediates 2/3- phosphoglycerate, pyruvate, dihydroxyacetone phosphate, and fructose 1,6 bisphosphate fructose carbons utilized by the glycolysis pathway in 5mM and 25mM IMKC, J774.1 and RAW cells respectively (Fig 8A-B, Fig 9A-C and Fig 10A-B, I). In contrast, TCA intermediates were not detected under fructose conditions in any macrophage cell lines (Fig 8E-F, Fig 9F-G, Fig 10E-F, L-M). Intracellular pyruvate and lactate levels were low but were found to be present in all cells. (Fig 8C-D, Fig 9D-E, Fig 10C-D, J-K). Similarly, fructose treatment reduced lactate secretion when compared to glucose in J774.1 cells (Fig 10P). However, C13 labeled fructose carbons were detected in the PPP intermediates, specifically ribose 5-phosphate, erythrose 4- phosphate and Sedoheptulose 7- phosphate in all cell lines (Fig 8G-H, Fig 9H-I and Fig 10G-H, N-O). These findings suggest fructose metabolism within macrophages involves glycolysis and the PPP with limited shuttling into the TCA cycle.

2.4.4 Pentose Phosphate Pathway May Regulate Fructose Mediated Inflammatory Gene Expression

As PPP intermediates were found in fructose treated IMKC and J774.1 cells expressing fructose induced inflammatory genes, we used inhibitor-based studies to determine if this pathway is involved in regulating the inflammatory response. We targeted glucose-6-phosphate dehydrogenase (G6PDH) activity, the rate limiting enzyme in the PPP, using 6AN and the noncompetitive inhibitor DHEA. 6AN attenuated fructose-induced increase of *Gpnmb* and *Il6* gene expression while having no effect on *Tnfα* in M1 IMKC (Fig 11A-C). Interestingly, 6AN and fructose augmented *Gpnmb* and *Il6* gene expression in M0 IMKC (Fig 11A-B). DHEA increased fructose induced expression of *Il6* in M0/M1 J774.1 (Fig 12A). Unlike IMKC, DHEA decreased *Tnfα* expression in M1 polarized J774.1 (Fig 12B). *Mmp12* was induced further with 6AN treatment in fructose treated M1 IMKC (Fig11 D). However, the opposite effect was observed in genes *Il1rn* and *Rsad2* (Fig 11E-F). In addition, fructose and 6AN increased expression of Rsad2 in M0 IMKC (Fig 11F). In J774.1 cells, DHEA decreased fructose induced expression of *Timp1* in

M1 groups (Fig 12D). Inhibition of the PPP further decreased proliferation when compared to fructose treatment alone in J774.1 (Fig 12E).

To specifically investigate the involvement of the PPP in the regulation of inflammatory gene expression, G6PDH silencing RNA (SiRNA) was used to reduce carbon shuttling through the PPP. Knockdown of G6PDH in fructose treated J774.1 and IMKC was confirmed by protein expression in M0 and M1macrophages (Fig 13A, B-C respectively). Knockdown of G6PDH led to increased expression of *Gpnmb* and *Il6* in fructose treated M0 IMKC (Fig 14A-B). In addition, G6PDH knockdown increased *Il6* expression in J774.1 cells although this was seen in M0 and M1 (Fig 12F). Not only was this seen in gene expression, but secretion of IL6 was also elevated in M1 G6PDH knockdown J774.1 cells (Fig 12G). Additionally, *Mmp12*, *Il1rn* and *Rsad2* were significantly increased in IMKCs in M0, although *Rsad2* expression also increased in M1 (Fig 14C-E). Taken together, these data indicate fructose carbon partitioning through the PPP is protective of inflammation, as inhibition increases inflammatory gene expression.

2.5 Discussion

Fructose metabolism within the non-parenchymal fraction of the liver, specifically within residential and recruited macrophages, is poorly studied. Recent studies have highlighted the importance of studying fructose metabolism within the liver, as large amounts of fructose bypass intestinal metabolism and are deposited in the liver [8]. Although much work has been done to study the effects of fructose in parenchymal cells, hepatocytes, there is little knowledge of how fructose directly affects the phenotype and function of macrophages within this environment. Here we show fructose metabolism in a new light by using IMKC, J774.1 and RAW macrophages to study phenotype and function within fructose conditions. We demonstrate that macrophages utilize fructose as a cellular regulator of inflammation uniquely between macrophages through metabolic partitioning within the PPP.

Fructose reduced cell metabolic activity and viability in both IMKC and J774.1 macrophages. Although cytotoxicity and apoptosis mechanisms were not affected by fructose in IMKC, both were increased in fructose treatments in J774.1 cells. Interestingly, the decrease in cell viability correlated with an increase in proliferation in IMKC. Recently Mmp12 has been linked to increases in cellular proliferation [102]. As IMKC highly expressed *Mmp12* in fructose treated cells, it is

possible *Mmp12* plays a role in proliferation and not only anti-inflammatory regulation in these cells. To determine the mechanism for reduced proliferation in J774.1 cells we analyzed AP-1 factor protein c-Jun as it has been shown to be a key proliferative factor in liver regeneration [103]. Correlating with reduction in protein, the phosphorylation and thus activation of c-Jun was also decreased in fructose conditions. As Ki67 proliferation protein levels did not change between groups, this may suggest a mechanism for reduced proliferation, although more studies would be necessary to conclude this.

C13 fructose MS tracing revealed novel insights into fructose metabolism in macrophages. Glucose transporters GLUT2, 5, or 8 are known to transport fructose within the liver. However only transporters GLUT 1 and 3 have currently been identified within macrophages. A recent paper indicated the presence of GLUT5 within bone marrow derived macrophages, although this mechanism may differ between macrophage subsets. Liang, R.J. et al reported multiple cancer cell lines are unable to utilize fructose which often leads to decreased proliferation and cell death [104]. However, overexpression of GLUT5 within cells recovered their ability to proliferate and survive in fructose conditions, indicating a potential for energy source plasticity and a regulatory role of GLUT transporters over HKs. Fructose is phosphorylated by ketohexokinase which is found in carbohydrate sensing organs like liver, kidney and pancreas. We analyzed ketohexokinase levels within IMKC treated with glucose or fructose and found no data to support the presence of KHK within these cells. Literature shows the presence of HK1 within macrophages which phosphorylates glucose and fructose [105]. Although glucose is the preferred substrate of HK1, concentrations of 5mM or more of fructose increases the rate of reaction to be equal of glucose [19] . HK not only contributes to fructose metabolism but is essential for NLRP3 inflammasome activation through increasing glycolytic flux [106] . Knockdown of HK decreased inflammatory protein IL-1β. Interestingly, our studies show HK1 to be present in IMKCs but downregulated in LPS conditions. In all macrophage cell lines, LPS stimulation with fructose treatment decreased *Il-1b* gene expression which may be caused by the decreased HK1 expression in LPS groups.

We analyzed gene expression of proteins involved in inflammation and fibrosis as reduced metabolic activity and cell death can lead to an induction of inflammation [107]. To our knowledge, this is the first report of fructose induced *Gpnmb* expression within macrophages. Recent studies have found Gpnmb to be protective in the context of NAFLD as its overexpression reduced fat

accumulation and fibrosis within the liver [108]. Although fructose significantly increased *Il6* expression with LPS stimulated in IMKC, the same conditions significantly decreased expression in J774.1 cells. Pro-inflammatory cytokine *Tnfα* gene expression was increased in all cell lines with fructose and LPS treatment. Inflammatory cytokine *Il-1b* gene expression was decreased across all macrophage cell lines when treated with fructose. Timp-1 is known to increase fibrosis within liver tissue [109]. In addition, Timp1 has recently been named as an apoptotic regulator, as increased Timp1 expression led to decreased apoptosis within breast cancer epithelial cells [110]. In J774.1 cells fructose itself, as well as with LPS, increased *Timp1* gene expression. It is possible that elevation of *Gpnmb* may be a protective cellular response to fibrotic *Timp1* rising levels within macrophages. However, elevated *Timp1* levels may regulate cell survival within alternative carbon treated J774.1 cells.

We utilized metabolic C13 MS tracing to determine a mechanism for fructose mediated changes in gene expression. Fructose metabolism utilizes fructose 1 phosphate which links fructolysis with glycolysis [111]. Given the connection between glycolysis and the TCA cycle it is interesting that glycolytic intermediates were seen in all cell lines, where TCA cycle intermediates were very low. Recently, Jones et. Al reported human peripheral blood monocytes treated with 11.1 mM C13 fructose induced fructose carbon flux through the TCA cycle [63]. This cycling was accompanied by increased secretion of inflammatory proteins. LPS stimulation of macrophages has been shown to upregulate glycolysis and the PPP to supply energy and intermediates for increased inflammatory cytokine production [112]. Our results indicate a preference of fructose carbon shuttling through the PPP. The differences between metabolic partitioning maybe be due to differences in cell type as well as fructose concentration. Inhibition of the PPP using 6AN has been shown to decrease LPS induced high fat diet macrophage inflammatory cytokine expression [113]. Similar to this study, our results indicate a decrease in expression of *Gpnmb*, *Il6* and *Il1rn* in fructose treated M1 IMKCs treated with 6AN. Unique to our study, fructose stimulated expression of *Mmp12* and *Il1rn*. The upregulation of gene expression was even further pronounced in G6PDH knockdown cells treated with fructose, especially in *Mmp12*, *Il1rn* and *Rsad2*. Taken together these data indicate a potential suppressive role of the PPP under fructose conditions, as knockdown of the pathway increases the anti-inflammatory and profibrotic response in IMKC.

In conclusion, fructose metabolism within macrophage cell lines is unique from glucose as cells rely on carbon shuttling through the PPP for energy. KCs are more likely equipped to handle alternate carbohydrate sources as they must adapt quickly to respond to surrounding stimuli. In cases of high concentrations of fructose IMKC have decreased viability at the same time as increasing proliferation, indicating the potential for residential macrophages to be influenced by surrounding carbohydrate levels. Macrophages responded to fructose through metabolic partitioning induced regulation of inflammatory gene expression. Inhibition of the PPP led to increased expression of anti-inflammatory and fibrosis genes indicating the PPP plays a protective role in cellular inflammation.

2.6 Figures and Figure Legends

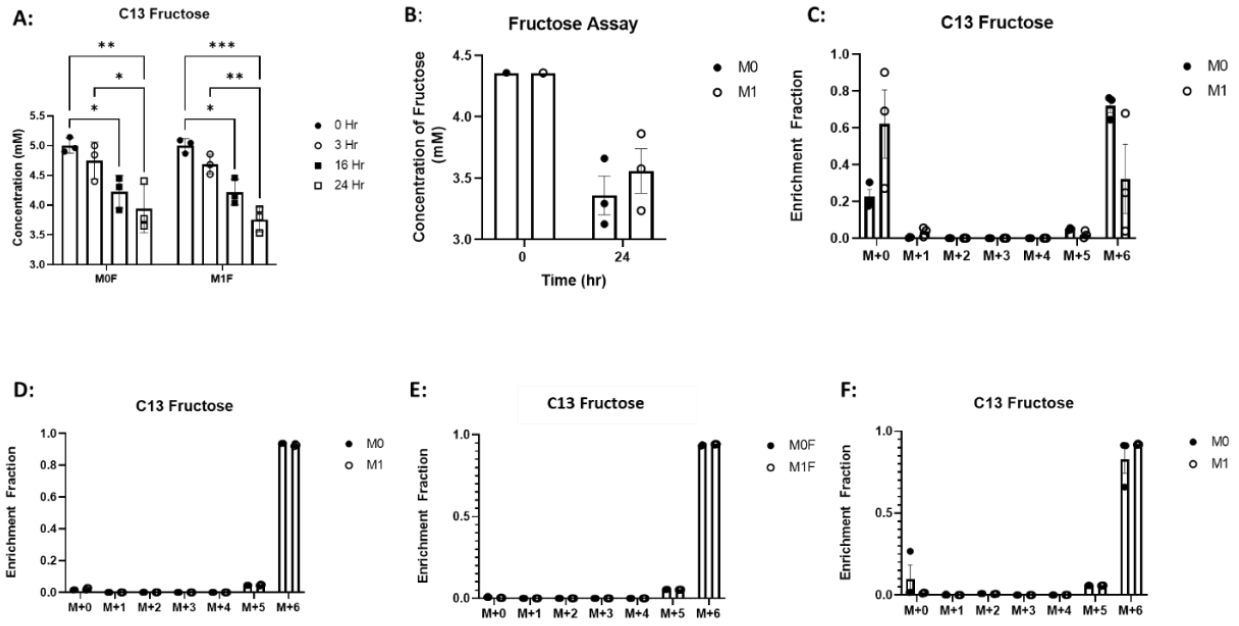

Figure 1: Fructose uptake in Macrophages. IMKC, RAW and J774.1 macrophages were plated in 25mM glucose 24 hours before media was switched to 5mM or 25mM fructose with or without LPS. **A:** J774.1 cells treated with 10ng/ml LPS media collection over 24 hours for NMR C13 tracing. **B:** J774.1 fructose assay comparing 5mM fructose at time of treatment versus 24 hours later. C13 fructose MS tracing of 5mM IMKC with 0.1ug/ml LPS **(C)**, 25mM **(D**), with 10ng/ml LPS J774.1 **(E)** and RAW **(D)** at 5mM. Data are representative of 2 independent experiments and shown as means ± SEMs (n=3). * $p<0.05$, ** $p<0.01$, *** $p<0.001$, **** $p<0.0001$.

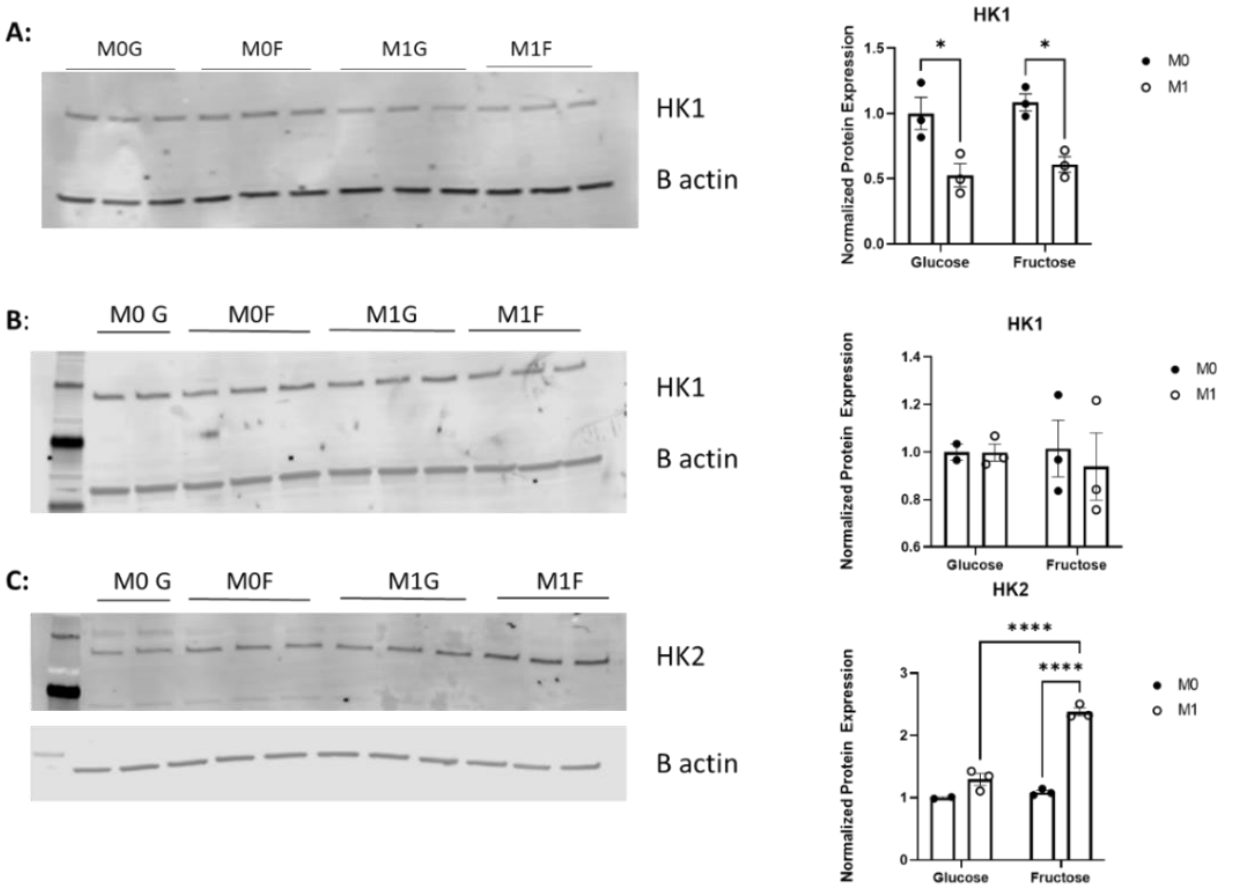

Figure 2: Fructose Uptake Mediated by HK. IMKC and J774.1 were plated in 25mM glucose 24 hours before media was switched to 25mM fructose with or without 0.1ug/ml LPS (IMKC) or 5mM with or without 10ng/ml LPS (J774.1). 24 hours later cells were harvested for protein. Western analysis of HK1, HK2 and B actin. **A:** IMKC. **B-C:** J774.1. Data are representative of 2 independent experiments and shown as means ± SEMs. * $p<0.05$, ** $p<0.01$, *** $p<0.001$, **** $p<0.0001$.

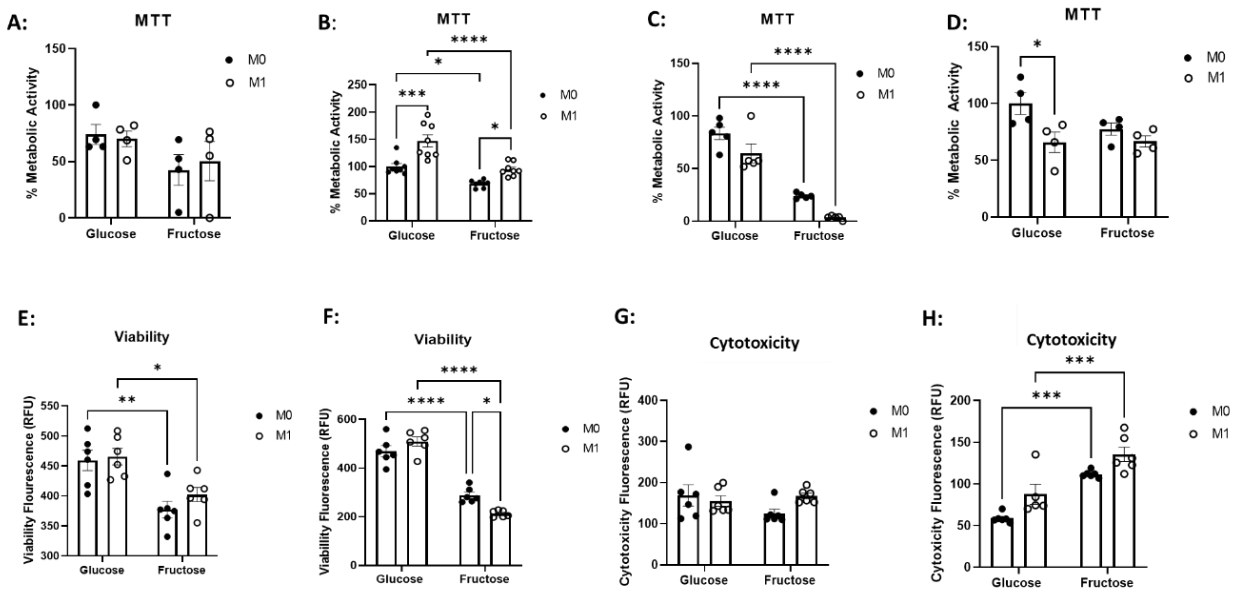

Figure 3: Fructose Decreases Cell Viability in IMKC and J774.1. Cell viability was measured by MTT labeling of cells for 2 hours before addition of dissolving agent DMSO. **A:** IMKC 5mM (n=4), **B:** IMKC 25mM (n=8), **C:** J774.1 5mM (n=5) and **D:** 25mM J774.1 (N=4). The viability assay was measured at 400/505 nm. **E:** IMKC (n=6), **F:** J774.1 (n=6). Cytotoxicity measured at 485/520 nm. **G:** IMKC (n=6), **H:** J774.1 (n=6). Data are representative of 3-2 independent experiments and shown as means ± SEMs. * $p<0.05$, ** $p<0.01$, *** $p<0.001$, **** $p<0.0001$.

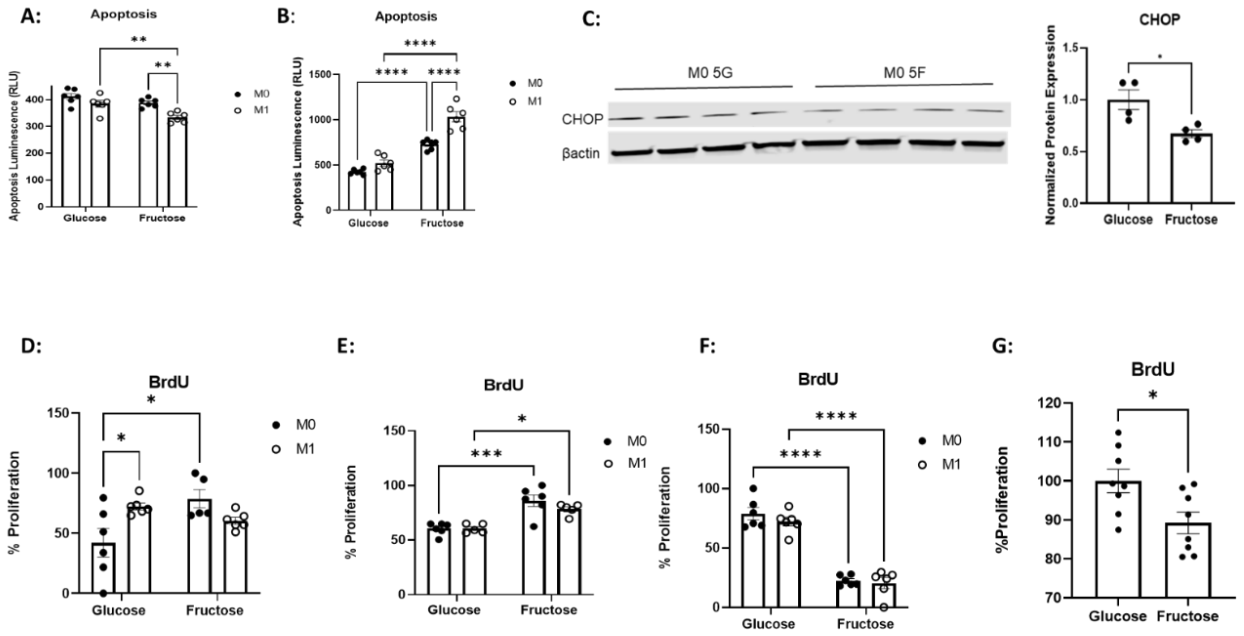

Figure 4: Fructose Induces IMKC Proliferation and Decreases J774.1 Proliferation. Measured luminescence for apoptosis assay. **A:** IMKC (n=6), **B:** J774.1 (n=6). **C:** J774.1 CHOP protein expression after 24 hr fructose treatment. Cells were plated with BrdU proliferation assay and treatment for 24 hours before antibody labelling and reading of colorimetric absorbance. **D:** IMKC 5mM (n=6) ,**E:** IMKC 25mM (n=6).**F:** J774.1 5mM (n=6) and **G:** J774.1 25mM M0 (n=8). Data are representative of 3 independent experiments and shown as means ± SEMs. * $p<0.05$, ** $p<0.01$, *** $p<0.001$, **** $p<0.0001$.

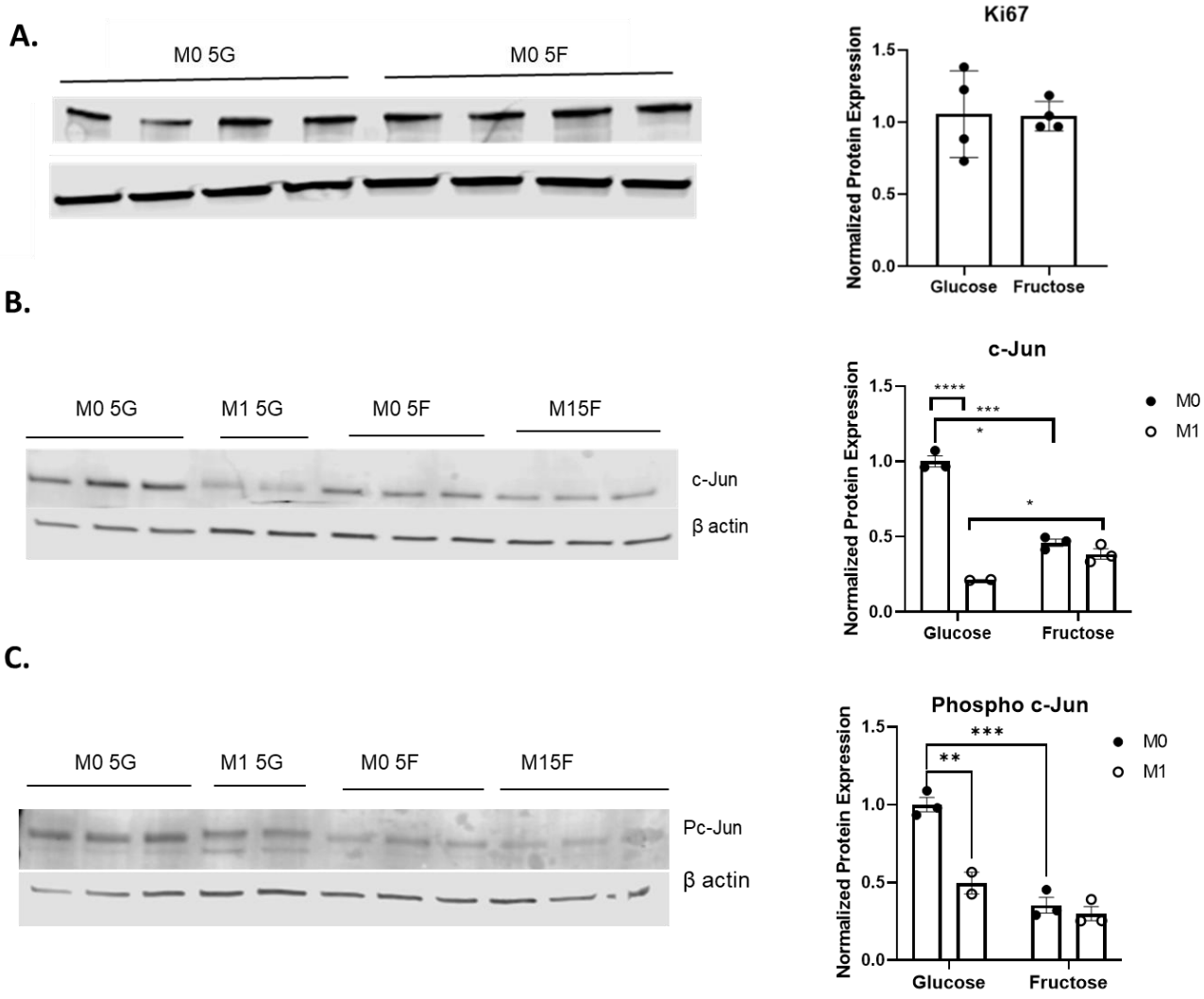

Figure 5: Fructose Reduces AP-1 Factor c-Jun Phosphorylation in M1 J774.1: Cells were plated in 25mM glucose 24 hours before media was changed to 5mM fructose with or without 10ng/ml LPS. Cells were harvested for protein expression with RIPA buffer. Lysate was resolved and analyzed for **A:** Ki67 (n=4) , **B:** c-Jun (n=3) and **C:** phosphor c-Jun (n=3) at 1:1000 dilution overnight. Secondary was added at 1:20,000 dilution. Data are representative of 3 independent experiments and shown as means ± SEMs. * $p<0.05$, ** $p<0.01$, *** $p<0.001$, **** $p<0.0001$.

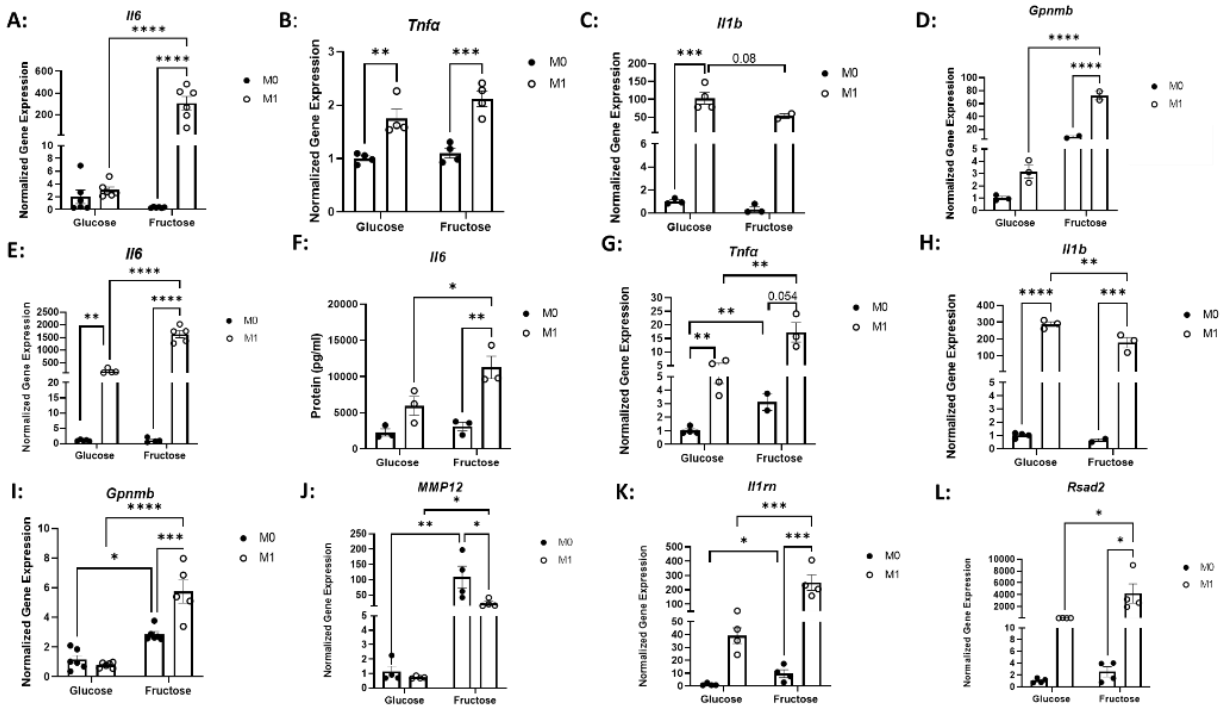

Figure 6: 25mM Fructose Increases Anti-inflammatory and Fibrosis Gene Expression in M0 IMKC: IMKCs were treated with 5mM or 25mM glucose or fructose for 24-hours and supplemented with/without LPS at 0.1ug/mL. cDNA was generated from RNA isolation and RT qPCR was analyzed for gene expression of pro-inflammatory cytokines. 5mM fructose **A:** *Il6*, **B:** *Tnfα* and **C:** *Il-1b*. 5mM anti-inflammatory gene expression of **D:** *Gpnmb*. 25mM gene expression of pro-inflammatory cytokines **E:** *Il6* **F:** ELISA analysis of IL6 protein secretion, **G:** *Tnfα,* and H: *Il1b*. 25mM Anti-inflammatory and fibrosis associated genes **I:** *Gpnmb*, **J:** *Mmp12*, **K:** *Il1rn*, and **L:** *Rsad2*. Gene expression (n=4). Data are representative of 3 independent experiments and shown as means ± SEMs.* $p<0.05$, ** $p<0.01$, *** $p<0.001$, **** $p<0.0001$.

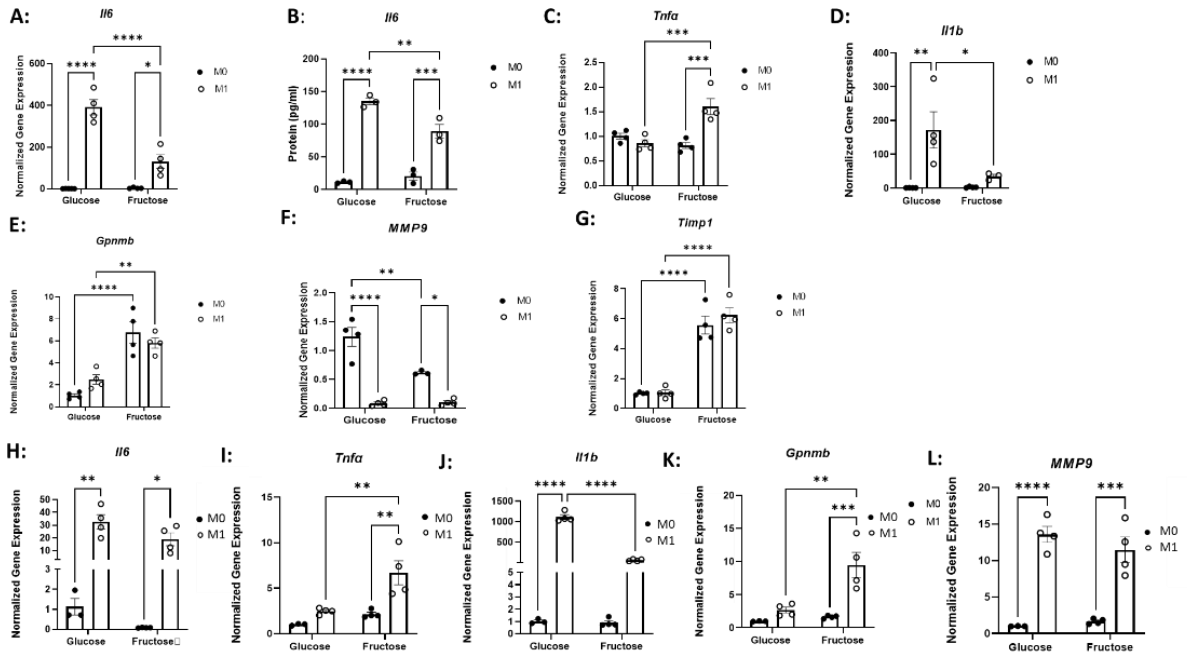

Figure 7: Fructose Regulates Genes Involved in Inflammation, and Fibrosis in J774.1 and RAW: Cells were treated with 5mM glucose or fructose for 24-hours and supplemented with/without LPS at 10 ng/ml. cDNA was generated from RNA isolation and RT qPCR was analyzed for gene expression of pro-inflammatory cytokines in J774.1 **A:** *Il6*, **B:** ELISA analysis of IL6 protein secretion, **C:** *Tnfα* and **D:** *Il-1b*. Anti-inflammatory gene **E:** *Gpnmb.* Fibrosis genes **F:** *Mmp9* and **G:** *Timp1*. RAW cell pro-inflammatory gene expression of **H:** *Il6*, **I:** *Tnfα,* and **J:** *Il1b.* Anti-inflammatory expression of **K:** *Gpnmb*. Fibrotic gene **L:** *Mmp9*. Gene expression (n=4). Data are representative of 3 independent experiments and shown as means ± SEMs.* $p<0.05$, ** $p<0.01$, *** $p<0.001$, **** $p<0.0001$.

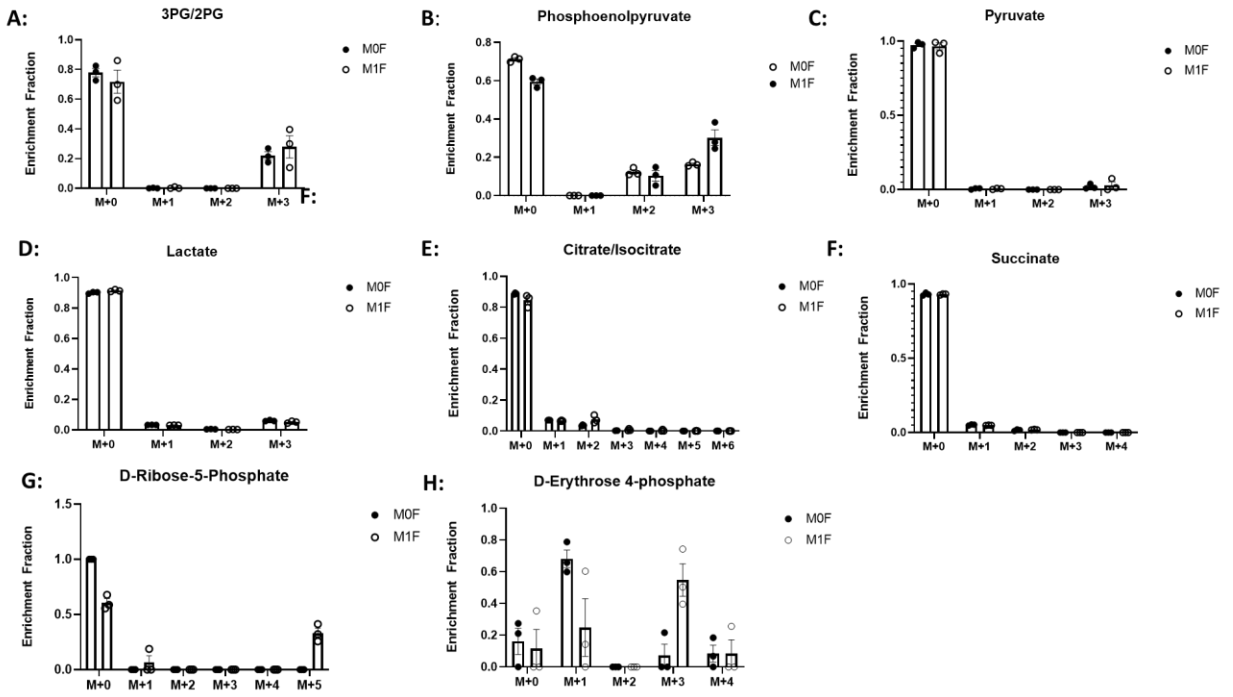

Figure 8: 5mM Fructose Metabolic Partitioning in IMKC: IMKCs were plated in 25mM glucose for 24 hours before media was changed to C13 5mM fructose with 0.1ug/mL LPS for M1 cells. 24 hours later cells were harvested for LC-MS via MetOH extraction for metabolite analysis and analyzed by MS peak intensity. Metabolites of interest were **A-D:** glycolysis intermediates, **E-F:** TCA cycle Intermediates, **G-H:** PPP intermediates**.** Metabolite tracing (n=3). Data are representative of 3 independent experiments and shown as means ± SEMs.

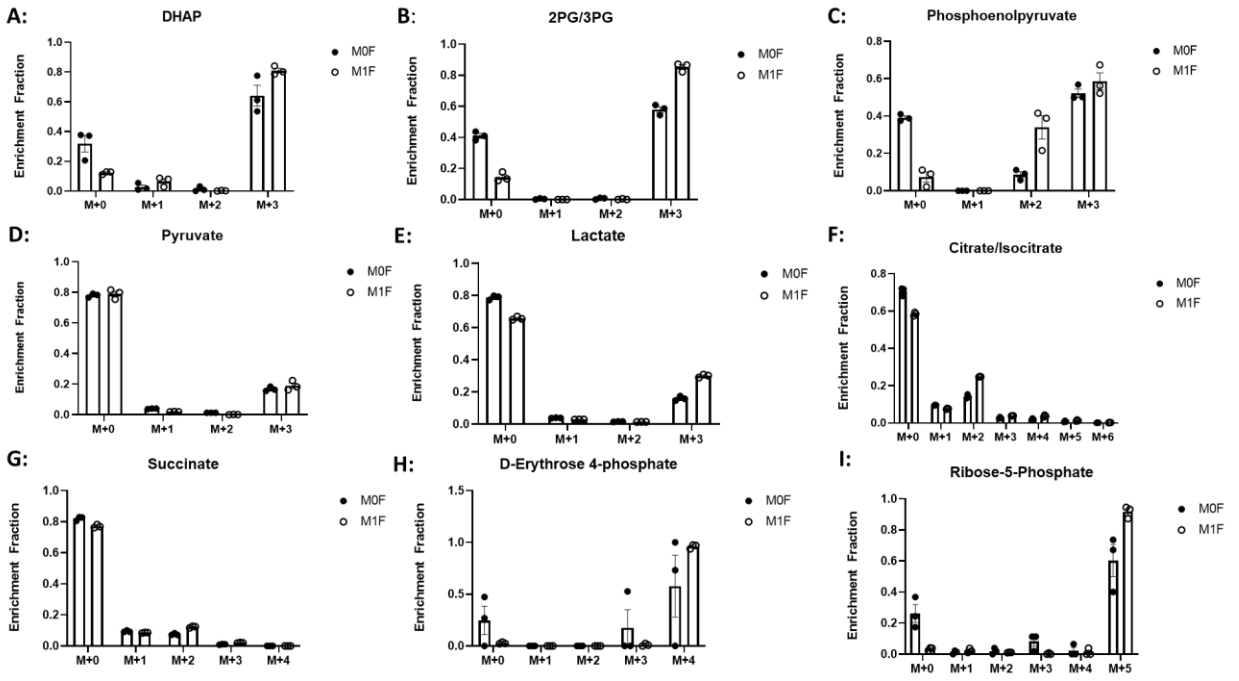

Figure 9: 25mM Fructose Metabolic Partitioning in IMKC: IMKCs were plated in 25mM glucose for 24 hours before media was changed to C13 25mM fructose with 0.1ug/mL LPS for M1 cells. 24 hours later cells were harvested for LC-MS via MetOH extraction for metabolite analysis and analyzed by MS peak intensity. Metabolites of interest were **A-E:** glycolysis intermediates, **F-G:** TCA cycle Intermediates, **H-I:** PPP intermediates**.** Metabolite tracing (n=3). Data are representative of 3 independent experiments and shown as means ± SEMs.

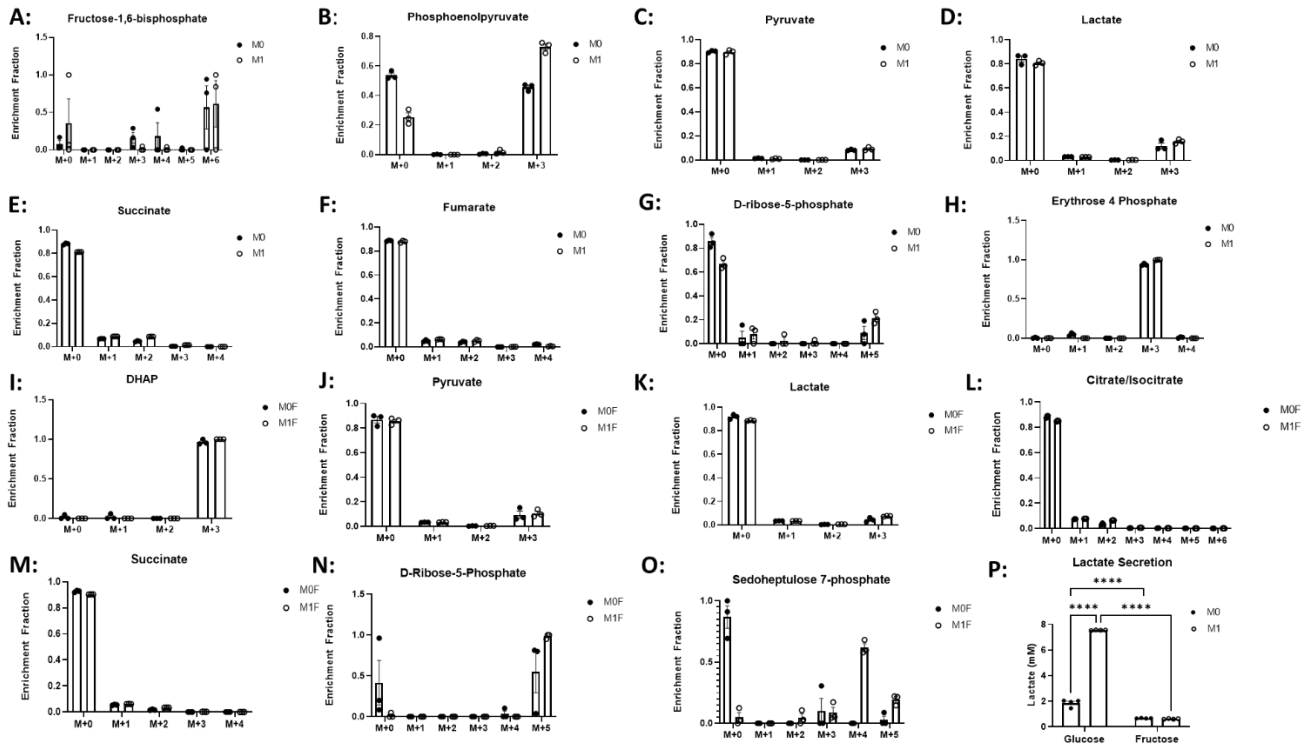

Figure 10: 5mM Fructose Metabolic Partitioning in J774.1 and RAW: Cells were plated in 25mM glucose for 24 hours before media was changed to C13 5mM fructose with 10 ng/mL LPS for M1 cells. 24 hours later cells were harvested for LC-MS via MetOH extraction for metabolite analysis and analyzed by MS peak intensity. Metabolites in J774.1 of interest were **A-D:** glycolysis intermediates, **E-F:** TCA cycle Intermediates, **G-H:** PPP intermediates**.** Metabolites of interest in RAW were **I-K:** Glycolysis, **L-M:** TCA and **N-P:** PPP. **P:** J774.1 media was collected after 24 hour exposure to fructose and analyzed for lactate secretion (n=4). Metabolite tracing (n=3). Data are representative of 2 independent experiments and shown as means ± SEMs.

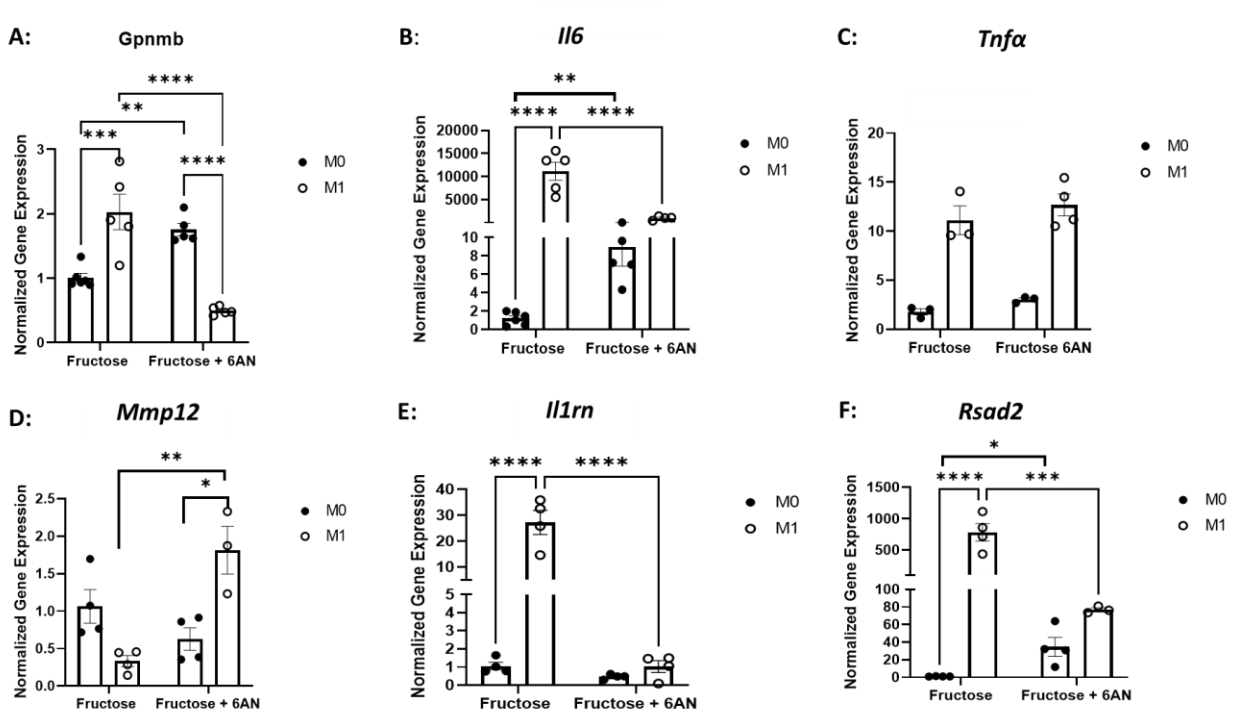

Figure 11: Pharmacological Inhibition of the PPP Increases Fructose Induced Expression of Anti-Inflammatory and Fibrosis Genes in M0 IMKC. IMKCs were treated with 25mM glucose or fructose for 24-hours and supplemented with/without LPS at 0.1ug/mL. Cells were treated with 100uM 6AN at time of treatment. Cells were isolated for RNA expression and genes of inflammation, **B-C:** *Il6* and *Tnfα,* and anti-inflammatory and fibrosis genes **A:** *Gpnmb* and **D-F:** *Mmp12*, *Il1rn* and *Rsad2*. (n=4). Data are representative of 2 independent experiments and shown as means ± SEMs. * p<0.1, ** p<0.01, *** p<0.001, **** p<0.0001.

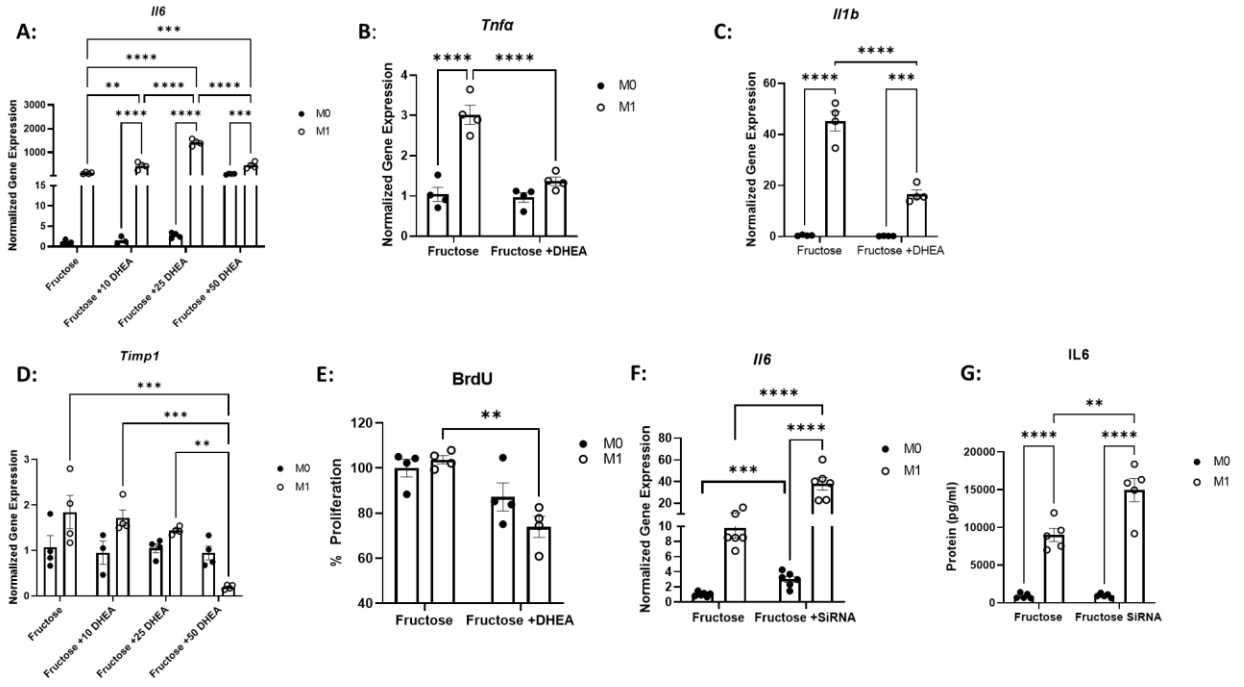

Figure 12: Pharmacological Inhibition of the PPP Increases IL6 Gene Expression in Fructose Treated J774.1 J774.1 cells were treated with 5mM fructose with or without 10, 25 or 50 μM DHEA for 24 hours as well as with or without 10ng/ml LPS. Cells were isolated for RNA and analyzed by RT qPCR inflammatory genes *Il6*, **(A),** *Tnfα* **(B)** and *Il1b* **(C)** and for fibrotic gene *Timp1* **(D). E:** BrdU proliferation assay after DHEA treatment. **F**: SiRNA knockdown was performed by adding 25pmol G6PDH SiRNA with lipofectamine for 48 hours in 5mM fructose conditions and analyzed by RT qPCR for *Il6* expression. **G:** SiRNA treatment media was kept and analyzed by ELISA for IL6 protein secretion (n=5). Data are representative of 2 independent experiments and shown as means ± SEMs.). n=4. Data are representative of 3 independent experiments and shown as means ± SEMs. ** $p<0.01$, *** $p<0.001$, **** $p<0.0001$.

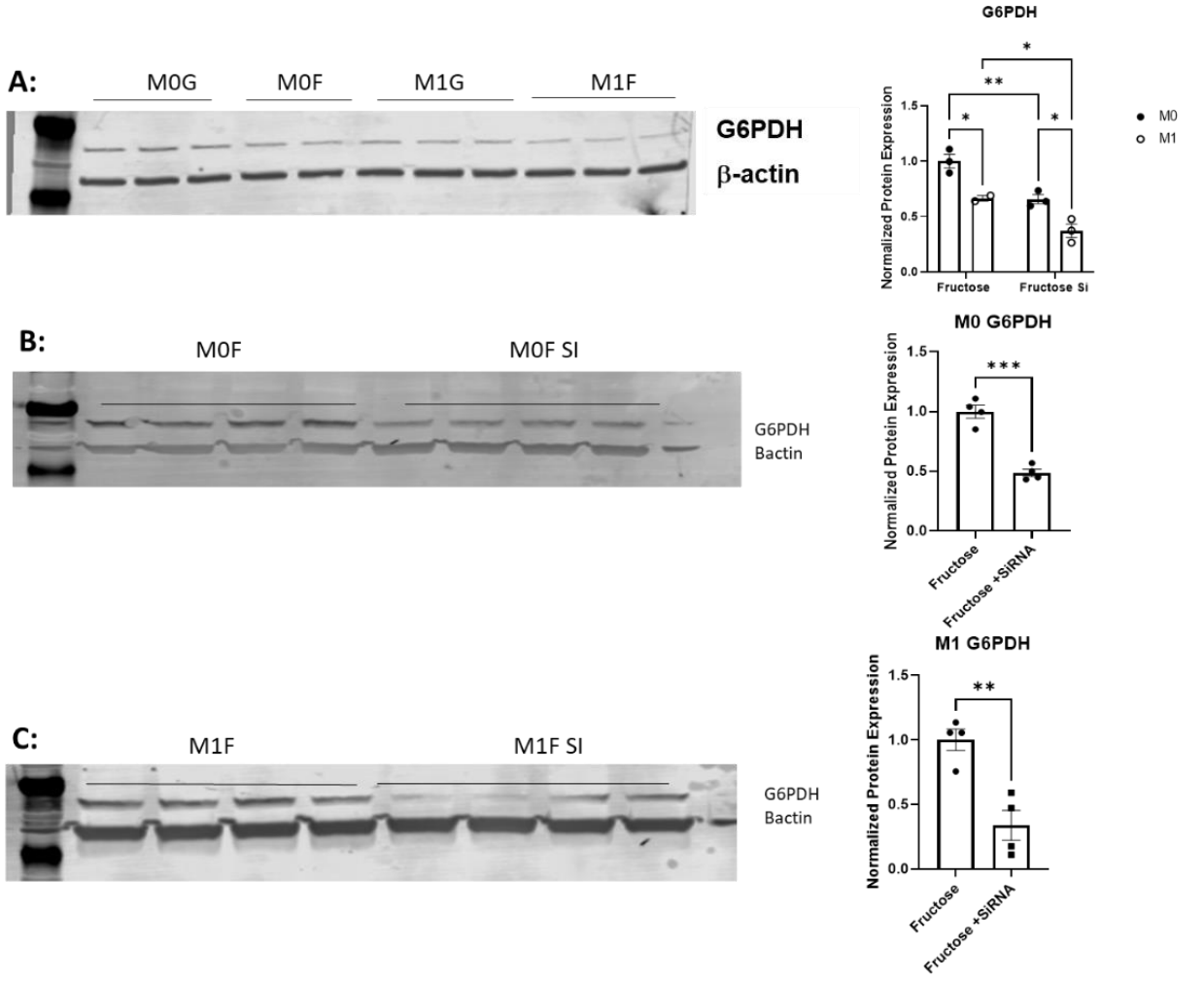

Figure 13: Establishing G6PDH Knockdown. Cells were plated in 25mM glucose for 24-hours. Media was changed to 25mM glucose with or without 25pmol G6PDH SiRNA for 48 hours. Cells received 5mM or 25mM fructose with or without 0.1 ug/ml LPS (IMKC) or 10 ng/ml (J774.1) for 24 hours and were harvested for protein expression. **A:** Primary antibody for G6PDH was used at 1:1000 dilution overnight at 8° C in J774 .1 (n=3) and IMKC (n=4) **(B-C).** Analysis was done by Image Lite. Data are representative of 3 independent experiments and shown as means ± SEMs. * $p<0.05$, ** $p<0.01$, *** $p<0.001$, **** $p<0.0001$.

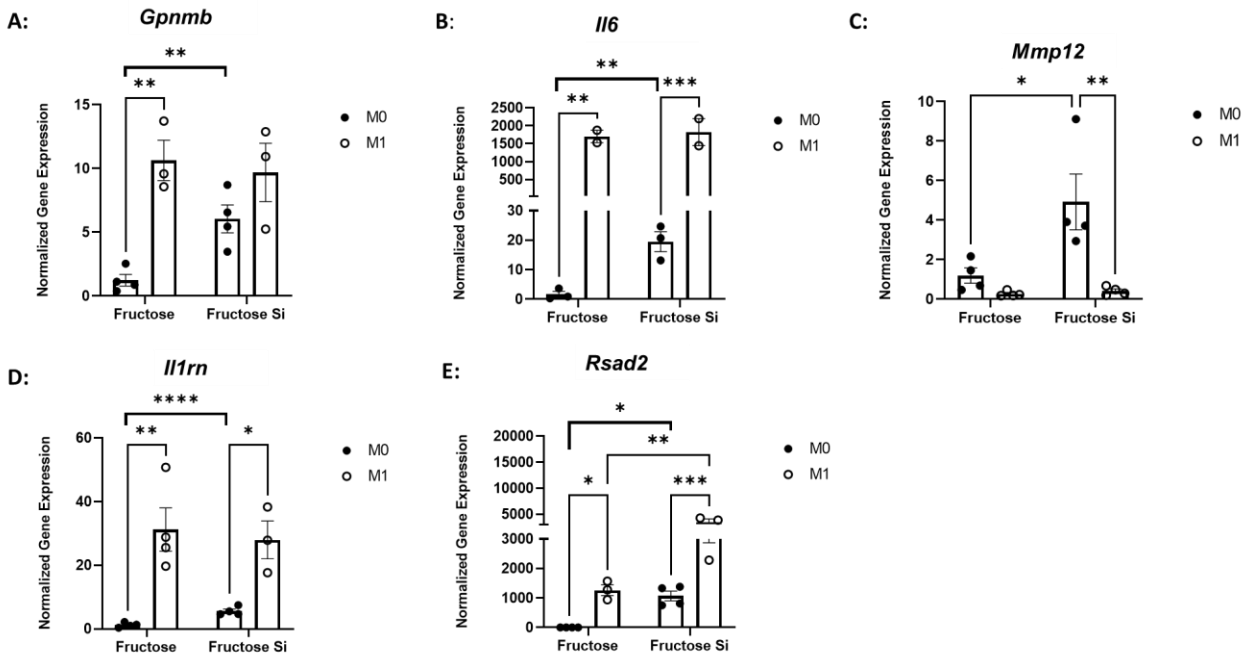

Figure 14: SiRNA Inhibition of the PPP Increases Fructose Induced Expression of Anti-Inflammatory and Fibrosis Genes in M0 IMKC. IMKCs were plated in 25mM glucose for 24-hours. Media was changed to 25mM glucose with or without 25pmol G6PDH SiRNA for 48 hours. Cells received 25mM fructose with or without 0.1 ug/ml LPS for 24 hours and were harvested for protein expression. Inflammatory gene (n=3) **B:** *Il6,* and anti-inflammatory and fibrosis genes **A:** *Gpnmb,* ***C:*** *Mmp12*, **D:** *Il1rn,* and **E:** *Rsad2* (n=4). Data are representative of 2 independent experiments and shown as means ± SEMs. * p<0.05, ** p<0.01, *** p<0.001, **** p<0.0001.

CHAPTER 3: Fructose Consumption Regulates Anti-Inflammatory and Extracellular Matrix Regulatory Gene Expression in Kupffer Cells.

3.1 Abstract

Over-consumption of fructose in adults and children has been linked to increased risk of Non-Alcoholic Fatty Liver Disease (NAFLD). Recent studies have highlighted the effect of fructose on liver inflammation, fibrosis, and immune cell activation. However, little work summarizes the direct impact of fructose on macrophage infiltration, phenotype, and function within the liver. We demonstrate chronic fructose diet increased liver, adipose and body weight gain compared to control groups. Fructose also increased acylcarnitine and diacylglyceride levels while inducing liver damage through oval hyperplasia and increased collagen deposition. In addition, fructose decreased Kupffer Cell populations while increasing transitioning monocytes. Fibrotic gene expression of *Col1a1* and *Timp1* as well as inflammatory gene expression of *Tnfa* and expression of *Gpnmb* in liver tissue was significantly increased compared to glucose and control diets. Single cell RNA sequencing (scRNAseq) revealed fructose elevated expression of *Mmp12*, *Il1rn,* and *Rsad2* in liver and hepatic macrophages. Although not specific to macrophages, fructose increased gene expression of genes involved in fructose metabolism and the PPP. These results indicate fructose may decrease KC populations while increasing transitioning monocytes. This response is accompanied by increased anti-inflammatory and fibrosis associated gene expression potentially in response to cell death.

3.2 Introduction

In recent years, the monosaccharide fructose has become one of the most studied carbohydrates as its consumption is more prevalent in our everyday diets [114]. Fructose consumption has been linked to obesity related insulin resistance, type 2 diabetes mellitus, non-alcoholic fatty liver disease (NAFLD) and atherogenic dyslipidemia, becoming a greater risk for cardiac stroke and potentially death [77]. Prevalence of steatosis in NAFLD has reached 25% of the worldwide population with the more aggressive form of Non-Alcoholic Steatohepatitis (NASH) reaching nearly 14% [77]. Fructose metabolism increases *de novo* lipogenesis (DNL) in the liver [39]. Given the prevalence of NAFLD, it is important to understand the mechanism in which fructose mediates inflammatory and fibrotic progression. Important work has summarized the effects of fructose on

hepatocyte function, but little is known about the effect of fructose on resident and infiltrating immune cell populations.

The liver is made of several macrophage populations ranging from residential Kupffer cells (KCs) to infiltrating bone marrow derived monocytes. Monocytes and macrophages play a large role in maintaining tissue function and phenotype as they scavenge for toxins and secrete cytokines which allow for crosstalk among cells in tissues [82]. KCs and recruited macrophages have been shown to play a massive role in the progression of NAFLD as they often display a pro-inflammatory phenotype (M1) secreting cytokines interleukin 6 (IL-6), tumor necrosis factor α (Tnfα) and interleukin 1β (IL-1β) [85-87]. KC depletion within rats and mice demonstrate a protective effect on the liver as the depletion prevented steatosis, hepatic insulin resistance, hepatic inflammation and apoptosis [93] [94]. Residential or recruited macrophages may express a fluid phenotype, displaying both proinflammatory and anti-inflammatory properties. External stimuli such as lipopolysaccharide (LPS) or interferon gamma (IFNγ) activate toll-like receptors (TLR) response of macrophages to secrete cytokines such as IL6 and TNFα to aid in wound repair through increased flux of glycolysis [55]. Under chronic inflammatory conditions, macrophages may switch to an anti-inflammatory phenotype releasing extracellular matrix proteins to signal wound healing.

Carbohydrate metabolism is a known stimulus of macrophage plasticity. Glucose is the primary energy source for macrophages. In contrast, limited studies address the impact of fructose metabolism on macrophage plasticity and the impact on NAFLD progression [115]. In LPS stimulated monocytes, fructose shifts glycolysis metabolism to the tri-carboxylic acid cycle (TCA) or oxidative phosphorylation (OXPHOS) cycling [63]. Furthermore, fructose increases secretion of pro-inflammatory cytokines IL-1β, IL6 and Tnfα which are dependent on hexokinase activity. In dendritic cells, fructose undergoes glycolytic metabolism while activating NFkb [116]. The increase in glucose metabolism drives cytokine production as induction of M1 phenotype is dependent upon glycolysis. In addition, utilization of the PPP produces NADPH pools needed for cytokine production. Given the importance of KCs in maintaining liver homeostasis, we describe the role of fructose in regulating KC metabolism, inflammation, and viability using chronic-fed mouse models and immortalized KCs in vitro.

In this study, fructose induced liver damage through oval cell hyperplasia and collagen deposition and was associated with increased acylcarnitine and diacyglycerides. Fructose reduced KC populations and increased transitioning monocytes. Interestingly, liver tissue and hepatic macrophages from chronic fructose diet displayed an anti-inflammatory and profibrotic phenotype by increasing gene expression of matrix metallopeptidase 12 (*Mmp12*), interleukin 1 receptor antagonist (*Il1rn*), glycoprotein NMB (*Gpnmb*) and radical s adenosyl methionine domain (*Rsad2*). Additionally, genes involved in fructose metabolism and PPP were upregulated in fructose conditions.

3.3 Materials and Methods

Mouse Model

C57BL/6J mice were housed at North Carolina State University Biological Resources Facility with ad libitum access to chow food (Laboratory Rodent Diet 5001) and water on a 12- hour light/dark cycle. At the age of 8 weeks, mice were administered 30% fructose, glucose or no supplementation in their drinking water for 4, 6, or 8 months. Chronic fructose exposure data is combined from 6- and 8-month studies. Food and water intake was monitored every week as well as body weight. Before tissue collection mice were fasted for 5 hours. Mice were then anesthetized with isoflurane and sacrificed via cervical dislocation. Liver was perfused by heart right ventricle puncture and 1X PBS until liver became tan in color. Liver and adipose tissue was removed and immediately snap-frozen in liquid nitrogen or fixed via formaldehyde. All animal procedures were approved by the Institutional Animal Care and Use Committee (IACUC) at North Carolina State University.

Liver Nonparenchymal Cell Isolation

Isolated livers were immediately processed for nonparenchymal cell isolation using Liver lymphocyte protocol adapted from (Breuer et al. 2020 AJP, [14]). Immune cells were separated by 443 xg spins and 33% percol gradient. Samples were resuspended in FACs buffer and stained with AO/PI for cell counting.

Flow Cytometry

Liver isolated cells were incubated with Fc block and incubated in FACS buffer with fluorophore conjugated antibodies on ice for the following macrophage panel: F480 (A700, 1:200, Biolegend), CD64 (PE, 1:200, BD Biosciences), CD11b (FITC, 1:200, BD Biosciences), Ly6c (PerCP-Cy5.5, 1:200, BD Biosciences), CLEC4F (Unconjugated, 1:200, R&D Systems). Following antibody incubation samples were washed twice with FACS buffer. After washing, CLEC4F samples were incubated with a secondary antibody (Donkey anti-goat AF647, 1:500, ThermoFisher) and washed twice after incubation. The Becton Dickinson LSRII machine at the NCSU flow Cytometry Core was used to acquire all flow data. Flow data was analyzed using FlowJo software v10.8.

Magnetic Labeling and Separation

Magnetic separation was performed following manufacturer's protocol. Remaining pellet and supernatant were counted and resuspend in buffer per 1 x 10^7 total cells. Anti-F4/80, Anti-FITC and Anti-CD11b MicroBeads UltraPure per 1 x 10^7 total cells were added within each sample. Cells were mixed well and incubated for 15 mins in the dark in the refrigerator (2-8°C). Cells were washed with FACS and centrifuged at 300 x g for 10 minutes. Supernatant was removed completely, and cells were resuspended up to 1 x 10^8 cells in FACS buffer.

Single Cell RNA Sequencing

All samples were submitted and processed by the NCSU Genomics Core. Sample preparation was conducted using the 5′ assay for the 10X Chromium Controller (10X Genomics) targeting 5,000 cells per sample. In all, 50,000 reads per cell were targeted for PE-150 sequencing on an Illumina NovaSeq. Sample processing and sequencing were completed in the NCSU Genomics Sciences Laboratory. Reads were further processed using CellRanger v4.1 (10X Genomics) with the mm9 mouse reference genome. Ambient RNA signal was estimated and removed using SoupX v1.5.2 [117] with the autoEstCont and adjustCounts functions. Filtered count matrices were passed to Seurat v4 [118] and cells with <10% mitochondrial RNA content and at least 500 unique reads that correspond to at least 200 features were retained. DoubletFinder [119]v2.0.3 was used to detect and remove heterotypic doublets. Counts were normalized using the NormalizeData function from Seurat.

Data Integration and Dimensional Reduction

Principal component analysis was performed using the RunPCA function from Seurat. Integration anchors were detected using the FindIntegrationAnchors function with reduction = "rpca" and independent samples were integrated with the IntegrateData function from Seurat. Nonlinear dimensional reduction was performed using the RunUMAP function from Seurat using the first 30 principal components.

Unsupervised Clustering and Cell Annotation

Unsupervised clustering was performed using the Louvain algorithm implemented in the FindClusters function with resolution = 0.4 in Seurat. Cell types were predicted using SingleR v1.6.1 [120] with the Immgen and MouseRNAseq references from the celldex v1.2.0 [120] package. Consensus between predicted cell type labels, differentially expressed markers found using the FindAllMarkers function, and established cell-specific markers were used to annotate clusters. For each major cell type, subclustering was performed to further delineate cell subtypes.

Downstream Single Cell Analysis

For assessment of differential abundance between conditions, MiloR v1.6.0 [121] was used generate neighborhoods of cells and comparisons were performed using the testNhoods function. For additional plotting, the integrated Seurat v4 object was converted to an anndata object using scDIOR [122] . Then, anndata objects were loaded into Scanpy v1.9.2 [123].

RNA Isolation and RT-PCR

Samples were isolated for RNA according to manufacturer's protocol using Direct-zol™ RNA MicroPrep kit (Genesee Scientific). RNA concentration was obtained by nanodrop, and cDNA was made using qscript cDNA supermix following instructions of manufacturer (Quantabio). cDNA was synthesized at 1000 ng using BioRAD iQ5 thermocycler. Cycles were: Priming for 5 minutes at 25°C, RT: 30 minutes at 42°C and RT inactivation for 5 minutes at 85°C. cDNA was used to analyze gene expression by real time polymerase chain reaction (RT q-PCR) using PerfeCTa qPCR FastMixII (QUantbio). TaqMan assays used were Il6, Tnfα, IL1β, Gpnmb, Col1a1, Timp1,

Mmp12, Rsad2, Ilrn1, Il1bp, Afp, Gcp3, Fn1, Cd11b, F4/80 and 18S eukaryotic endogenous control (Thermo Fisher Scientific). Samples were normalized to 18S.

Statistical Analysis

GraphPad Prism 9.3.1 software was used for all statistical analyses. Two-tailed unpaired Student's t-tests were performed for two group comparisons. Two-way ANOVA was performed for genotype versus diet studies followed by multiple T test comparisons. All data is presented as the mean ± SEM. Data was considered statistically significant for $P<0.05$ (*), $P<0.01$ (**), $P<0.001$(***), and $P<0.0001$(****).

3.4 Results

3.4.1 Chronic Fructose Diet Induces Liver and Body Weight Gain

To gain insight into the impact of short- and long-term fructose exposure on the liver, mice were fed chow diet supplemented with control water, 30% glucose water or 30% fructose water for 4, 6, or 8 months. Mice on glucose and fructose water had elevated body weight compared to control in short- and long-term conditions (Fig 1A, D). Interestingly, mice on fructose had decreased weight gain compared to glucose even when consuming a similar number of calories (Fig 1A,C and D,F). Fructose supplementation for 4 months increased liver weight compared to glucose but had no effect on adipose tissue weight (Fig 1B). Fructose diet for 8 months showed no difference in liver or adipose weight compared to glucose(Fig 1E). In all studies, fructose increased adipose weight compared to control (Fig 1B, E). Both acute and chronic studies revealed mouse preference of glucose over fructose, as they consumed less water with fructose supplementation than glucose (Fig 1C, F).

Fructose is known to increase *de novo* lipogenesis leading to increased lipid accumulation and stored triglycerides. We confirmed fructose elevated fatty acid synthase (*fasn)* gene expression at both 4 months and chronic exposure as liver phenotype was similar (Fig 2A, C). Although trending in increase at 4 months, targeted mass spectrometry lipidomics profiling revealed fructose increased saturated long chain fatty acid acyl-carnitines, specifically 18:0, 18:1 and 20:1 and long chain diacylglycerides compared to both control and glucose fed mice on chronic diet (Fig 1B, D respectively). Interestingly, fructose supplementation not only increased lipid accumulation but

pathology scoring revealed and increase in liver damage through oval cell hyperplasia and lipid accumulation (Fig 2E). Collagen deposition analyzed by siris red staining was increased in mice that had fructose treatment (Fig 2E). Additionally, mice on fructose diet displayed tumor growth compared to control and glucose fed mice.

3.4.2 Chronic Fructose Diet Reveals Gene Signature of Hepatic Macrophages

To determine the potential mechanism of fructose induced liver damage, we analyzed the gene signature of hepatic macrophage subsets. Studies have shown mice on fructose diet have elevated KCs, as well as infiltrating monocytes, and macrophages, within liver compared to control diets [73, 124]. We used single cell RNA sequencing (scRNAseq) to determine how fructose regulates hepatic macrophage subsets (Fig 3A). Fructose treatment decreased KCs expressing *Clecf4*, *Tim4*, *Adreg* and B cells expressing *Cd79a*, *Ms4a1*, *Ly6d* (Fig 3B-C). In contrast, transitioning monocytes expressing *Cxcl10*, *Ptafr*, *Cd74*, *Clec4e*, *H2ab1*, *Fabp5* and *Cxcl9* increased with fructose diet compared to control and glucose (Fig 3B-C). To confirm the reduction in KCs and increase in transitioning monocytes, flow cytometry analysis identified significant reductions in KC ($Lyc6^{-}CD11b^{+}F480^{+}CD64^{-}CLEC4F^{+}$) populations but showed a trending increase in monocyte derived macrophages ($Lyc6^{-}CD11b^{+}F480^{+}CD64^{-}$) in fructose treated mice compared to control and glucose (Fig 4D).

ScRNAseq of KCs revealed chronic fructose diet upregulated pathways involved in metabolism, signal transduction, and the immune system (Fig 4A). From the scRNAseq data set, we examined genes upregulated in KCs, and found fructose increased expression of *Mmp12*, *Il1rn*, *Rsad2,* and *Il18bp* (Fig 4B-C). By examining scRNAseq genes by treatment, *Tnfa, Gpnmb, Hk2, Hk3, Aldoa,* which is involved in fructose metabolism, and *G6pdx*, the rate limiting step of the PPP, had a higher frequency in fructose fed mice (Fig 4B). While the frequency was higher under fructose conditions, these genes were not found to be upregulated in KCs.

3.4.3 Fructose Increases Anti-inflammatory Gene Expression in Acute and Chronic Studies

Fructose is associated with increased inflammation and fibrosis [15]. Short term fructose water decreased Tnfα gene expression compared to control and glucose water (Fig 5A). In addition, this length of study did not have any effect on fibrosis of the liver as *Col1al* and *Timp1* gene expression

were unchanged between groups (Fig 5A). In contrast, chronic fructose diet had a trending increase of *Tnfα* gene expression compared to control (Fig 5C) and significantly increased fibrosis markers *Col1a1* and *Timp1* compared to control (Fig 5C). In addition to fibrotic and inflammatory cytokine expression we analyzed genes often upregulated in cancer. There was no change in expression across any groups, although this may be because RNA samples were not taken from liver tumors for gene expression (Fig 5F). These data model chronic fructose exposure increases inflammation and fibrosis where glucose diet did not have the same effect.

Recently, GPNMB protein has been reported to protect the liver from liver fat toxicity and is highly expressed in NASH associated lipid laden macrophages and stellate cells. Gpnmb gene expression was elevated in both acute and chronic fructose water diets potentially as a response to induced fibrosis (Fig 5B,D). To confirm scRNAseq genes that were upregulated in KCs of the liver, we analyzed liver tissue and isolated Cd11b+ F4/80+ macrophages. Although single cell data indicated an increase in transitioning monocytes and a decrease in macrophages in the fructose group, we did not see changes in expression of *Cd11b* or *F4/80* in total liver tissue (Fig 5F). In liver tissue, anti-inflammatory genes *Mmp12*, *Il1rn* and *Rsad2* were significantly increased in fructose treated mice compared to control water at both acute and chronic timed studies (Fig 5B,D). Fructose had no effect on *Il18bp,* although gene expression was elevated in glucose compared to control (Fig 5D). To determine if upregulated anti-inflammatory gene expression was regulated by macrophages in fructose fed mice, we analyzed isolated CD11b+ F4/80+ cells. Fructose increased *Gpnmb, Mmp12, I11rn1* and *Rsad2* (Fig 5E). Additionally, primary KCs were isolated for in vitro 24-hour fructose and LPS exposure (Fig 6A). Similar to chronic fructose studies, primary KCs had trending elevated gene expression of *Gpnmb, Mmp12* and *Il1rn* in fructose treated KCs (Fig 6B). Additionally, these cells had elevated *Il18bp* in fructose LPS conditions. These findings suggest fructose directly regulates anti-inflammatory and fibrosis associated gene expression in acute and chronic exposure.

3.5 Discussion

Fructose metabolism in residential and recruited macrophages is poorly understood. Recent studies have highlighted the importance of studying fructose metabolism as researchers show large quantities of consumed fructose bypass initial intestinal metabolism and is deposited directly in

the liver [20]. Although literature has summarized the effects of fructose on hepatocytes, little is known of how fructose directly impacts the function and phenotype of macrophages under fructose conditions [21, 22]. By using fructose fed mice we demonstrate that chronic fructose exposure increases transitioning monocyte populations while decreasing KC populations. In addition, acute and chronic fructose conditions regulate anti-inflammatory and extracellular matrix gene expression in liver and primary KCs.

Studies of fructose exposure and its effects on NAFLD have varying results, making it hard to summarize the total effects of fructose. Some studies demonstrate fructose exposure for as small as 3-8 weeks increase liver steatosis without affecting body mass or liver weight gain [23-25]. In addition, these mice had elevated infiltrating neutrophils and hepatic Tnfα gene expression. However, others show fructose diet increases lipid vacuoles as well as increases weight gain. In our study we did not detect elevations in body weight until 20 weeks of fructose supplemented water, although liver steatosis was seen at 4- and 8-months. The development of fructose induced steatosis is consistent throughout fructose diet studies, however, the difference in body weight gain may be due to differences in fat content in chow diets over length of fructose exposure [26]. We found 30% carbohydrate supplemented water for 8 months did increase liver and adipose tissue weights, although these were not significantly different from each other. The difference between our study with other groups may be due to limited fat content in chow diet.

We demonstrate chronic fructose feeding for 8 months leads to elevated prevalence of steatosis from lipid accumulation and damage of the liver. The increase in accumulating lipids may be due to upregulation of proteins involved in de novo lipogenesis such as FASN. A recent study showed chow diet with 30% fructose (w/v) for 10 weeks with and without high fat diet had elevated saturated acylcarnitines [27]. Here we demonstrate chronic fructose diet increased acylcarnitines and diacylglycerides, specifically saturated long chain fatty acids, although we did not see these changes until over 20 weeks of diet. The increase in acylcarnitines may indicate inhibition of FAO as well as cause mitochondria dysfunction through increased ROS as shown in previous studies, although more work would need to be done to confirm this [28]. Increased acylcarnitine levels activate pro-inflammatory Tnfα expression, especially within macrophages, [29] therefore,

chronic fructose diet induced acylcarnitines may be a driver for increased inflammatory cytokine gene expression within KCs of the liver.

Recently, increased levels of uric acid have been reported through intestinal microbiome and hepatic cell fructose metabolism [30]. Fructose mediated uric acid production and oxidative stress triggers inflammation in human macrophages and mouse kidney [31, 32]. 30% fructose water for 8 weeks was shown to elevate Tnfα protein expression and increase macrophage infiltration within mouse liver [33]. This response was mediated through oxidative stress from fructose induced intestinal leaky gut endotoxin release. Interestingly, our chronic fructose diet showed significant elevation of Tnfα gene expression in liver tissue. Interestingly, fructose can play an anti-inflammatory role as it increases microbiome butyrate production in the small intestine [20]. The increase in butyrate led to improved intestinal barrier disruption and decreased endotoxin release from the small intestines [34]. It is possible the increase in Tnfα observed in our study may come from microbiome induced oxidative stress by endotoxin release or uric acid mediated inflammatory signaling, although this hypothesis would need to be further tested.

Along with upregulated inflammatory gene expression, chronic fructose diet increased fibrotic gene expression of *Col1a1* and *Timp1* in the liver. These tissues also scored higher in liver damage and had elevated collagen. Diet studies monitoring patients with NAFLD found that daily fructose consumption rather than high fructose consumption over short periods of time decreased steatosis and increased the presence of fibrosis in human liver biopsies [15]. In addition, the release of Tnfα from activated Kupffer cells has been reported to drive liver fibrosis by increasing Timp1 expression from hepatic stellate cells (HSCs) [35]. Tnfα signaling deficiencies were shown to attenuate liver steatosis and fibrosis, indicating a critical role of KCs in the pathogenesis of NAFLD. Although studies have found IL6 to be upregulated in both serum and liver tissue of mice on fructose diet, our studies did not indicate an effect of fructose on IL6 expression in liver tissue [36, 37]. As we show in our studies, KCs can increase fibrotic gene expression of proteins such as Col1a1 and Timp1. This aids in progressing liver fibrosis through activation of HSCs [38]. Interestingly this pro-fibrotic response of KCs was congruent with increased anti-inflammatory and fibrosis associated genes *Gpnmb, Mmp12, Il1rn* and *Rsad2* in liver and $Cd11b^{+}F4/80^{+}$ cells.

Recent studies have found Gpnmb to be protective in the context of NAFLD as its overexpression reduces fat accumulation and fibrosis in the liver [39]. The protective effect of Gpnmb may be due to its anti-oxidative properties in the liver, specifically in KCs. To our knowledge, this is the first report of fructose induced Gpnmb expression within macrophages. In liver injury, KCs secrete MMPs to aid in regression of fibrosis and resolution of tissue tearing. One study found Mmp12 to be the main secretory protein of macrophages that is involved in this process [40]. In addition, Mmp12 is important for regulating elastin in fibrosis and leukocyte chemotaxis [125] Interestingly, Mmp12 plays an additional role in stimulating pro-inflammatory cytokine expression as well as regulating macrophage proliferation [41]. This may explain the induction of inflammatory cytokine Tnfα and increased populations of transitioning monocytes. From our data, fructose leads to a reduction of KCs which may be regulated by their increased *Mmp12* expression. Under fructose conditions, transitioning monocytes were found to be increased while macrophage populations were decreased. It is possible that fructose inhibits transitioning monocyte differentiation as macrophage populations are reduced. In addition, the increase of transitioning monocytes could be due to fructose induced signaling leading to monocyte recruitment.

Glucose transporters GLUT2 or 8 are known to transport fructose within the liver. However only transporters GLUT 1 and 3 have currently been identified within macrophages [42-44]. A recent paper indicated the presence of GLUT5 within bone marrow derived macrophages, although this mechanism may differ between macrophage subsets. Liang, R.J. et al reported multiple cancer cell lines are unable to utilize fructose which often leads to decreased proliferation and cell death [45]. However, overexpression of GLUT5 within cells recovered their ability to proliferate and survive in fructose conditions, indicating a potential for energy source plasticity and a regulatory role of GLUT transporters over HKs. This may be the case in KCs where chronic fructose exposure may upregulate fructose transporters. Fructose is phosphorylated by ketohexokinase which is found in carbohydrate sensing organs like liver, kidney and pancreas. We found KHK and HK2 to be upregulated in fructose samples of scRNAseq data although this was not specific to macrophages. Literature shows the presence of HK1 within macrophages which phosphorylates glucose and fructose [46]. Although glucose is the preferred substrate of HK1, concentrations of 5mM or more of fructose increases the rate of reaction to be equal of glucose [47]. HK not only contributes to

fructose metabolism but is essential for NLRP3 inflammasome activation through increasing glycolytic flux [48].

In conclusion, fructose exposure increased liver, adipose and weight gain compared to control groups. In addition, fructose increased acylcarnitine and diacylglyceride levels while increasing liver damage through increased oval cell hyperplasia and collagen deposition. ScRNAseq data revealed fructose increased genes associated with the anti-inflammatory and wound healing response in liver as well as $Cd11b^{+}$ $F4/80^{+}$ cells. The increase in gene expression was accompanied by a decrease in KC populations and an increase in transitioning monocytes. Genes involved in fructose metabolism and the PPP were also upregulated in fructose, although these genes were not specific to KCs in the liver. Taken together our results demonstrate fructose decreases KC populations while increasing the wound healing response in the liver.

3.6 Figures and Figures Legends

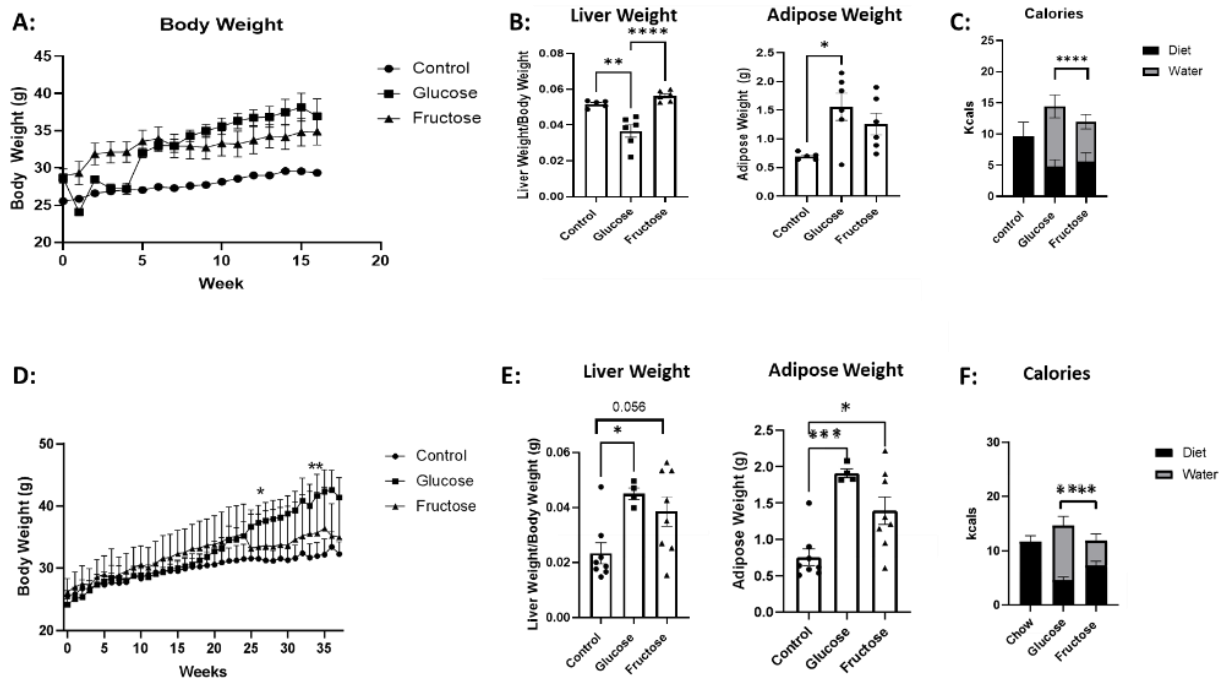

Figure 15: Chronic Fructose Diet Induces Liver and Adipose Tissue Weight Gain. C57BL/6 mice were fed chow diet supplemented with 30% glucose, fructose or control water for 4 months or 6-8 months. **A:** Body weight gain over time for 4 months (n=6). **B:** Liver and adipose tissue were removed and weighed at 4 months **C:** Chow and water

calorie intake over 4 months, water consumption analyzed between groups. **D:** Body weight gain over time for 8 months. **E:** Liver and adipose tissue were removed and weighed at 8 months. **F:** Chow and water calorie intake over 8 months, water consumption analyzed between groups * p<0.05 ** p<0.01, *** p<0.001, **** p<0.0001. Control (n=8), Glucose (n=4) and Fructose (n=8). Data are representative of 2 independent experiments and shown as means ± SEMs.

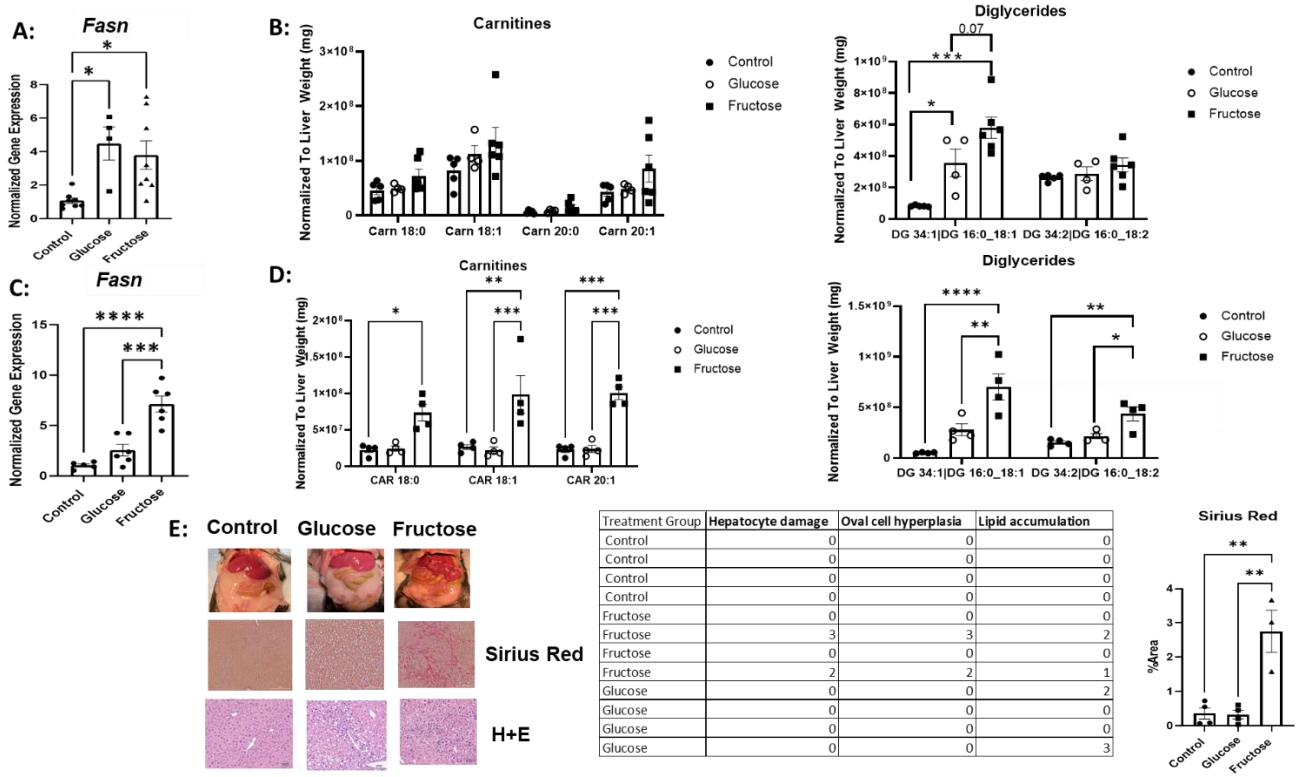

Treatment Group	Hepatocyte damage	Oval cell hyperplasia	Lipid accumulation
Control	0	0	0
Control	0	0	0
Control	0	0	0
Control	0	0	0
Fructose	0	0	0
Fructose	3	3	2
Fructose	0	0	0
Fructose	2	2	1
Glucose	0	0	2
Glucose	0	0	0
Glucose	0	0	0
Glucose	0	0	3

Figure 16: Fructose Increases Long Chain Carnitines and DGs and Liver Damage. Liver tissue was isolated and processed for RT qPCR and mass spectrometry lipidomics analysis. Gene expression of lipid synthesis gene *Fasn* at 4 months (n=6) **(A)**. **B:** Intensity of long chain fatty acid acyl carnitines and diglycerides normalized to liver weight, from mass spectrometry profiling at 4 months. Gene expression of lipid synthesis gene *Fasn* at 8 months (n=6) **(C)**. **D:** Intensity of long chain fatty acid acyl carnitines and diglycerides normalized to liver weight, from mass spectrometry profiling at 8 months. **E:** Liver morphology and histology using H+E and Sirius red * p<0.05, ** p<0.01, *** p<0.001, **** p<0.0001. Control (n=8), Glucose (n=4) and Fructose (n=8). Data are representative of 2 independent experiments and shown as means ± SEMs.

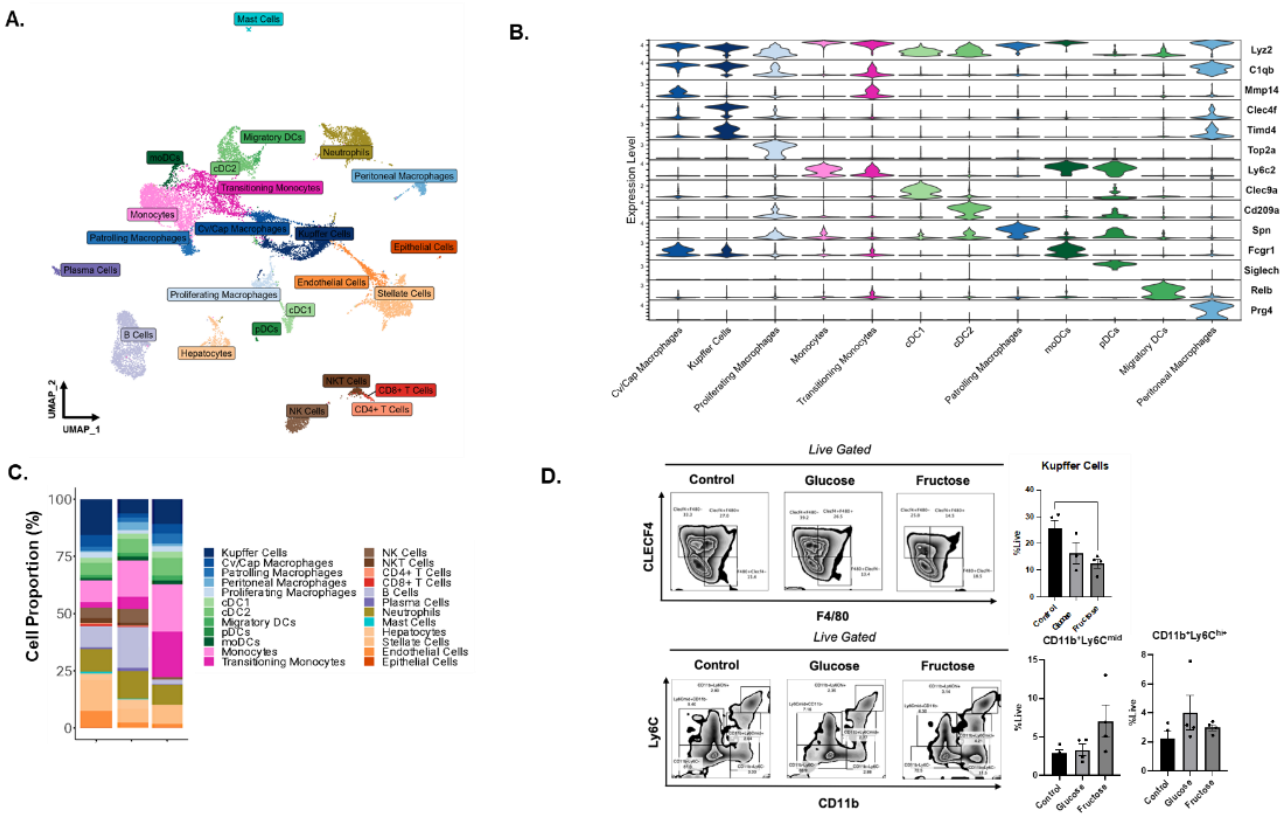

Figure 17: Chronic Fructose Diet Decreases Kupffer Cells and Increases Transitioning Monocytes. A-C: Chronic fructose, glucose, and control mouse livers were isolated and processed for Cd11b+/F4/80+ cells. Cells were unsupervised and clustered using the Louvain algorithm **D:** Cells were stained with F4/80+, CD64+, Cd11b+, Ly6c+, and Clec4f and analyzed by flow cytometry. Control (n=4), Glucose (n=4) and Fructose (n=4).

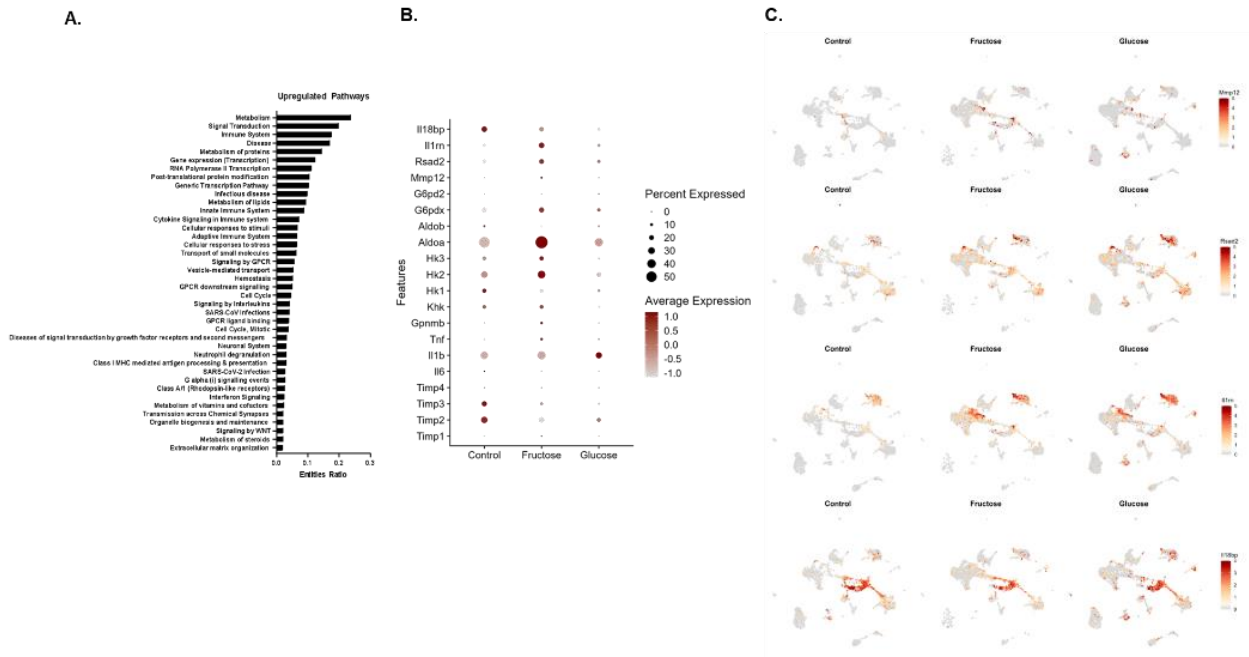

Figure 18: Impact of Chronic Fructose Diet on Molecular Pathways and Genes Associated with Metabolism, Inflammation, and Fibrosis. Livers were isolated from chronic fructose fed mice and processed for Cd11b+ F4/80+ cells. Pathway analysis was performed with metascape **(A)**. **B-C:** RNA SEQ data was analyzed for significantly upregulated genes in fructose treatments compared to glucose and control. * $p<0.05$, *** $p<0.001$. Control (n=4), Glucose (n=4) and Fructose (n=4). Data are representative of 1 independent experiment and shown as means ± SEMs.

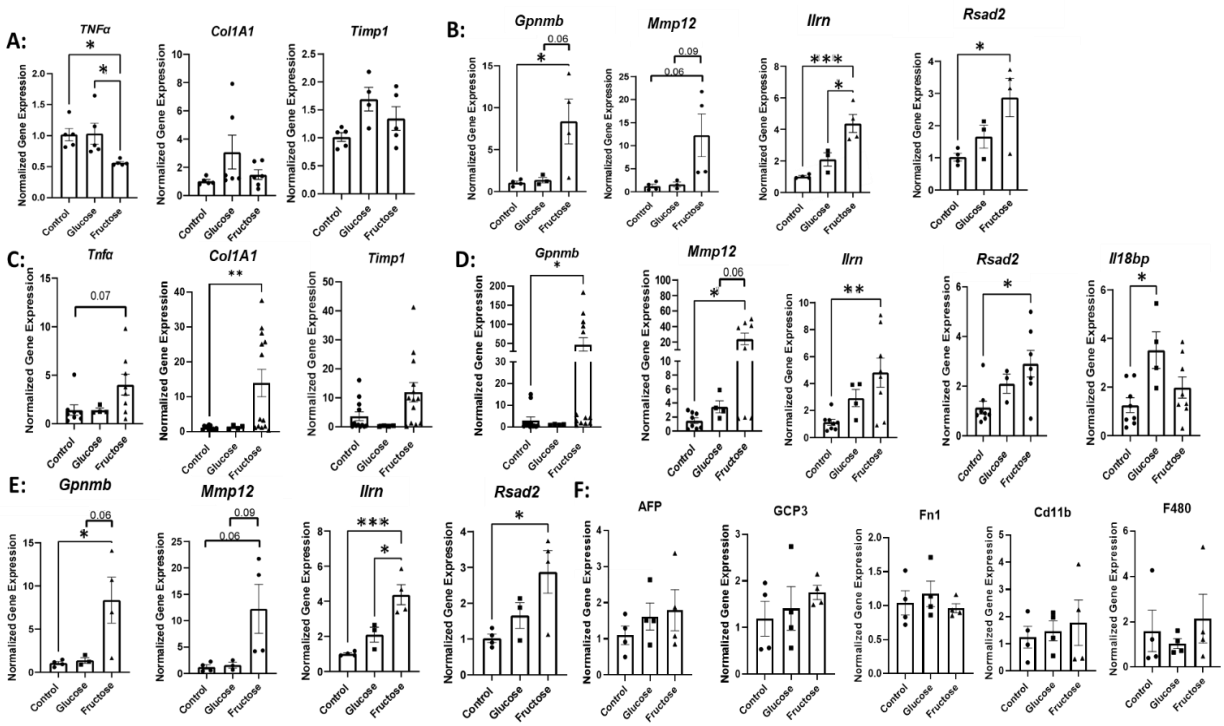

Figure 19: Chronic Fructose Diet Increases Anti-Inflammatory and Profibrotic Associated Gene Expression in Liver and CD11b^{+}F4/80^{+} Cells. Livers were harvested and processed for RT qPCR as well as sorted into Cd11b+F4/80+ populations for RT qPCR. **A:** 4-month liver RNA expression of inflammatory and fibrotic proteins *Tnfα Col1a1* and *Timp1*. **B:** 4-month anti-inflammatory and fibrosis associated genes *Gpnmb*, *Mmp12*, *Il1rn* and *Rsad2*. **C:** 8 month inflammatory and fibrotic expression of *Tnfα Col1a1* and *Timp1*. **D:** 8 month anti-inflammatory and fibrosis associated genes *Gpnmb, Mmp12*, *Il1rn*, *Rsad2* and *I18bp*. **E:** Cd11b^{+}F4/80^{+} cell fractions analyzed by RT qPCR for genes *Gpnmb, Mmp12*, *Il1rn* and *Rsad2*. **F:** Genes associated with liver cancer in 8 month liver tissues. * $p<0.05$, *** $p<0.001$. Control (n=8), Glucose (n=4) and Fructose (n=8) for Liver. Data are representative of 2 independent experiments and shown as means ± SEMs. Control (n=4), Glucose (n=4), Fructose (n=4) for Cd11b^{+}F4/80^{+} cells. Data are representative of 1 independent experiment and shown as means ± SEMs.

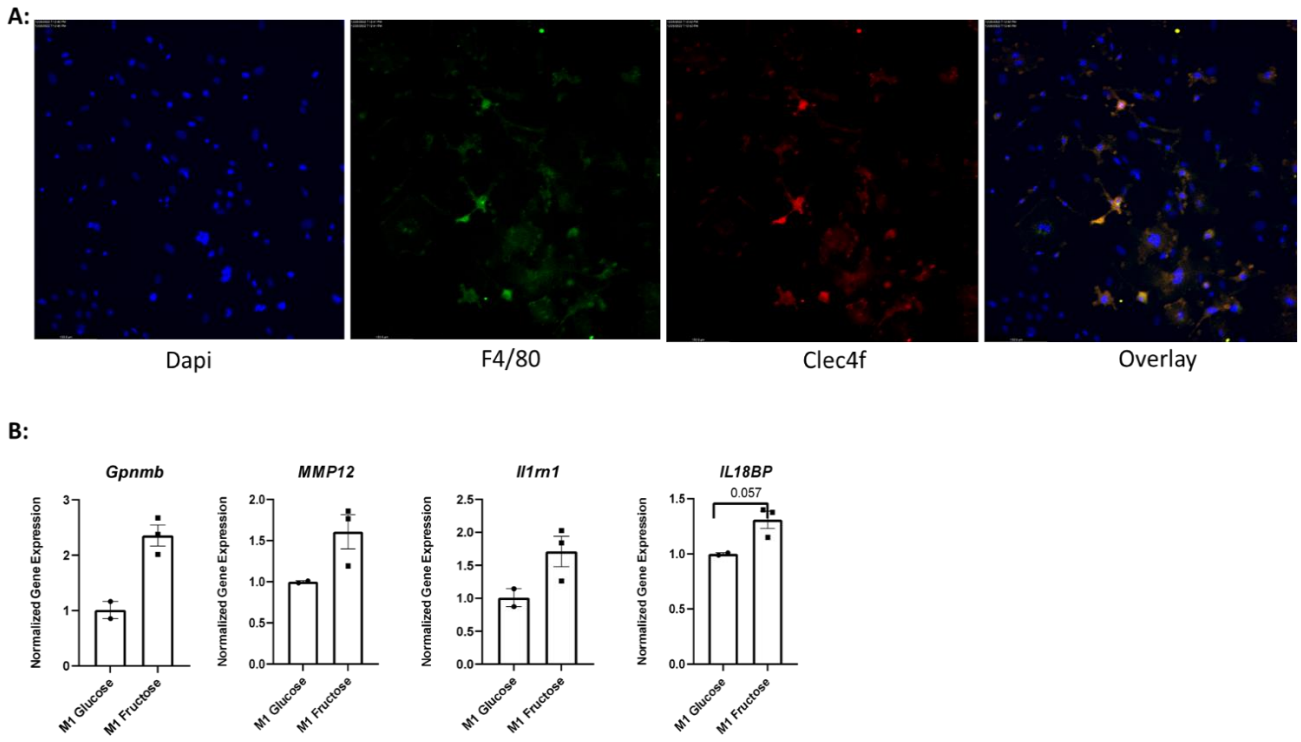

Figure 20: Fructose Increases Anti-inflammatory and Fibrosis Gene Expression in Primary M1 Polarized KC. A: Primary KCs were isolated from livers and cultured in RPMI culturing media. 8 days later KCs were stained for F4/80 and Clec4f for immunohistochemistry confirmation of KC isolation. **B:** Cells were treated with 5mM glucose or fructose with or without 10 ng/ml LPS. Cells were collected for RNA for RT qPCR. Genes of interest are *Gpnmb, Mmp12*, *Il1rn* and *Il18BP* (n=3). Data are representative of 1 experiment and shown as means ± SEMs.

CHAPTER 4: Effect of Fructose Metabolism and Localization in Primary Liver Macrophages After Chronic and Short-Term Fructose Feeding.

4.1 Abstract

Hepatocytes have long been studied as the cell type that is responsible for fructose metabolism in the liver. Many studies have shown the effects of fructose on hepatocyte cell signaling, lipid accumulation and cell activation. However, 30% of the liver is made up of residential macrophages called Kupffer cells. Kupffer cells reside in the liver sinusoid giving them direct access to portal vein mediated circulating fructose. After chronic fructose exposure, hepatocytes may become overwhelmed and can no longer clear fructose from blood capillaries. In this study we use C13 fructose perfusions as well as liver cell fraction isolations to analyze the potential of Kupffer cells to uptake and utilize fructose from the diet after acute and chronic exposure. We have shown both hepatocytes and the non-parenchymal cell fraction containing macrophages utilize fructose through analyzing their metabolic phenotype. We also highlight the technical difficulties of metabolic experiments under physiological conditions.

4.2 Introduction

The short- and long-term effects of fructose diet on non-alcoholic fatty liver disease (NAFLD) progression have long been studied within the liver. Until recently, most research has focused on hepatocyte utilization of fructose as they make up the bulk of the liver and play a role in fructose metabolism and cellular signaling. Recently there has been a push to understand fructose metabolism in non-parenchymal cells of the liver such as monocytes and macrophages. Although groups have characterized the phenotype of immune cells in a fructose environment, the field is lacking in knowledge of how direct fructose exposure and metabolism affects immune cell phenotype and function.

The long standing "two hit" hypothesis explains the importance of hepatocyte fructose metabolism which increases *de novo* lipogenesis (DNL) and lipid accumulation [126]. Short term fructose diets have been shown to increase % fat mass of mice without affecting liver weight [37] [127]. Mice on fructose diet also have elevated triglycerides (TAG) and diglycerides (DAG) in the liver. The increase in lipid storage is accompanied by increased activity of genes involved in fatty acid

synthesis such as acetyl coA carboxylase (ACC), fatty acid synthase (FAS) and Stearoyl-CoA desaturase enzyme 1 (SCD1). In addition, fructose mediated increased citrate synthesis activity may be a mechanism of de novo lipogenesis aiding in the increased lipids of the liver. The effect of induced TAG and DNL has also been reported in long term fructose diet studies in humans showing postprandial hypertriglyceridemia [128-130]. The initial "hit" of lipid accumulation leads to increased prevalence of liver injury, cellular apoptosis and inflammatory signaling as the liver is overwhelmed with lipid metabolism, causing the "second hit" [131] [132]. This hit leaves the liver damaged, scarred, and potentially progressing to a more aggressive form of NAFLD called non-alcoholic steatohepatitis (NASH). Choi et.al. explained the potential for high fructose diet to increase hepatocyte apoptosis through adipocyte cytokine signaling and increased oxidative stress [133]. Although hepatocytes make up the majority of the liver, disease states that cause increased cell death may cause increased immune cell infiltration and proliferation and reduced parenchymal cell populations. Immune cell populations could encounter circulating fructose. For this reason, it is imperative to understand how fructose metabolism affects their function and phenotype over short- and long-term exposure.

Macrophages are important immune cells needed for tissue homeostasis as they assist in dead cell removal, pathogen clearance and stimulate other immune cells. Residential liver macrophages, Kupffer cells (KCs), reside in the liver sinusoid making them the first line of defense when in the presence of pathogens from portal vein blood. Studies have shown fructose diets increase intestinal endotoxin release which activates KCs through toll like receptor 4 (TLR4) signaling. Activation of KCs can lead to increased reactive oxygen species (ROS), tumor necrosis factor alpha (Tnfα) signaling and insulin resistance, ultimately aiding in disease progression [134]. Similarly, Kohli et. al. demonstrates that NASH progression may be fueled by fructose induced macrophage infiltration to the liver which progresses fibrosis and collagen deposition [135]. In both cases, macrophage populations seem to be affected by fructose exposure whether through indirect or direct molecular mechanisms. In addition, our previous works have shown fructose can directly drive KC inflammation and reduce cell viability, potentially through pentose phosphate pathway (PPP) metabolic partitioning.

In this study we aim to understand the effect and metabolism of direct acute and chronic fructose exposure within non-parenchymal cells (NPC)s of the liver. We use portal vein C13 fructose

perfusions to mimic physiological nutrient circulation to gain insight into fructose metabolism within liver cell fractions. Here we demonstrate the need for optimal NPC separation protocols as cell fractioning protocols are not ideal for fructose metabolism tracing. We show that both acute and chronic fructose exposure leads to fructose metabolism in both hepatocytes and NPCs indicating the potential for both cell types to continually metabolize fructose even after chronic exposure.

4.3 Materials and Methods

Mouse Model

C57BL/6 mice were housed at North Carolina State University Biological Resources Facility with ad libitum access to chow food (Laboratory Rodent Diet 5001) and water on a 12- hour light/dark cycle. At the age of 8 weeks, mice were administered 30% fructose or no supplementation in their drinking water for 6 months. Food and water intake was monitored every week as well as body weight. Mice were anesthetized with isoflurane and sacrificed via cervical dislocation. The liver was perfused by portal vein catheter insertion and heart right atrium puncture with 1X PBS until liver became tan in color. PBS was switched to C13 fructose tracing media. The liver was removed and immediately placed in collagenase buffer. All animal procedures were approved by the Institutional Animal Care and Use Committee (IACUC) at North Carolina State University.

C13 Closed Loop Perfusion Optimization for NPC Fraction Separation

This protocol was adapted from Choi [136] and Cabral [137] and is described briefly here as major edits were made for optimization.

Buffers:

Wash- 2%FBS in PBS.

C13 Fructose Perfusion Media- Buffers- 1640 RPMI no glucose with 11.1 mM C13 fructose

Collagenase- 15 mls RPMI, Collagenase II- 12.75mg, Collagenase IV- 9.375 mg, Dnase1 75ul, and protease 15mg.

C13 Closed Loop Perfusion Protocol

1. All buffers and PBS were pre-warmed to 37°C, collagenase should be warmed roughly 30 mins before use.
2. C57BL/6 mice were sacrificed using isoflurane and cervical dislocation.
3. The lower abdomen was cut to expose the body cavity and diaphragm was cut to reveal the heart.
4. A 25G needle and catheter was inserted into the portal vein and clamped to create a tight grip. The pump with PBS started at 60 rpm and the liver began to swell and lose color.
5. Clip the Inferior vena cava (IVC) to alleviate PBS flow through.
6. Clamp IVC and add catheter into the suprahepatic IVC.
    a. PBS should flow from pump through portal vein and out the suprahepatic IVC.
7. PBS was perfused for 5 mins to wash debris and red blood cells.
8. 11.1 mM C13 fructose was perfused for an additional 15 mins at 60rpm.
9. After the fructose, the collagenase mixture was added and perfused for 15 mins.
    a. Liver should start to lose shape and rigidity. Remove liver and place into15mls wash buffer.
10. Cut Gibson's capsule and let cells flow out. Transfer to 50 ml conical tube.
11. Added 15 mls wash buffer and spun at 100xg 3 mins 4C with minimal brake.
12. Pour supernatant which is non-parenchymal cells (NPC) and dead hepatocytes and keep on ice.
13. Wash the cells 3X by removing the supernatant, keeping, adding 15mls to pellet and repeating. You should have 4 supernatant collections.
14. The hepatocyte pellet was resuspended in 600ul triazol and split in 300ul and stored in freezer for RNA isolation.
15. Pellet the supernatants at 163 xg 10 mins. Discard the supernatant and resuspend the pellet in 35mls wash.
16. Centrifuge the mix at 25Xg for 3 min. Remove 25mls of buffer and keep (NPC).
17. Add 25mls of fresh buffer to pellet. Spin at 25xg 3 min. This is the second wash. Keep the supernatant and toss the pellet.
18. Pool all supernatants and pellet at 163 xg 10 min. Resuspend in 600ul triazol and split into 2 300ul.

Optimized C13 Perfusion Protocol

Protocol was adapted from Zeng [138] and briefly described here as edits were made for optimization.

Buffers:

Wash Buffer: RPMI no glucose, 2mM L-glutamate, 20mM Hepes (Ph7), 11.1 mM fructose, with phenol

C13 Fructose media- RPMI no glucose, 20mM Hepes (pH 7), 11.1 mM C13 fructose, L-glutamate, with phenol

Collagenase Digestion Media- RPMI no glucose, 11.1 mM fructose, 20mM Hepes (pH 7), L glutamate, phenol, 1mg/1ml Collagenase IV.

1. All buffers were pre-warmed to 37^0C besides C13 fructose. Collagenase should be warmed at least 30 mins before use.
2. C57BL/6 mice were sacrificed using isoflurane and cervical dislocation.
3. The lower abdomen was cut to expose the body cavity and diaphragm was cut to reveal the heart.
4. 22G needle and catheter were inserted into portal vein.
5. Pump with PBS was turned on at 170 RPM. Liver should swell and instantly begin to lose color.
6. Immediately cut the right atrium and allow PBS flow through for 50 mls.
7. Remove liver and wash once with PBS. Place into clean Petri dish with 3 mls of Collagenase IV media.
    a. One lobe was cut for RNA and formalin preparations.
8. Mince the liver in 3mls of digestive buffer and add back to 30 mls of buffer. Keep in water bath for 30 mins, shaking every 5 mins.
9. Repeat until all livers have been done.
10. After digestion, filter the liver sample through 70µm filter into new conical tube.
11. Centrifuge at 300 xg for 5 mins at 4^0C.
12. Remove supernatant and toss. Resuspend pellet in 25mls wash buffer. Repeat centrifugation.

13. Remove supernatant and toss. Resuspend in 25mls of wash buffer. Spin at 50xg 3 mins to pellet hepatocytes. Keep the supernatant that contains NPCs.
14. Spin down the NPCs at 300 xg 5 mins and resuspend in 1 ml wash buffer.
15. Take a cell count of both fractions.
16. Continue to MS sample preparation.

Mass Spectrometry Sample Preparation

Isolated cells were centrifuged at 500 g for 3min before removing medium for a brief wash with 1ml ice cold 0.9% NaCl. Cells were centrifuged at same speed and media was removed. 1mL 80% methanol/water (both HPLC grade) (pre-cooled in -20°C freezer for at least 1hr) was added to samples. Samples were put in-80°C freezer for 15min to further inactivate enzyme activities. Samples were removed and put on dry ice and split into 2, 1.5mL centrifuge tubes. In a pre-cooled centrifuge (4C) samples were spun at 20,000 xg for 10 mins. The supernatant was removed and placed into newly labelled tubes, still 400ul each. The Pellet was kept for protein analysis and supernatant was transferred to a new tube for speed evaporation.

RNA Isolation

Samples were isolated for RNA according to manufacturer's protocol using Direct-zol™ RNA MicroPrep kit (Genesee Scientific). RNA concentration was obtained by nanodrop, and cDNA was made using qscript cDNA supermix following instructions of manufacturer (Quantabio). cDNA was synthesized at 1000 ng using BioRAD iQ5 thermocycler. Cycles were: Priming for 5 minutes at 25°C, RT: 30 minutes at 42°C and RT inactivation for 5 minutes at 85°C. cDNA was used to analyze gene expression by real time polymerase chain reaction (RT q-PCR) using PerfeCta qPCR FastMixII (QUantbio). TaqMan assays used were albumin and F4/80.

Immunohistochemistry

Cells were seeded into black bottom 96 well plates at 1 x 10^5 cells/mL in RPMI culturing media (VWR 1640) with 10% fetal bovine serum (FBS), 5% L-Glutamine, 1% Penicillin/Streptomycin. 2 hours later the wells were washed with 1X PBS 2 times and media was replaced with culturing media. Media was replaced every other day until day 8 where cells were fixed using 4%

formaldehyde. Formaldehyde was replaced with PBS and the plate was stored in fridge until stained. IHC protocol was adapted from cellsignaling.com. Each well received blocking buffer (1X PBS / 5% normal serum / 0.3% Triton™ X-100 buffer) for one hour before being replaced with primary antibody (1X PBS / 1% BSA / 0.3% Triton™ X-100 buffer) which was kept overnight at 4^0C. Antibodies used were Dapi (1:1000), Clec4F (1:400) and F4/80 (1:400) purchased from cell signaling. Primary antibody buffer was removed, and wells were washed 3 times with 1X PBS. The secondary buffer was added at 1:500 in goat anti rat A488 and donkey anti goat A647 which were purchased from cell signalling. The secondary was removed, and wells were washed 3 times with PBS.

Cell Viability

Isolated cells were diluted with 1:2 AO/PI live/dead staining optimized for the cellometer. Cells were focused in brightfield mode before being adjusted via fluorescence focus.

Statistical Analysis

GraphPad Prism 9.3.1 software was used for all statistical analyses. Two-tailed unpaired Student's t-tests were performed for two group comparisons. Two-way ANOVA was performed for genotype versus diet studies followed by multiple T test comparisons. All data is presented as the mean ± SEM. Data was considered statistically significant for $P<0.05$ (*), $P<0.01$ (**), $P<0.001$(***), and $P<0.0001$(****).

4.4 Results

4.4.1 Closed Loop Perfusion Results in Decreased Cell Viability

In order to separate hepatocytes from NPCs of the liver we combined a 15-minute liver perfusion protocol with a cell separation protocol for optimal fructose tracing and cell fraction separation. After isolation, cells were counted using AO/PI dead/live cell staining optimized for cellometer usage. Unfortunately, cell counts revealed a low yield as well as low viability (Table 1). Analysis of RNA expression revealed the separated hepatocyte fraction had elevated expression of albumin compared to NPC while the NPC fraction had increase F4/80 expression compared to hepatocytes (Fig 21A). These results indicate that the closed loop perfusion does not inhibit optimal cell

centrifugation separation. In addition to analyzing gene expression, we confirmed separation by plating the NPC fraction and staining for Clec4f and F4/80 which are known KC surface markers (Fig 21B). After verification of cell separation, we incorporated 11.1 mM C13 fructose in our perfusion buffer to determine the rate of fructose metabolism in both cell fractions. MS tracing revealed fructose carbons in glycolysis and the pentose phosphate pathway (PPP) in both NPC and hepatocytes (Fig 21C, Fig 22A-B,D). Interestingly, carbon partitioning through the tricarboxylic acid cycle (TCA) was limited (Fig 22C). When analyzing upper glycolytic metabolites, we found DHAO and 2PG/3PG to be significantly increased in hepatocytes compared to NPC. This may be due to increased metabolic activity in the hepatocyte fraction, however further metabolic processing looks similar in both fractions, so this cannot be concluded at this time. Taken together, these data indicate the combined C13 fructose perfusion and cell separation protocol work to deliver both pure fractionation and C13 tracing capabilities. In addition, hepatocytes and NPCs are both able to take up and metabolize fructose within 15 minutes of exposure.

Although results indicated fructose metabolism may be happening in NPC fractions early on in fructose exposure, we found our cells to be low in yield and viability after taking a cell count. Not only did this protocol lead to low viability of cells (Table 1), but it was also very hard to reproduce. To achieve the most accurate representation of fructose metabolism in hepatocyte and NPC fractions we next optimized our C13 perfusion and cell separation protocols.

4.4.2 New C13 Fructose Perfusion Increased Cell Yield and Viability

Next, we sought to optimize the perfusion and separation protocol to increase cell yield and viability for MS fructose tracing. A cell count revealed increased cell yield and viability (Table 2), indicating this protocol will be effective in our tracing studies. Immunohistochemistry (IHC) was used to test the separation of liver cells in this new protocol. Wells were stained with KC markers Clec4f and F4/80 followed by dapi to stain for nuclei of cells. IHC revealed effective separation as NPC fractions had high levels of Clec4f and F4/80 expression (Fig 23A). These results confirmed cell separation and increased cell yield and viability, so we continued with this protocol for our C13 fructose tracing studies.

To determine the utilization of fructose in hepatocyte and NPC fractions over chronic exposure, C57BL/6 mice were on chow diet supplemented with 30% fructose drinking water or control water

for 6 months. Mice on fructose water had elevated %weight gain over 6 months, although this was not seen until week 9 and was not significant (Fig 23B). The liver weight of these mice was also slightly increased compared to control, although this was not significant (Fig 24A). Mice on fructose and control diet consumed similar amounts of calories per day of chow food, however, mice on fructose water had elevated calorie consumption compared to control due to excess calories from carbohydrates (Fig 24B). It is important to highlight the increase in calorie consumption in fructose fed mice did not cause significant increase in mouse weight gain over 6 months. Mice were euthanized and both chronic fructose exposed, and control water exposed mice were perfused with 30% C13 fructose for 30 mls. A cell count was taken to verify optimal viability (Table 3).

After separation, cells were prepared for metabolite MS analysis. Although low levels of fructose were detected (Fig 24C), all groups showed intracellular hexose phosphate was present (Fig 24C). Limited upper-level glycolytic metabolites were present in any samples (Fig 24C) which could be due to fast metabolism of hexose phosphate pools, or a lack of metabolic partitioning. Of note, fructose carbons were found in lactate in both cell fractions and at both time points of exposure (Fig 25 A). However, little carbons were found in TCA metabolites, specifically succinate (Fig 25 B). Interestingly, carbon shuttling is present in PPP intermediate Ribose 5 Phosphate in all groups, although this was very minimal and may lead to falsified data (Fig 5C). Taken together these data indicate hepatocytes and NPCs exposed to acute or chronic fructose are able to metabolize fructose, although it is limited.

4.5 Discussion

Historically, studying metabolism *in vivo* has been difficult due to many interworking metabolite pathways as well as metabolite secretion. With the advancements in technology, we gain insight into cellular metabolism within physiological conditions. Understanding KC function and phenotype has been difficult due to limited KC isolation protocols as well as limited cell surface identifying markers of KCs. Most current protocols are hard to execute and reproduce, needing excellent skills in liver perfusion and cell isolation technique. Additionally, protocols vary considerably in digestion buffers, equipment, centrifugation steps and even culturing conditions. These variations make it hard to establish a working protocol for cell isolations that can be used

for culture, metabolic tracing, or RNA extraction. Additionally, the various methods used can lead to unaccountable cell yield and viability as well as sample purity. Although isolation purity and cell viability are tested using flow cytometry or immunohistochemistry staining, these isolations do not always lead to optimized cell culture conditions. However, most protocols agree that some type of liver perfusion is essential for optimal cell separation. The benefit of doing a liver perfusion is that it cleans the liver of red blood cells and debris. The addition of digestion buffer in the perfusion aids in liver digestion and better cell isolation.

Here we show the technical difficulties in replicating KC isolation protocols as our initial protocol led to ideal separation and metabolic tracing but provided limited cell yield and viability. Interestingly, the low cell viability may be a contributing factor to why we saw more fructose carbon shuttling in this experiment compared to our C13 study in which cells had higher viability. The decreased cell viability may slow down metabolism allowing for increased metabolite pools that are captured in C13 tracing studies. However, the danger that lies in accepting these results is that dying cells may have a unique metabolic flux that falsifies the shuttling pattern. To avoid issues with cell viability we found an alternative KC isolation protocol that increased cell yield and viability that was optimal to combine with C13 fructose prefusion. In this study we used mice that were on 30% fructose water for 6 months to compare chronic fructose exposure to cells receiving fructose for the first time. Both groups were perfused with 30% C13 fructose and livers were isolated for MS analysis. Interestingly, the detection of intracellular C13 fructose was very minimal in all groups. However, hexose phosphate was seen in all samples. Hexose phosphate can be either- or- both glucose-6-phosphate and fructose-1-phosphate as the MS cannot separate the metabolites. In the case of this study, the strong M+6 patterning of fructose carbons on hexose phosphate allows for confirmation that fructose was taken up by all cells.

Interestingly, carbons were not found in lower-level glycolytic metabolites, TCA metabolites or PPP metabolites. Lactate was fully labeled which could be due to two different phenomena within the cells. First, there are other cells that reside in the liver that may be able to take up free circulating fructose and begin metabolism. Lactate is a metabolite that is often secreted by cells. It is possible that NPC and Hepatocyte fractions had large lactate pools as they could have taken up the C13 lactate mediated from fructose metabolism from their environment. Second, lactate can be produced through fructose metabolism. In the case of our study, it is likely that lactate was made

from fructose metabolism. The M+3 patterning of lactate would mostly come from an M+6 pattern, like fructose. In addition, M+3 lactate can undergo gluconeogenesis where it is converted back through upper-level glycolysis intermediates. If lactate pools were from the surrounding environment, we would expect to see strong M+3 labeling in hexose phosphate, where we see M+6. Taken together this data indicates that both cell types can take up C13 fructose and begin metabolism, specifically through hexose phosphate and lactate in both acute and chronic fructose exposure.

Although we can conclude NPC and hepatocyte fractions utilize circulating fructose at the same rate, we have limited knowledge about fructose metabolism in either fraction. Again, this highlights the difficulties in these types of experiments where perfusions and isolations are very technically advanced and hard to repeat. Another reason we may see limited carbon shuttling is due to the increased viability of our cell collection. It is possible the length of time it takes to isolate cell fractions and harvest for MS is too long and we missed the metabolic partitioning pattern. Although we see hexose phosphate and lactate present, it may be due to these metabolites being at higher concentrations that withstand the period of time in which it takes to isolate cells for MS analysis. In conclusion, our work highlights the difficulties of carbon tracing in physiological conditions, but we show the potential for NPC and hepatocytes to uptake circulating fructose after both acute and chronic exposure.

4.6 Figures and Figure Legends

Table 1: Representative Cell Yield and Viability from Closed Loop Circulation

Closed Circulation	Fraction	Cells/ml	Viability (%)
	Hep	2* 10^5	18
	NPC	2.9* 10^5	2

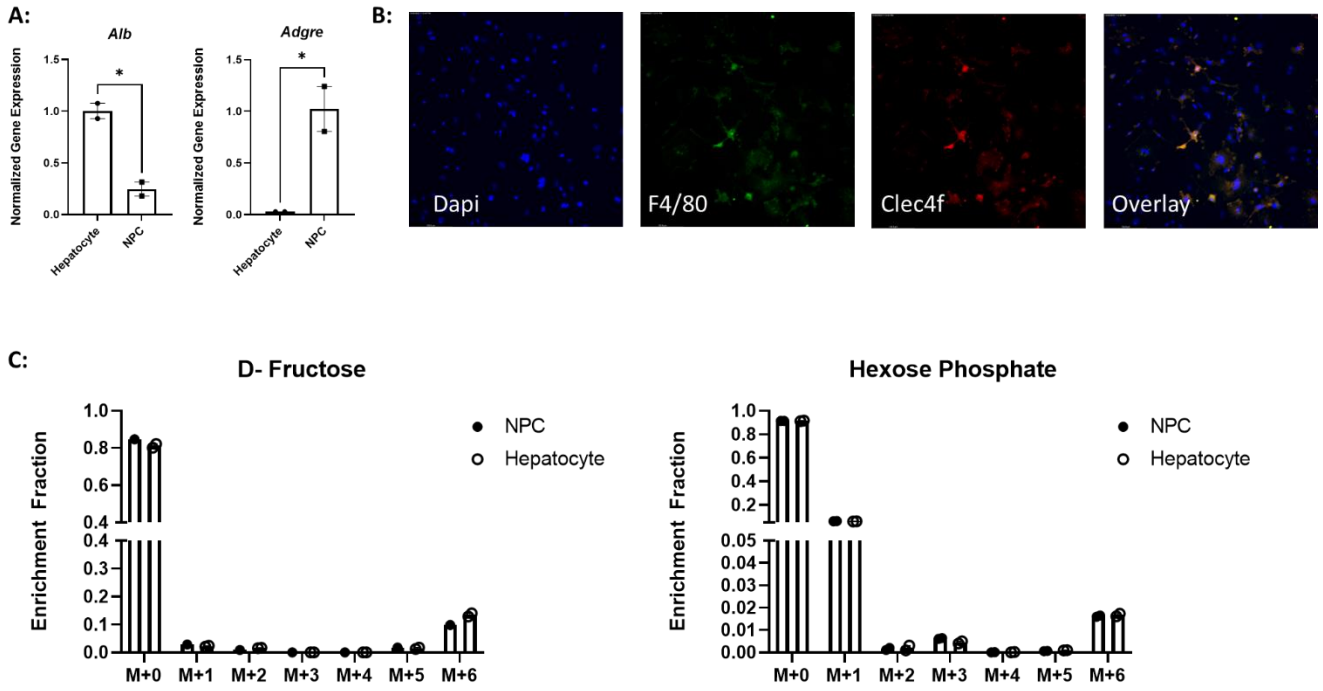

Figure 21: Closed Loop Perfusion leads to NPC and Hepatocyte Separation. Livers were perfused with PBS to wash out red blood cells and debris. C13 fructose was perfused for 15 minutes before the liver was excised and mechanically digested. Cell fractions were separated by centrifugation and fractions were plated for immunohistochemistry or harvested in triazol for RNA. A: RT qPCR analysis of albumin and F4/80 in hepatocyte and NPC fractions. B: Cells were plated and stained for F4/80 and Clec4f at 1:400 dilution overnight to verify KC isolation. Cells were harvested for C13 MS tracing by methanol extraction. C: Metabolites fructose and hexose phosphate.

Table 2: Representative Cell Yield and Viability from PLOS

PLOS	Fraction	Cells/ml	Viability (%)
	Hep	4.8* 10^5	56
	NPC	7.35* 10^5	52

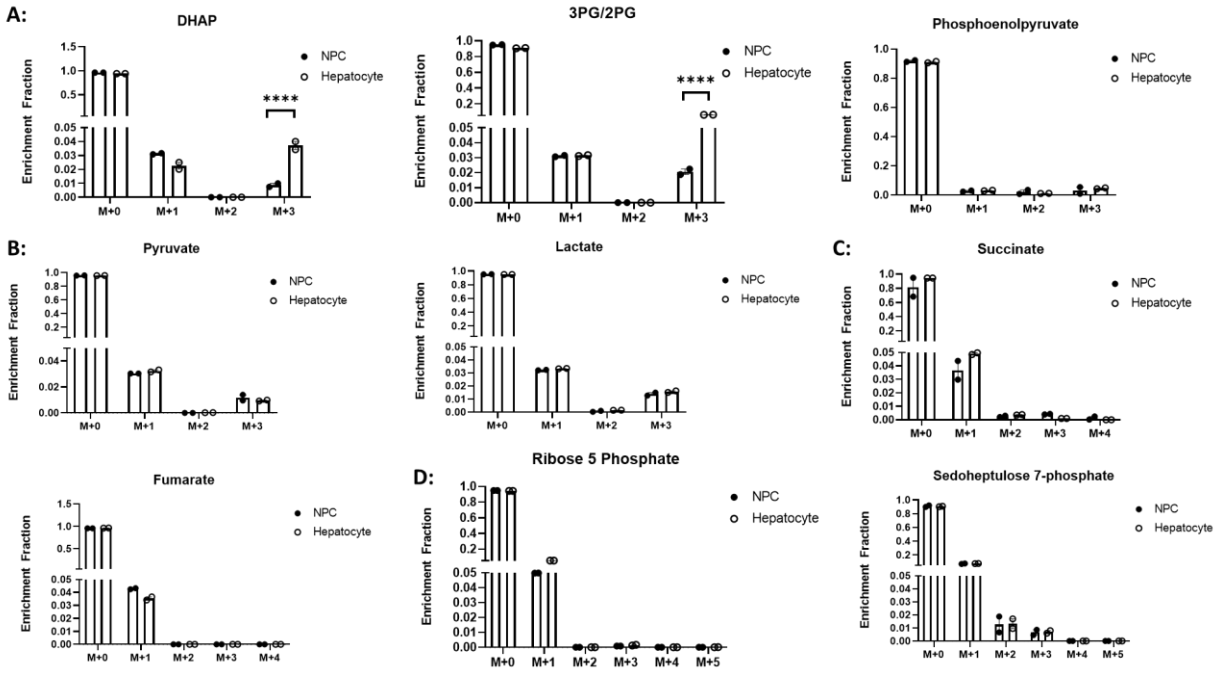

Figure 22: Fructose Carbon Partitioning in NPC and Hepatocyte Fractions. Cells were isolated from the liver using the PLOS one protocol. Cells were harvested for MS using methanol extraction. A: glycolysis intermediates. B: Pyruvate and Lactate. C: TCA cycle intermediates. D: PPP intermediates.

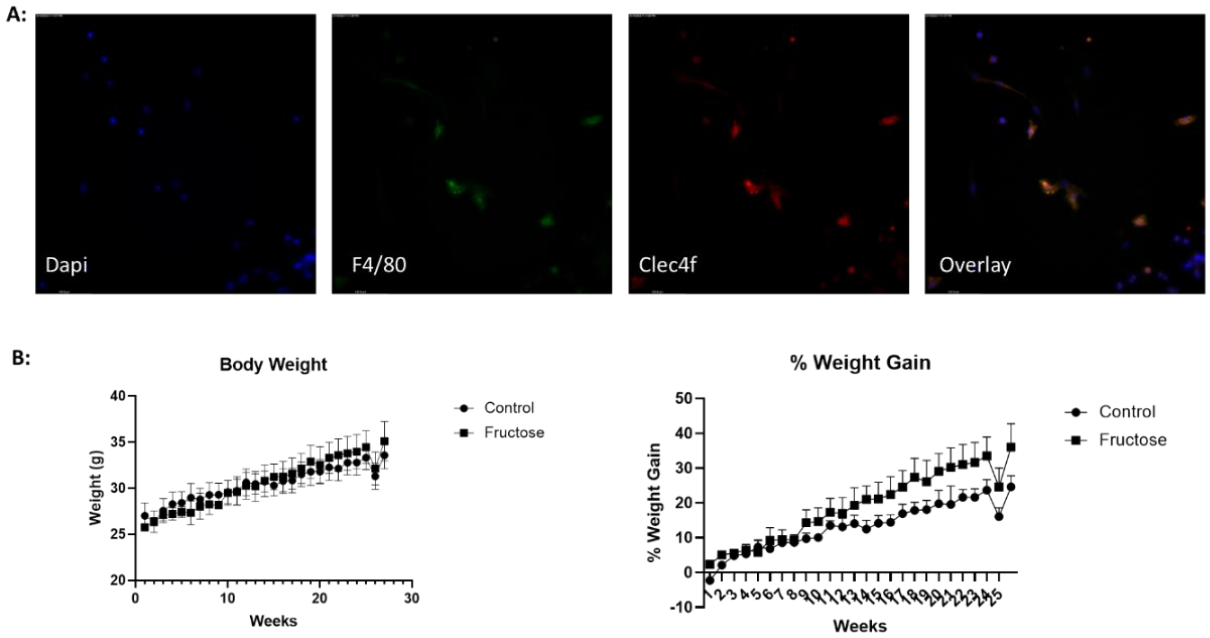

Figure 23: Mice on Fructose Diet do not Gain Weight. C57BL/6 were on chow diet for 6 months supplemented with 30% fructose water or control water. **A:** Livers were perfused and isolated for NPC fraction. Cells were plated and stained for KC markers F4/80 and Clec4f at 1:400 dilution overnight. **B:** Body weight.

Table 3: Representative Cell Yield and Viability from C13 Study

C13 Experiment	Treatment	Fraction	Cells/ml	Viability (%)
	Control	Hep	4.12* 10^5	61
		NPC	1.78* 10^6	54
	Fructose	Hep	1.1* 10^6	40
		NPC	1.33* 10^6	30

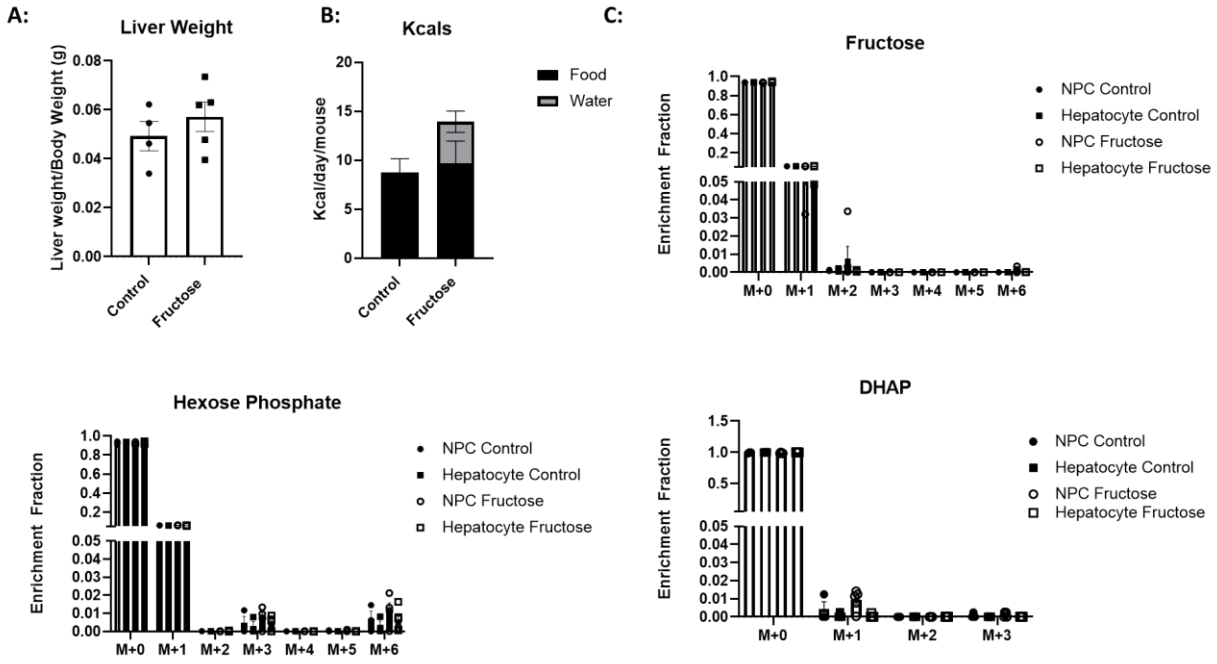

Figure 24: Fructose Metabolites After Acute and Chronic Fructose Exposure. C57BL/6 were on chow diet for 6 months supplemented with 30% fructose water or control water. **A:** Livers were excised and weighed. **B:** Food and water consumption was taken weekly and analyzed for total calories consumed per day per mouse. **C:** Livers were perfused with C13 fructose and mechanically digested for NPC and Hepatocyte fractions. Cells were harvested for MS using MetOH extraction. Data representative of 1 experiment, n=3.

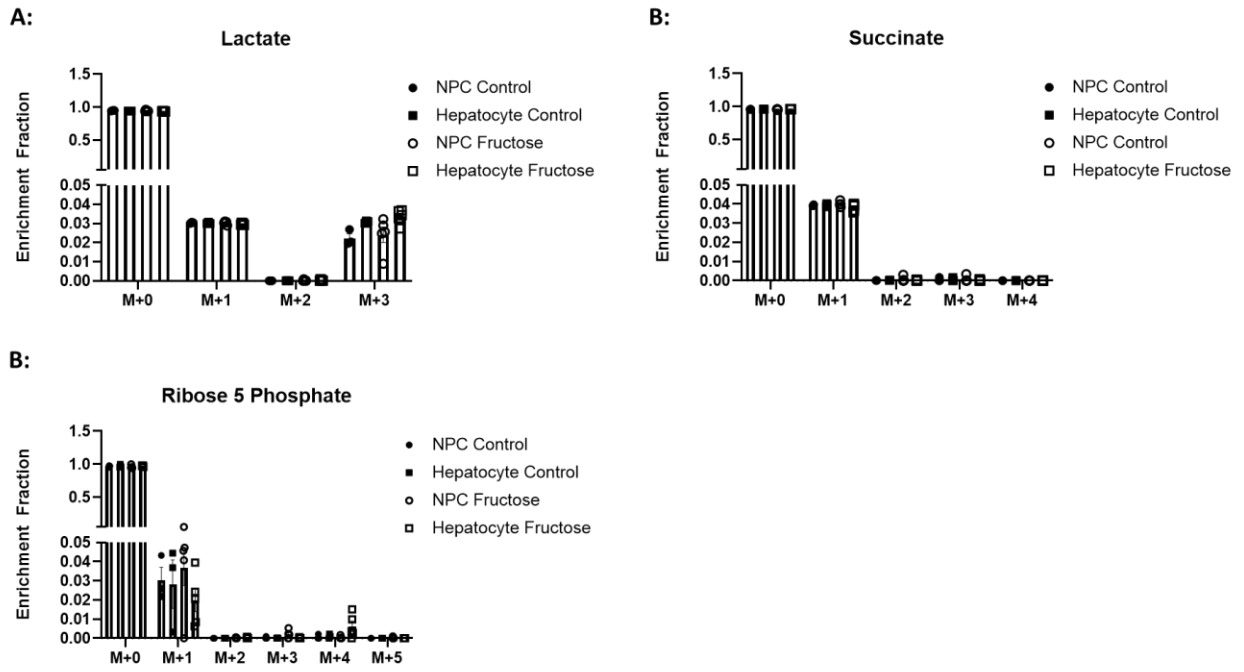

Figure 25: Fructose Metabolite Shuttling After Acute and Chronic Fructose Exposure. C57BL/6 were on chow diet for 6 months supplemented with 30% fructose water or control water. Livers were perfused with C13 fructose and mechanically digested for NPC and Hepatocyte fractions. Cells were harvested for MS using MetOH extraction. **A:** glycolysis intermediates, **B:** TCA intermediates, and **C:** PPP intermediates. Data representative of 1 experiment, n=3.

CHAPTER 5: Conclusions

5.1 Fructose Metabolism and Macrophages

The monosaccharide fructose has become a point of interest as studies show correlations between increased weight gain, insulin resistance and prevalence of NAFLD with increased fructose consumption. Although many works have summarized the effects of fructose on hepatocytes of the liver, the effect of fructose metabolism on residential and recruited macrophages is widely unknown. This work combines *in vitro* and *in vivo* methodology to gain insight into fructose metabolism and its effects on KC phenotype and function. By using IMKC, RAW and J774.1 macrophages we show the ability of fructose uptake potentially through HK mediated phosphorylation within these cells. In addition, fructose uptake and metabolism decrease cell viability in IMKC and J774 .1 while increasing proliferation in IMKC. Fructose significantly upregulated *Tnfα* in M1 macrophages. Interestingly, *Il6* expression was unique across M1 macrophages where fructose increased *Il6* in IMKC, decreased expression in J774.1 and had no response in RAW cells compared to glucose. Although fructose had no effect of fibrotic gene expression of *Timp1* in IMKC, fructose increased expression in J774.1 in both M0 and M1 conditions. Similar in both IMKC and J774.1, fructose induced expression of *Gpnmb* (M0 and M1) but decreased expression of *Il1b* in M1 cells. Fructose increased genes associated with the anti-inflammatory and fibrosis response in M0 and M1 IMKC. These data indicate the direct involvement of fructose metabolism in regulation of genes associated with inflammation and fibrosis.

5.2 Pentose Phosphate Pathway and Inflammation

To determine the mechanism for fructose induced gene expression within macrophages we used C13 fructose tracing through MS analysis. Analysis revealed fructose carbon shuttling through glycolysis and the PPP with little carbon partitioning in the TCA cycle. This result is unique to our studies as others have found fructose to increase TCA partitioning. Our results may be indicative of using IMKC which have a similar phenotype as residential KCs. However, this response was also seen in RAW and J774.1 cells. In addition, other studies used higher concentrations of fructose at 11.1 mM fructose compared to 5mM in our studies. However, we also analyzed fructose metabolism at 25mM and still detected significant partitioning through the PPP. In order to

determine if PPP carbon partitioning had an effect on fructose mediated gene regulation, we used 6-AN, DHEA and G6PDH siRNA to inhibit the PPP. In IMKC, PPP inhibition increased gene expression of *Il6*, *Gpnmb* and *Rsad2* in M0 conditions. In addition, 6-AN decreased fructose induced expression of *Il6*, *Gpnmb*, *Il1rn* and *Rsad2* in M1. DHEA mediated inhibition of the PPP caused an increase in both M0 and M1 of *Il6* expression. Unique to J774.1 cells, DHEA decreased fructose and LPS induced *Tnfα* and *Timp1* expression. The use of G6PDH siRNA for PPP inhibition further induced fructose mediated increase of *Gpnmb*, *Mmp12,* and *Il1rn* in M0 IMKC and increased *Il6* in M0 of J774.1. Although fructose alone stimulated genes associated with inflammation and fibrosis compared to glucose, metabolites generated by the PPP may serve to suppress the expression of these genes as inhibition of the PPP lead to increased expression.

5.4 Genes Associated with NASH Phenotype

With insights into fructose metabolism and regulation of gene expression *in vitro*, we sought to determine the effect of chronic fructose exposure on macrophage liver populations. Mice on 6-8 months of fructose water showed elevated weight gain, liver weight and adipose weight compared to control diets. The increase in liver weight was accompanied by increased acylcarnitine and diglyceride lipid species, increased liver damage through oval hyperplasia and collagen deposition. In addition, fructose samples had upregulated levels of *Fasn*, a gene upregulated in cases of fatty acid elongation. To gain insight into fructose mediated effects on liver macrophages we used scRNAseq to genetically map macrophage subsets. After genetic clustering, this analysis revealed fructose treatment led to KC population decrease and increasing transitioning monocytes. The reduction of KCs was further confirmed by flow cytometry where KCs ($F480^{+}CD64^{-}CLEC4F^{+}$) were significantly reduced in fructose treated mice. Interestingly, genes associated with fructose metabolism (*Hk2, Hk3* and *Aldoa*) and the PPP (*G6pdx*) were upregulated in fructose treated samples, although these were not specific to KCs. After analyzing upregulated genes specific to fructose in KCs, we found genes associated with fibrosis and the anti-inflammatory response *Mmp12*, *Il1rn* and *Rsad2* to be increased. Although we cannot be sure the upregulated anti-inflammatory gene expression is a direct response to fructose metabolism, the similarities between the chronic fructose diet mouse study and *in vitro* IMKC study are undeniable. Based on our *in vitro* data supplemented with new *in vivo* findings, fructose metabolism through the PPP regulates genes involved in inflammation and fibrosis while causing a decrease in KC viability.

5.5 Impact of fructose Concentration and Delivery

High concentrations of fructose have been shown to cause intestinal overload and un-metabolized fructose can be deposited into the liver via the portal vein. As macrophages reside in the liver sinusoid, they have direct exposure to circulating free fructose. Currently, literature summarizes that hepatocytes take on the bulk of fructose metabolism. In our studies, we show that KCs can uptake and utilize fructose. For this reason, we investigated if macrophages could metabolize fructose at the time of exposure or over chronic fructose exposure. Optimization of C13 fructose perfusion with NPC and hepatocyte cell fractionation showed fructose metabolism within both fractions. At the same time, fructose metabolites in both conditions of acute and chronic fructose exposure were seen in both fractions. These results indicate fructose metabolism may be happening within macrophages of the liver at the same time as hepatocyte metabolism. In addition, chronic fructose exposure does not seem to inhibit NPC or hepatocyte ability to utilize fructose.

5.6 Limitations of Study

Although these studies offer insight into fructose metabolism in macrophages, there are limitations to our studies. Chronic diet studies are a challenge due to physiological variation between biological replicates that is hard to avoid with low replicate numbers. For example, two out of five fructose treated mice had fibrotic livers and higher prevalence of genes associated with fibrosis and liver damage. However, not every mouse responded this way, where some had elevated adipose and liver tissue as well as increased weight gain. The differences in liver phenotype can lead to variations in gene expression and analysis of macrophage phenotype and function. In addition, providing fructose in the water at libitum causes inconsistencies with concentrations of fructose each mouse is consuming. Based on our findings of supplementing fructose through water, we will conduct a power analysis which will help to determine the number of mice per fructose treatment that would be needed to provide statistical relevance to our studies. In addition, providing fructose treatment through oral gavage would control fructose dosage in each mouse to confirm equal concentrations of consumption. These changes are difficult to implement due to mouse housing facilities and costs as well as intensity and frequency of oral gavage over a period of multiple months.

In addition to these limitations, liver cell isolation and culture has been an issue. Although we have worked on many protocols, we have yet to culture KCs successfully for extended fructose

treatments. For example, the current perfusion protocol has increased our KC yield and viability, but culturing these cells has been difficult. To start, KCs are isolated from selective adherence which leaves room for potential contamination of semi-adherent cells. In addition, cells need to be cultured for at least 8 days before any treatment which has been difficult to do when seeding low viability and low yield cells. To gain insight into primary KC fructose metabolism, isolation and culture of KCs with C13 fructose is essential. Although the use of IMKC could offer information into carbon shuttling, the use of primary KCs would provide more physiological relevance. The limitations of this experiment reside in proper cell isolation and culturing conditions as well as duration of cell harvest for MS tracing. The fructose perfusion studies are limited by perfusion and isolation protocols as they are labor intensity and time consuming. The protocol itself is very technically difficult and is complicated to replicate for every sample. Once C13 fructose is supplied to the liver, metabolism begins immediately. During the cell isolation and MS sample preparations, it is possible the cells have metabolized C13 fructose in its entirety, leading to inaccurate MS tracing data. In addition, the multiple steps of washing and centrifugation may decrease metabolite pools aiding in missed information for metabolite tracing.

We propose an alternative *in vivo* method to determine which cells take up fructose that would alleviate the stresses of quick digestion and preparation for MS. One method includes utilizing fluorescent tagged fructose that is unable to be metabolized by cells. This system would trap fructose in cell populations that are able to uptake fructose at time of exposure. Flow cytometry or fluorescent imagining will provide insight into NPC and hepatocyte fructose uptake, although this would not provide information about fructose metabolism.

Although these studies offer insight into the role of fructose metabolism in liver macrophages, there remains a gap in knowledge relating to the involvement of the PPP in chronic fructose environments. Glucose 6 Phosphate Dehydrogenase (G6PDH) is an enzyme that catalyzes the rate limiting step in the oxidative phase of the PPP. The oxidative pathway is important for cell redox maintenance as it produces reducing reagent NADPH. Fructose has been shown to increase G6PDH activity in liver and increase serum triglycerides in G6PDH knockout mice [139]. NADPH pools are also utilized by hepatocytes as reducing reagents for alpha glycerol phosphate production, fatty acid elongation and triglyceride synthesis in DNL [140]. Of interest, fructose exposure has been shown to increase DNL through upregulation of genes involved in fatty acid

elongation. Our data may demonstrate that this response is also mediated through fructose upregulation of PPP shuttling thus providing reducing reagent NADPH for DNL production. Future directions for this project would be to measure NADP+/NADPH levels in the presence of fructose in macrophages. Lipid synthesis is important for macrophage phagocytosis, cytokine production and bioenergetics [141]. Recent studies have found lipid laden macrophages may be a result of hypoxia induced glucose uptake leading to lipid synthesis and storage [142]. It is possible that fructose partitioning could drive lipid synthesis through increased NADPH pools yielding increased lipid accumulation in macrophages. However, our current findings do not find elevations in saturated fatty acids and acetyl CoA in IMKC or J774.1 macrophages. Future studies will conduct a targeted lipidomics analysis of fructose treated macrophages.

In addition to playing a role in DNL, NADPH is also important for ROS production, especially in macrophages. G6PDH deficiency can lead to increased ROS as NADPH pools with antioxidant properties are decreased. However, NADPH is also the substrate for NADPH oxidase (NOX) which functions to produce ROS needed for macrophage phagocytosis and immune response [143] [144]. G6PDH suppression has been shown to downregulate NOX, thus reducing ROS which leads to decreased pro-inflammatory response in M1 [145]. Although M1 macrophages can lead to uncontrolled inflammation and disease, it is important to establish injury signaling and activation of immune cells to clear debris and pathogens. Obesity is hallmarked by increased white adipose tissue (WAT) and is often coupled with NAFLD. The increase in WAT induces Tnfα secreting macrophage and immune cell infiltration to adipose which increases overall adipose inflammation [146]. However, G6PDH deficiency in adipocytes may lead to decreased disease status as the reduction in inflammatory signaling reducing adipocyte inflammation and thus macrophage infiltration [147]. In our studies, we showed macrophage exposure to fructose increased *Tnfα* expression in both M0 and M1 conditions. The upregulation of *Tnfα* may be due to increased NADPH availability from carbon shuttling through the PPP. Future directions may include monitoring ROS levels in the presence of fructose with and without an active PPP and compare the impact on anti-inflammatory and wound healing genes and proteins. This could offer insight into the direct mechanism for how fructose mediates macrophage inflammation, potentially through NADPH mediated increased ROS production from NOX.

As G6PDH deficiency has implications in disease and inflammation another future project would be to use G6PDH knockout mice to examine liver morphology and macrophage phenotype in mice on acute and chronic fructose diet. If the PPP does play an important role in suppressing the anti-inflammatory response of KCs, then knockdown of this pathway may lead to a lessened disease state mediated by fructose exposure. In addition to increased anti-inflammatory response, G6PDH KO background with fructose may increase KC populations as we have shown fructose to increase *Mmp12.* MMP12 is associated with regulating cell proliferation but also promotes scar formation, angiogenesis, and monocyte trafficking [125]. In our studies, we show fructose treatment decreases KC populations while having a fully active PPP. It is possible that G6DPH KO mice on fructose diet may have elevated KC proliferation due to increases in *Mmp12* expression.

5.7 Final Summary of Work

In conclusion, this work has elevated our knowledge of fructose metabolism within macrophages of the liver. We have shown through *in vitro* and *in vivo* studies that fructose induces an anti-inflammatory and profibrotic response while decreasing cell viability. In addition, the PPP plays a suppressive role in anti-inflammatory response in KC. Although our results have a large impact on understanding the effects of fructose on liver disease, we strive to uncover the missing links between fructose metabolism through the PPP and its connection with impaired resolution of hepatic inflammation that leads to liver fibrosis and complications.

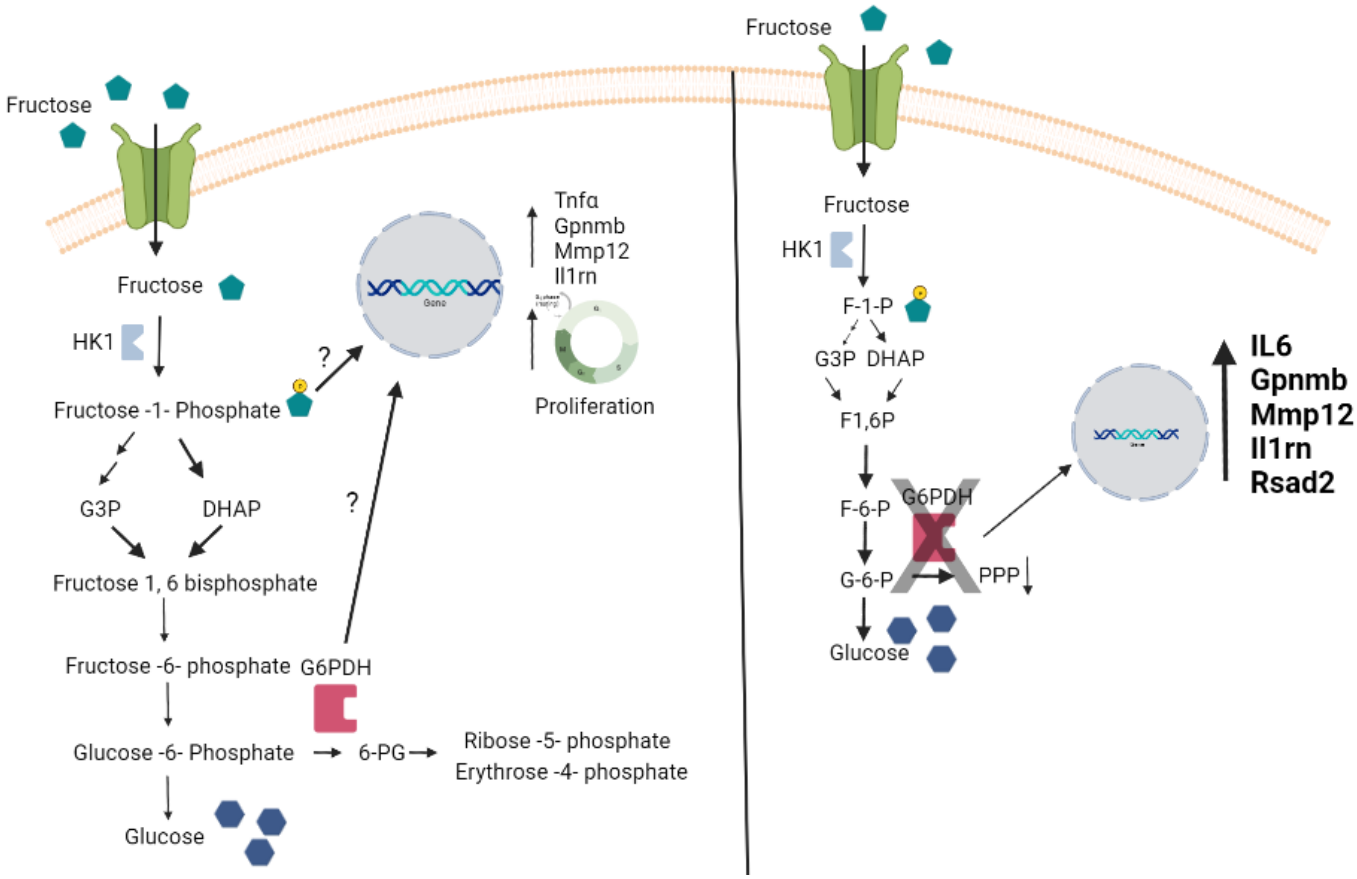

Figure 3.1: Fructose metabolic partitioning through the PPP Increases Anti-inflammatory Gene Expression. Fructose is phosphorylated by HK1 within IMKC. MS tracing reveals fructose carbon shuttling through the PPP. Phosphorylation and metabolism lead to increased cell proliferation and anti-inflammatory gene expression. G6PDH knockdown reveals the PPP is suppressive of anti-inflammatory gene expression as inhibition increases expression.

REFERENCES

1. Bray, G.A., S.J. Nielsen, and B.M. Popkin, *Consumption of high-fructose corn syrup in beverages may play a role in the epidemic of obesity.* Am J Clin Nutr, 2004. **79**(4): p. 537-43.
2. Bergheim, I., et al., *Antibiotics protect against fructose-induced hepatic lipid accumulation in mice: role of endotoxin.* J Hepatol, 2008. **48**(6): p. 983-92.
3. Aoun, R., et al., *Dietary fructose and its association with the metabolic syndrome in Lebanese healthy adults: a cross-sectional study.* Diabetol Metab Syndr, 2022. **14**(1): p. 29.
4. Hallfrisch, J., *Metabolic effects of dietary fructose.* FASEB J, 1990. **4**(9): p. 2652-60.
5. Bhosale, S.H., M.B. Rao, and V.V. Deshpande, *Molecular and industrial aspects of glucose isomerase.* Microbiol Rev, 1996. **60**(2): p. 280-300.
6. Rippe, J.M. and T.J. Angelopoulos, *Sucrose, high-fructose corn syrup, and fructose, their metabolism and potential health effects: what do we really know?* Adv Nutr, 2013. **4**(2): p. 236-45.
7. Diggle, C.P., et al., *Ketohexokinase: expression and localization of the principal fructose-metabolizing enzyme.* J Histochem Cytochem, 2009. **57**(8): p. 763-74.
8. Jang, C., et al., *The Small Intestine Converts Dietary Fructose into Glucose and Organic Acids.* Cell Metab, 2018. **27**(2): p. 351-361.e3.
9. Lambertz, J., et al., *Fructose: A Dietary Sugar in Crosstalk with Microbiota Contributing to the Development and Progression of Non-Alcoholic Liver Disease.* Front Immunol, 2017. **8**: p. 1159.
10. Falony, G., et al., *Cross-feeding between Bifidobacterium longum BB536 and acetate-converting, butyrate-producing colon bacteria during growth on oligofructose.* Appl Environ Microbiol, 2006. **72**(12): p. 7835-41.
11. Burant, C.F. and M. Saxena, *Rapid reversible substrate regulation of fructose transporter expression in rat small intestine and kidney.* Am J Physiol, 1994. **267**(1 Pt 1): p. G71-9.
12. Douard, V. and R.P. Ferraris, *Regulation of the fructose transporter GLUT5 in health and disease.* Am J Physiol Endocrinol Metab, 2008. **295**(2): p. E227-37.
13. Barone, S., et al., *Slc2a5 (Glut5) is essential for the absorption of fructose in the intestine and generation of fructose-induced hypertension.* J Biol Chem, 2009. **284**(8): p. 5056-66.
14. Davidson, N.O., et al., *Human intestinal glucose transporter expression and localization of GLUT5.* Am J Physiol, 1992. **262**(3 Pt 1): p. C795-800.
15. Ferraris, R.P., *Dietary and developmental regulation of intestinal sugar transport.* Biochem J, 2001. **360**(Pt 2): p. 265-76.
16. Kretowicz, M., et al., *The impact of fructose on renal function and blood pressure.* Int J Nephrol, 2011. **2011**: p. 315879.
17. Khitan, Z. and D.H. Kim, *Fructose: a key factor in the development of metabolic syndrome and hypertension.* J Nutr Metab, 2013. **2013**: p. 682673.
18. Mäenpää, P.H., K.O. Raivio, and M.P. Kekomäki, *Liver adenine nucleotides: fructose-induced depletion and its effect on protein synthesis.* Science, 1968. **161**(3847): p. 1253-4.
19. Grossbard, L. and R.T. Schimke, *Multiple hexokinases of rat tissues. Purification and comparison of soluble forms.* J Biol Chem, 1966. **241**(15): p. 3546-60.
20. Andres-Hernando, A., et al., *Deletion of Fructokinase in the Liver or in the Intestine Reveals Differential Effects on Sugar-Induced Metabolic Dysfunction.* Cell Metab, 2020. **32**(1): p. 117-127.e3.

21. Shepherd, E.L., et al., *Ketohexokinase inhibition improves NASH by reducing fructose-induced steatosis and fibrogenesis.* JHEP Rep, 2021. **3**(2): p. 100217.
22. Gutierrez, J.A., et al., *Pharmacologic inhibition of ketohexokinase prevents fructose-induced metabolic dysfunction.* Mol Metab, 2021. **48**: p. 101196.
23. Li, X., et al., *A splicing switch from ketohexokinase-C to ketohexokinase-A drives hepatocellular carcinoma formation.* Nat Cell Biol, 2016. **18**(5): p. 561-71.
24. Kim, J., et al., *Ketohexokinase-A acts as a nuclear protein kinase that mediates fructose-induced metastasis in breast cancer.* Nat Commun, 2020. **11**(1): p. 5436.
25. Hannou, S.A., et al., *Fructose metabolism and metabolic disease.* J Clin Invest, 2018. **128**(2): p. 545-555.
26. Todoric, J., et al., *Fructose stimulated de novo lipogenesis is promoted by inflammation.* Nat Metab, 2020. **2**(10): p. 1034-1045.
27. Taylor, S.R., et al., *Dietary fructose improves intestinal cell survival and nutrient absorption.* Nature, 2021. **597**(7875): p. 263-267.
28. Tan, R., et al., *Intestinal Microbiota Mediates High-Fructose and High-Fat Diets to Induce Chronic Intestinal Inflammation.* Front Cell Infect Microbiol, 2021. **11**: p. 654074.
29. Montrose, D.C., et al., *Dietary Fructose Alters the Composition, Localization, and Metabolism of Gut Microbiota in Association With Worsening Colitis.* Cell Mol Gastroenterol Hepatol, 2021. **11**(2): p. 525-550.
30. DiNicolantonio, J.J. and S.C. Lucan, *Is fructose malabsorption a cause of irritable bowel syndrome?* Med Hypotheses, 2015. **85**(3): p. 295-7.
31. Jones, H.F., R.N. Butler, and D.A. Brooks, *Intestinal fructose transport and malabsorption in humans.* Am J Physiol Gastrointest Liver Physiol, 2011. **300**(2): p. G202-6.
32. Kawabata, K., et al., *A high-fructose diet induces epithelial barrier dysfunction and exacerbates the severity of dextran sulfate sodium-induced colitis*. 2018: International Journal of Molecular Medicine.
33. Masoodi, M., et al., *Metabolomics and lipidomics in NAFLD: biomarkers and non-invasive diagnostic tests.* Nat Rev Gastroenterol Hepatol, 2021. **18**(12): p. 835-856.
34. Taskinen, M.R., C.J. Packard, and J. Borén, *Dietary Fructose and the Metabolic Syndrome.* Nutrients, 2019. **11**(9).
35. Janevski, M., et al., *Fructose containing sugars modulate mRNA of lipogenic genes ACC and FAS and protein levels of transcription factors ChREBP and SREBP1c with no effect on body weight or liver fat.* Food Funct, 2012. **3**(2): p. 141-9.
36. Mamikutty, N., Z.C. Thent, and F. Haji Suhaimi, *Fructose-Drinking Water Induced Nonalcoholic Fatty Liver Disease and Ultrastructural Alteration of Hepatocyte Mitochondria in Male Wistar Rat.* Biomed Res Int, 2015. **2015**: p. 895961.
37. Softic, S., et al., *Divergent effects of glucose and fructose on hepatic lipogenesis and insulin signaling.* J Clin Invest, 2017.
38. Abdelmalek, M.F., et al., *Increased fructose consumption is associated with fibrosis severity in patients with nonalcoholic fatty liver disease.* Hepatology, 2010. **51**(6): p. 1961-71.
39. Ter Horst, K.W. and M.J. Serlie, *Fructose Consumption, Lipogenesis, and Non-Alcoholic Fatty Liver Disease.* Nutrients, 2017. **9**(9).
40. Yu, S., et al., *The Contribution of Dietary Fructose to Non-alcoholic Fatty Liver Disease.* Front Pharmacol, 2021. **12**: p. 783393.

41. Loos, R.J.F. and G.S.H. Yeo, *The genetics of obesity: from discovery to biology.* Nat Rev Genet, 2022. **23**(2): p. 120-133.
42. Toop, C.R. and S. Gentili, *Fructose Beverage Consumption Induces a Metabolic Syndrome Phenotype in the Rat: A Systematic Review and Meta-Analysis.* Nutrients, 2016. **8**(9).
43. Jürgens, H., et al., *Consuming fructose-sweetened beverages increases body adiposity in mice.* Obes Res, 2005. **13**(7): p. 1146-56.
44. Legeza, B., et al., *Fructose, Glucocorticoids and Adipose Tissue: Implications for the Metabolic Syndrome.* Nutrients, 2017. **9**(5).
45. Varma, V., et al., *Metabolic fate of fructose in human adipocytes: a targeted.* Metabolomics, 2015. **11**(3): p. 529-544.
46. Pektas, M.B., et al., *Dietary Fructose Activates Insulin Signaling and Inflammation in Adipose Tissue: Modulatory Role of Resveratrol.* Biomed Res Int, 2016. **2016**: p. 8014252.
47. Magliano, D.C., et al., *Short-term administration of GW501516 improves inflammatory state in white adipose tissue and liver damage in high-fructose-fed mice through modulation of the renin-angiotensin system.* Endocrine, 2015. **50**(2): p. 355-67.
48. Barroso, E., et al., *PPARβ/δ ameliorates fructose-induced insulin resistance in adipocytes by preventing Nrf2 activation.* Biochim Biophys Acta, 2015. **1852**(5): p. 1049-58.
49. Hernández-Díazcouder, A., et al., *High fructose exposure modifies the amount of adipocyte-secreted microRNAs into extracellular vesicles in supernatants and plasma.* PeerJ, 2021. **9**: p. e11305.
50. Zhuang, G., et al., *A novel regulator of macrophage activation: miR-223 in obesity-associated adipose tissue inflammation.* Circulation, 2012. **125**(23): p. 2892-903.
51. Lozano, I., et al., *High-fructose and high-fat diet-induced disorders in rats: impact on diabetes risk, hepatic and vascular complications.* Nutr Metab (Lond), 2016. **13**: p. 15.
52. Kawanishi, N., et al., *Exercise training attenuates hepatic inflammation, fibrosis and macrophage infiltration during diet induced-obesity in mice.* Brain Behav Immun, 2012. **26**(6): p. 931-41.
53. Kohli, R., et al., *High-fructose, medium chain trans fat diet induces liver fibrosis and elevates plasma coenzyme Q9 in a novel murine model of obesity and nonalcoholic steatohepatitis.* Hepatology, 2010. **52**(3): p. 934-44.
54. Wen, Y., et al., *Hepatic macrophages in liver homeostasis and diseases-diversity, plasticity and therapeutic opportunities.* Cell Mol Immunol, 2021. **18**(1): p. 45-56.
55. Mosser, D.M. and J.P. Edwards, *Exploring the full spectrum of macrophage activation.* Nat Rev Immunol, 2008. **8**(12): p. 958-69.
56. Tannahill, G.M., et al., *Succinate is an inflammatory signal that induces IL-1β through HIF-1α.* Nature, 2013. **496**(7444): p. 238-42.
57. Castegna, A., et al., *Pharmacological targets of metabolism in disease: Opportunities from macrophages.* Pharmacol Ther, 2020. **210**: p. 107521.
58. Stein, M., et al., *Interleukin 4 potently enhances murine macrophage mannose receptor activity: a marker of alternative immunologic macrophage activation.* J Exp Med, 1992. **176**(1): p. 287-92.
59. Doyle, A.G., et al., *Interleukin-13 alters the activation state of murine macrophages in vitro: comparison with interleukin-4 and interferon-gamma.* Eur J Immunol, 1994. **24**(6): p. 1441-5.
60. Liu, Y., et al., *Metabolic reprogramming in macrophage responses.* Biomark Res, 2021. **9**(1): p. 1.

61. Jha, A.K., et al., *Network integration of parallel metabolic and transcriptional data reveals metabolic modules that regulate macrophage polarization.* Immunity, 2015. **42**(3): p. 419-30.
62. Guilliams, M., et al., *Spatial proteogenomics reveals distinct and evolutionarily conserved hepatic macrophage niches.* Cell, 2022.
63. Jones, N., et al., *Fructose reprogrammes glutamine-dependent oxidative metabolism to support LPS-induced inflammation.* Nat Commun, 2021. **12**(1): p. 1209.
64. Gligorovska, L., et al., *Macrophage migration inhibitory factor deficiency aggravates effects of fructose-enriched diet on lipid metabolism in the mouse liver.* Biofactors, 2021. **47**(3): p. 363-375.
65. Elchaninov, A., et al., *An Eye on Kupffer Cells: Development, Phenotype and the Macrophage Niche.* Int J Mol Sci, 2022. **23**(17).
66. Dixon, L.J., et al., *Kupffer cells in the liver.* Compr Physiol, 2013. **3**(2): p. 785-97.
67. Gomez Perdiguero, E., et al., *Tissue-resident macrophages originate from yolk-sac-derived erythro-myeloid progenitors.* Nature, 2015. **518**(7540): p. 547-51.
68. Ait Ahmed, Y., et al., *Kupffer cell restoration after partial hepatectomy is mainly driven by local cell proliferation in IL-6-dependent autocrine and paracrine manners.* Cell Mol Immunol, 2021. **18**(9): p. 2165-2176.
69. Hashimoto, D., et al., *Tissue-resident macrophages self-maintain locally throughout adult life with minimal contribution from circulating monocytes.* Immunity, 2013. **38**(4): p. 792-804.
70. Tran, S., et al., *Impaired Kupffer Cell Self-Renewal Alters the Liver Response to Lipid Overload during Non-alcoholic Steatohepatitis.* Immunity, 2020. **53**(3): p. 627-640.e5.
71. Wan, J., et al., *M2 Kupffer cells promote M1 Kupffer cell apoptosis: a protective mechanism against alcoholic and nonalcoholic fatty liver disease.* Hepatology, 2014. **59**(1): p. 130-42.
72. Kim, J.K., *Fat uses a TOLL-road to connect inflammation and diabetes.* Cell Metab, 2006. **4**(6): p. 417-9.
73. Seki, K., et al., *Oral administration of fructose exacerbates liver fibrosis and hepatocarcinogenesis via increased intestinal permeability in a rat steatohepatitis model.* Oncotarget, 2018. **9**(47): p. 28638-28651.
74. Futatsugi, K., et al., *Discovery of PF-06835919: A Potent Inhibitor of Ketohexokinase (KHK) for the Treatment of Metabolic Disorders Driven by the Overconsumption of Fructose.* J Med Chem, 2020. **63**(22): p. 13546-13560.
75. Kazierad, D.J., et al., *Inhibition of ketohexokinase in adults with NAFLD reduces liver fat and inflammatory markers: A randomized phase 2 trial.* Med, 2021. **2**(7): p. 800-813.e3.
76. Lazarus, J.V., et al., *Advancing the global public health agenda for NAFLD: a consensus statement.* Nat Rev Gastroenterol Hepatol, 2022. **19**(1): p. 60-78.
77. Harrison, S.A., et al., *Prospective evaluation of the prevalence of non-alcoholic fatty liver disease and steatohepatitis in a large middle-aged US cohort.* J Hepatol, 2021. **75**(2): p. 284-291.
78. Geidl-Flueck, B., et al., *Fructose- and sucrose- but not glucose-sweetened beverages promote hepatic de novo lipogenesis: A randomized controlled trial.* J Hepatol, 2021. **75**(1): p. 46-54.
79. Muriel, P., P. López-Sánchez, and E. Ramos-Tovar, *Fructose and the Liver.* Int J Mol Sci, 2021. **22**(13).

80. Chaudhry, S., J. Emond, and A. Griesemer, *Immune Cell Trafficking to the Liver.* Transplantation, 2019. **103**(7): p. 1323-1337.
81. Robinson, M.W., C. Harmon, and C. O'Farrelly, *Liver immunology and its role in inflammation and homeostasis.* Cell Mol Immunol, 2016. **13**(3): p. 267-76.
82. Ju, C. and F. Tacke, *Hepatic macrophages in homeostasis and liver diseases: from pathogenesis to novel therapeutic strategies.* Cell Mol Immunol, 2016. **13**(3): p. 316-27.
83. Thibaut, R., et al., *Liver macrophages and inflammation in physiology and physiopathology of non-alcoholic fatty liver disease.* FEBS J, 2022. **289**(11): p. 3024-3057.
84. Tosello-Trampont, A.C., et al., *Kuppfer cells trigger nonalcoholic steatohepatitis development in diet-induced mouse model through tumor necrosis factor-α production.* J Biol Chem, 2012. **287**(48): p. 40161-72.
85. Miura, K., et al., *Hepatic recruitment of macrophages promotes nonalcoholic steatohepatitis through CCR2.* Am J Physiol Gastrointest Liver Physiol, 2012. **302**(11): p. G1310-21.
86. Ramadori, G. and T. Armbrust, *Cytokines in the liver.* Eur J Gastroenterol Hepatol, 2001. **13**(7): p. 777-84.
87. Obstfeld, A.E., et al., *C-C chemokine receptor 2 (CCR2) regulates the hepatic recruitment of myeloid cells that promote obesity-induced hepatic steatosis.* Diabetes, 2010. **59**(4): p. 916-25.
88. Tang, T., et al., *Pro-inflammatory activated Kupffer cells by lipids induce hepatic NKT cells deficiency through activation-induced cell death.* PLoS One, 2013. **8**(12): p. e81949.
89. Baffy, G., *Kupffer cells in non-alcoholic fatty liver disease: the emerging view.* J Hepatol, 2009. **51**(1): p. 212-23.
90. Jegatheesan, P. and J.P. De Bandt, *Fructose and NAFLD: The Multifaceted Aspects of Fructose Metabolism.* Nutrients, 2017. **9**(3).
91. Ge, T., et al., *The Role of the Pentose Phosphate Pathway in Diabetes and Cancer.* Front Endocrinol (Lausanne), 2020. **11**: p. 365.
92. Galván-Peña, S. and L.A. O'Neill, *Metabolic reprograming in macrophage polarization.* Front Immunol, 2014. **5**: p. 420.
93. Huang, W., et al., *Depletion of liver Kupffer cells prevents the development of diet-induced hepatic steatosis and insulin resistance.* Diabetes, 2010. **59**(2): p. 347-57.
94. Traeger, T., et al., *Kupffer cell depletion reduces hepatic inflammation and apoptosis but decreases survival in abdominal sepsis.* Eur J Gastroenterol Hepatol, 2010. **22**(9): p. 1039-49.
95. Gladys Ferrere , 2 Anne Leroux , 1, 2 Laura Wrzosek , 1, 2 Virginie Puchois , 1, 2 Françoise Gaudin , 1, 3 Dragos Ciocan , 1, 2, 4 Marie-Laure Renoud , 1, 2 Sylvie Naveau , 1, 2, 4 Gabriel Perlemuter , 1, 2, 4 and Anne-Marie Cassard 1, 2, *, *Activation of Kupffer Cells Is Associated with a Specific Dysbiosis Induced by Fructose or High Fat Diet in Mice.* PLOS ONE, 2016.
96. Hu, H., et al., *The C/EBP Homologous Protein (CHOP) Transcription Factor Functions in Endoplasmic Reticulum Stress-Induced Apoptosis and Microbial Infection.* Front Immunol, 2018. **9**: p. 3083.
97. Jenkins, S.J., et al., *Local macrophage proliferation, rather than recruitment from the blood, is a signature of TH2 inflammation.* Science, 2011. **332**(6035): p. 1284-8.

98. Scholzen, T. and J. Gerdes, *The Ki-67 protein: from the known and the unknown.* J Cell Physiol, 2000. **182**(3): p. 311-22.
99. Himes, S.R., et al., *The JNK are important for development and survival of macrophages.* J Immunol, 2006. **176**(4): p. 2219-28.
100. Li, L., Z. Feng, and A.G. Porter, *JNK-dependent phosphorylation of c-Jun on serine 63 mediates nitric oxide-induced apoptosis of neuroblastoma cells.* J Biol Chem, 2004. **279**(6): p. 4058-65.
101. Saade, M., et al., *The Role of GPNMB in Inflammation.* Front Immunol, 2021. **12**: p. 674739.
102. Guan, C., et al., *MMP-12 regulates proliferation of mouse macrophages via the ERK/P38 MAPK pathways during inflammation.* Exp Cell Res, 2019. **378**(2): p. 182-190.
103. Stepniak, E., et al., *c-Jun/AP-1 controls liver regeneration by repressing p53/p21 and p38 MAPK activity.* Genes Dev, 2006. **20**(16): p. 2306-14.
104. Liang, R.J., et al., *GLUT5 (SLC2A5) enables fructose-mediated proliferation independent of ketohexokinase.* Cancer Metab, 2021. **9**(1): p. 12.
105. Wolf, A.J., et al., *Hexokinase Is an Innate Immune Receptor for the Detection of Bacterial Peptidoglycan.* Cell, 2016. **166**(3): p. 624-636.
106. Moon, J.S., et al., *mTORC1-Induced HK1-Dependent Glycolysis Regulates NLRP3 Inflammasome Activation.* Cell Rep, 2015. **12**(1): p. 102-115.
107. Yang, Y., et al., *Programmed cell death and its role in inflammation.* Mil Med Res, 2015. **2**: p. 12.
108. Katayama, A., et al., *Beneficial impact of Gpnmb and its significance as a biomarker in nonalcoholic steatohepatitis.* Sci Rep, 2015. **5**: p. 16920.
109. Lachowski, D., et al., *Matrix stiffness modulates the activity of MMP-9 and TIMP-1 in hepatic stellate cells to perpetuate fibrosis.* Sci Rep, 2019. **9**(1): p. 7299.
110. Liu, X.W., et al., *Tissue inhibitor of metalloproteinase-1 protects human breast epithelial cells against intrinsic apoptotic cell death via the focal adhesion kinase/phosphatidylinositol 3-kinase and MAPK signaling pathway.* J Biol Chem, 2003. **278**(41): p. 40364-72.
111. Nakagawa, T., et al., *Endogenous Fructose Metabolism Could Explain the Warburg Effect and the Protection of SGLT2 Inhibitors in Chronic Kidney Disease.* Front Immunol, 2021. **12**: p. 694457.
112. Erlich, J.R., et al., *Glycolysis and the Pentose Phosphate Pathway Promote LPS-Induced NOX2 Oxidase- and IFN-β-Dependent Inflammation in Macrophages.* Antioxidants (Basel), 2022. **11**(8).
113. Baardman, J., et al., *A Defective Pentose Phosphate Pathway Reduces Inflammatory Macrophage Responses during Hypercholesterolemia.* Cell Rep, 2018. **25**(8): p. 2044-2052.e5.
114. Lancaster, K.J., *Current Intake and Demographic Disparities in the Association of Fructose-Rich Foods and Metabolic Syndrome.* JAMA Netw Open, 2020. **3**(7): p. e2010224.
115. Antonella Viola 1 * , F.M., Ricardo Sánchez-Rodríguez 1 , Tommaso Scolaro 1 and Alessandra Castegna 2,3 *, *The Metabolic Signature of Macrophage Responses.* Front. Immunol, 2019.

116. Jaiswal, N., S. Agrawal, and A. Agrawal, *High fructose-induced metabolic changes enhance inflammation in human dendritic cells.* Clin Exp Immunol, 2019. **197**(2): p. 237-249.
117. Young, M.D. and S. Behjati, *SoupX removes ambient RNA contamination from droplet-based single-cell RNA sequencing data.* Gigascience, 2020. **9**(12).
118. Hao, Y., et al., *Integrated analysis of multimodal single-cell data.* Cell, 2021. **184**(13): p. 3573-3587.e29.
119. McGinnis, C.S., L.M. Murrow, and Z.J. Gartner, *DoubletFinder: Doublet Detection in Single-Cell RNA Sequencing Data Using Artificial Nearest Neighbors.* Cell Syst, 2019. **8**(4): p. 329-337.e4.
120. Aran, D., et al., *Reference-based analysis of lung single-cell sequencing reveals a transitional profibrotic macrophage.* Nat Immunol, 2019. **20**(2): p. 163-172.
121. Dann, E., et al., *Differential abundance testing on single-cell data using k-nearest neighbor graphs.* Nat Biotechnol, 2022. **40**(2): p. 245-253.
122. Feng, H., L. Lin, and J. Chen, *scDIOR: single cell RNA-seq data IO software.* BMC Bioinformatics, 2022. **23**(1): p. 16.
123. Wolf, F.A., P. Angerer, and F.J. Theis, *SCANPY: large-scale single-cell gene expression data analysis.* Genome Biol, 2018. **19**(1): p. 15.
124. Jensen, V.S., et al., *Dietary fat stimulates development of NAFLD more potently than dietary fructose in Sprague-Dawley rats.* Diabetol Metab Syndr, 2018. **10**: p. 4.
125. Mouton, A.J., et al., *Matrix metalloproteinase-12 as an endogenous resolution promoting factor following myocardial infarction.* Pharmacol Res, 2018. **137**: p. 252-258.
126. Day, C.P. and O.F. James, *Steatohepatitis: a tale of two "hits"?* Gastroenterology, 1998. **114**(4): p. 842-5.
127. Montgomery, M.K., et al., *Disparate metabolic response to fructose feeding between different mouse strains.* Sci Rep, 2015. **5**: p. 18474.
128. Stanhope, K.L., et al., *Consuming fructose-sweetened, not glucose-sweetened, beverages increases visceral adiposity and lipids and decreases insulin sensitivity in overweight/obese humans.* J Clin Invest, 2009. **119**(5): p. 1322-34.
129. Faeh, D., et al., *Effect of fructose overfeeding and fish oil administration on hepatic de novo lipogenesis and insulin sensitivity in healthy men.* Diabetes, 2005. **54**(7): p. 1907-13.
130. Parks, E.J., et al., *Dietary sugars stimulate fatty acid synthesis in adults.* J Nutr, 2008. **138**(6): p. 1039-46.
131. Peverill, W., L.W. Powell, and R. Skoien, *Evolving concepts in the pathogenesis of NASH: beyond steatosis and inflammation.* Int J Mol Sci, 2014. **15**(5): p. 8591-638.
132. Syn, W.K., S.S. Choi, and A.M. Diehl, *Apoptosis and cytokines in non-alcoholic steatohepatitis.* Clin Liver Dis, 2009. **13**(4): p. 565-80.
133. Choi, Y., M.A. Abdelmegeed, and B.J. Song, *Diet high in fructose promotes liver steatosis and hepatocyte apoptosis in C57BL/6J female mice: Role of disturbed lipid homeostasis and increased oxidative stress.* Food Chem Toxicol, 2017. **103**: p. 111-121.
134. Spruss, A., et al., *Toll-like receptor 4 is involved in the development of fructose-induced hepatic steatosis in mice.* Hepatology, 2009. **50**(4): p. 1094-104.
135. *High-fructose, medium chain trans fat diet induces liver fibrosis and elevates plasma coenzyme Q9 in a novel murine model of obesity and nonalcoholic steatohepatitis*†.
136. Choi, W.M., et al., *Experimental Applications of.* Mol Cells, 2019. **42**(1): p. 45-55.

137. Cabral, F., et al., *Purification of Hepatocytes and Sinusoidal Endothelial Cells from Mouse Liver Perfusion.* J Vis Exp, 2018(132).
138. Zeng, W.Q., et al., *A new method to isolate and culture rat kupffer cells*. PLoS One, 2013. **8**(8): p. e70832.
139. Hecker, P.A., et al., *Effects of glucose-6-phosphate dehydrogenase deficiency on the metabolic and cardiac responses to obesogenic or high-fructose diets.* Am J Physiol Endocrinol Metab, 2012. **303**(8): p. E959-72.
140. Park, J., J.J. Chung, and J.B. Kim, *New evaluations of redox regulating system in adipose tissue of obesity*. Diabetes Res Clin Pract, 2007. **77 Suppl 1**: p. S11-6.
141. Yan, J. and T. Horng, *Lipid Metabolism in Regulation of Macrophage Functions.* Trends Cell Biol, 2020. **30**(12): p. 979-989.
142. Li, L., et al., *The importance of GLUT3 for de novo lipogenesis in hypoxia-induced lipid loading of human macrophages.* PLoS One, 2012. **7**(8): p. e42360.
143. Bedard, K. and K.H. Krause, *The NOX family of ROS-generating NADPH oxidases: physiology and pathophysiology.* Physiol Rev, 2007. **87**(1): p. 245-313.
144. Sanna, F., et al., *Production of inflammatory molecules in peripheral blood mononuclear cells from severely glucose-6-phosphate dehydrogenase-deficient subjects*. J Vasc Res, 2007. **44**(4): p. 253-63.
145. Ham, M., et al., *Macrophage glucose-6-phosphate dehydrogenase stimulates proinflammatory responses with oxidative stress*. Mol Cell Biol, 2013. **33**(12): p. 2425-35.
146. Xu, H., et al., *Chronic inflammation in fat plays a crucial role in the development of obesity-related insulin resistance.* J Clin Invest, 2003. **112**(12): p. 1821-30.
147. Ham, M., et al., *Glucose-6-Phosphate Dehydrogenase Deficiency Improves Insulin Resistance With Reduced Adipose Tissue Inflammation in Obesity.* Diabetes, 2016. **65**(9): p. 2624-38.